

THE ASTROPHYSICAL JOURNAL

An International Review of Spectroscopy and
Astronomical Physics

FOUNDED IN 1895 BY GEORGE E. HALE AND JAMES E. KEELER

EDITORS

HENRY G. GALE
*Ryerson Physical Laboratory of the
University of Chicago*

FREDERICK H. SEARES
*Mount Wilson Observatory of the Carnegie
Institution of Washington*

OTTO STRUVE
*Yerkes Observatory of the University
of Chicago*

COLLABORATORS

WALTER S. ADAMS, *Mount Wilson Observatory*; JOSEPH S. AMES, *Johns Hopkins University*; WILLIAM W. CAMPBELL, *Lick Observatory*; HENRY CREW, *Northwestern University*; CHARLES FABRY, *Université de Paris*; ALFRED FOWLER, *Imperial College, London*; EDWIN HUBBLE, *Mount Wilson Observatory*; HEINRICH KAYSER, *Universität Bonn*; ROBERT A. MILLIKAN, *Institute of Technology, Pasadena*; HUGH F. NEWALL, *Cambridge University*; FRIEDRICH PASCHEN, *Reichsanstalt, Charlottenburg*; HENRY N. RUSSELL, *Princeton University*; FRANK SCHLESINGER, *Yale Observatory*; HARLOW SHAPLEY, *Harvard College Observatory*

VOLUME 82

JULY-DECEMBER 1935



THE UNIVERSITY OF CHICAGO PRESS
CHICAGO, ILLINOIS

THE CAMBRIDGE UNIVERSITY PRESS, LONDON
THE MARUZEN COMPANY LIMITED, TOKYO
THE COMMERCIAL PRESS, LIMITED, SHANGHAI

PUBLISHED JULY, SEPTEMBER, OCTOBER, NO-
VEMBER, DECEMBER 1935

COMPOSED AND PRINTED BY THE UNIVERSITY OF CHICAGO PRESS
CHICAGO, ILLINOIS, U.S.A.

Astronomy
Hall

CONTENTS

NUMBER I

	PAGE
RELATIVE MULTIPLY STRENGTHS IN <i>LS</i> COUPLING. Leo Goldberg . . .	I
MEASUREMENT OF THE VELOCITY OF LIGHT IN A PARTIAL VACUUM. A. A. Michelson, F. G. Pease, and F. Pearson	26
STUDIES OF EXTRA-GALACTIC NEBULAE. PART I: DETERMINATION OF MAGNITUDES. Philip C. Keenan	62
HETEROCHROMATIC STUDIES OF THE COMPANIONS OF SIRIUS, OF α CETI, AND OF α_2 ERIDANI. Charles Hetzler	75
ULTRA-VIOLET STELLAR SPECTRA WITH ALUMINUM-COATED REFLECTORS. III. THE SPECTRUM OF α LYRAE. R. William Shaw	87
NOTES	
VARIABLE <i>Hα</i> EMISSION IN ϵ AURIGAE. Dean B. McLaughlin . . .	95
VARIATIONS IN THE SPECTRUM OF 29 CANIS MAJORIS. O. Struve, C. T. Elvey, and W. W. Morgan	95

NUMBER II

THE VISUAL REGION OF THE SPECTRA OF EARLY-TYPE STARS. Roy K. Marshall	97
THE ASTROPHYSICAL OBSERVATORY OF THE CALIFORNIA INSTITUTE OF TECHNOLOGY. George E. Hale	111
TEMPERATURE CLASSIFICATION OF SAMARIUM LINES. Arthur S. King . .	140
SOME NOTES ON THE STRUCTURE OF ELLIPTICAL NEBULAE. Sinclair Smith	192
THE RADIAL VELOCITIES OF THE STARS OF SPECTRAL CLASSES R AND N. Roscoe F. Sanford	202
REVIEWS	
<i>A Finding List for Observers of Eclipsing Variables</i> , Raymond Smith Dugan (Dean B. McLaughlin), 222; <i>Fine Structure in Line Spectra and Nuclear Spin</i> , S. Tolansky (Carl Eckart), 223; <i>Elementary Quantum Mechanics</i> , R. W. Gurney (F. C. Hoyt), 224.	

NUMBER III

	PAGE
PHOTOMETRIC ELEMENTS OF BOSS 5070. Gerald E. Kron	225
ABSORPTION LINES DUE TO AN EXPANDING STAR. O. C. Wilson	233
A NEW ORBIT FOR 29 CANIS MAJORIS. W. J. Luyten and E. G. Ebbighausen	246
A TEST OF THERMODYNAMIC EQUILIBRIUM IN THE ATMOSPHERES OF EARLY-TYPE STARS. Otto Struve	252
THE EFFECT OF REFLECTION UPON THE PROFILES OF ABSORPTION LINES IN SPECTROSCOPIC BINARIES. E. L. McCarthy	261
REVIEWS	
<i>Mathematical Problems of Radiative Equilibrium</i> , Eberhard Hopf (B. P. Gerasimovič), 268; <i>Etude de la lumière du fond du ciel nocturne</i> , C. Fabry, J. Dufay, and J. Cojan (O. Struve), 270; <i>The Structure of Spectral Terms</i> , W. M. Hicks (Carl Eckart), 272.	

NUMBER IV

CHARLES EDWARD ST. JOHN. C. G. Abbot	273
KINEMATICS AND WORLD-STRUCTURE. H. P. Robertson	284
TWO METHODS OF INVESTIGATING THE NATURE OF THE NEBULAR RED-SHIFT. Edwin Hubble and Richard C. Tolman	302
A QUANTITATIVE STUDY OF CERTAIN PHASES OF F-TYPE SPECTRA. J. A. Hynek	338
REVIEWS	
<i>The Binary Stars</i> , Robert Grant Aitken (G. V. B.) 368	

NUMBER V

THE DISTRIBUTION OF CENTERS OF ATTRACTION FOR PROMINENCES. Philip C. Keenan	369
RELATIVE f -VALUES FOR LINES OF $Fe\ I$ FROM ELECTRIC-FURNACE ABSORPTION SPECTRA. Robert B. King and Arthur S. King	377
THE GLOBULAR CLUSTER NGC 2419. W. Baade	396
THE SPECTRUM OF NOVA HERCULIS $\lambda\lambda$ 5150-6550 Å. Paul W. Merrill	413
NOTES	
NOTE ON THE PHYSICAL SIGNIFICANCE OF THE n AND s CLASSIFICATION OF A STARS. Emma T. R. Williams 432	
MICROMETRIC OBSERVATIONS OF NOVA HERCULIS. G. Van Biesbroeck 433	
REVIEWS	
<i>The Rise of Modern Physics</i> , Henry Crew (P. C. Keenan), 435; <i>Relativity, Thermodynamics and Cosmology</i> , R. C. Tolman (O. Heckmann), 435.	
INDEX	439

VOLUME 82

JUL 18 1935
NUMBER 1

THE ASTROPHYSICAL JOURNAL

AN INTERNATIONAL REVIEW OF SPECTROSCOPY
AND ASTRONOMICAL PHYSICS

Founded in 1895 by GEORGE E. HALE and JAMES E. KEELER

HENRY G. GALE
Ryerson Physical Laboratory of the
University of Chicago

Edited by

FREDERICK H. SEARES
Mount Wilson Observatory of the
Carnegie Institution of Washington

OTTO STRUVE
Yerkes Observatory of the
University of Chicago

JULY 1935

RELATIVE MULTIPLET STRENGTHS IN LS COUPLING - - - - Leo Goldberg 1

MEASUREMENT OF THE VELOCITY OF LIGHT IN A PARTIAL VACUUM
A. A. Michelson, F. G. Pease, and F. Pearson 26

STUDIES OF EXTRA-GALACTIC NEBULAE. PART I: DETERMINATION OF MAGNITUDES - - - - Philip C. Keenan 62

HETEROCHROMATIC STUDIES OF THE COMPANIONS OF SIRIUS, OF α CETI, AND OF α_2 ERIDANI - - - - Charles Hetzler 75

ULTRA-VIOLET STELLAR SPECTRA WITH ALUMINUM-COATED REFLECTORS. III. THE SPECTRUM OF α LYRAE - - - - R. William Shaw 87

NOTES

VARIABLE H α EMISSION IN α AURIGAE - - - - Dean B. McLaughlin 95

VARIATIONS IN THE SPECTRUM OF β CANIS MAJORIS
O. Struve, C. T. Elvey, and W. W. Morgan 95

THE UNIVERSITY OF CHICAGO PRESS
CHICAGO, ILLINOIS, U.S.A.

THE ASTROPHYSICAL JOURNAL

AN INTERNATIONAL REVIEW OF SPECTROSCOPY
AND ASTRONOMICAL PHYSICS

Edited by

HENRY G. GALE

Ryerson Physical Laboratory of the
University of Chicago

FREDERICK H. SEARES

Mount Wilson Observatory of the
Carnegie Institution of Washington

OTTO STRUVE

Yerkes Observatory of the
University of Chicago

WITH THE COLLABORATION OF

WALTER S. ADAMS, Mount Wilson Observatory

JOSEPH S. AMES, Johns Hopkins University

WILLIAM W. CAMPBELL, Lick Observatory

HENRY CREW, Northwestern University

CHARLES FABRY, Université de Paris

ALFRED FOWLER, Imperial College, London

EDWIN HUBBLE, Mount Wilson Observatory

HEINRICH KAYSER, Universität Bonn

ROBERT A. MILLIKAN, Institute of Technology, Pasadena

HUGH F. NEWALL, Cambridge University

FRIEDRICH PASCHEN, Reichsanstalt, Charlottenburg

HENRY N. RUSSELL, Princeton University

FRANK SCHLESINGER, Yale Observatory

HARLOW SHAPLEY, Harvard College Observatory

Former Editors:

GEORGE E. HALE

JAMES E. KEELER

EDWIN B. FROST

The *Astrophysical Journal* is published by the University of Chicago at the University of Chicago Press, 5750 Ellis Avenue, Chicago, Illinois, during each month except February and August. ¶ The subscription price is \$6.00 a year; the price of single copies is 75 cents. Orders for service of less than a half-year will be charged at the single-copy rate. ¶ Postage is prepaid by the publishers on all orders from the United States, Mexico, Cuba, Porto Rico, Panama Canal Zone, Republic of Panama, Dominican Republic, Canary Islands, El Salvador, Argentina, Bolivia, Brazil, Colombia, Chile, Costa Rica, Ecuador, Guatemala, Honduras, Nicaragua, Peru, Hayti, Uruguay, Paraguay, Hawaiian Islands, Philippine Islands, Guam, Samoan Islands, Balearic Islands, Spain, and Venezuela. ¶ Postage is charged extra as follows: for Canada and Newfoundland, 30 cents on annual subscriptions (total \$6.30); on single copies, 3 cents (total 78 cents); for all other countries in the Postal Union, 80 cents on annual subscriptions (total \$6.80), on single copies, 8 cents (total 83 cents). ¶ Patrons are requested to make all remittances payable to The University of Chicago Press, in postal or express money orders or bank drafts.

The following are authorized agents:

For the British Empire, except North America, India, and Australasia: The Cambridge University Press, Fetter Lane, London, E.C. 4. Prices of yearly subscriptions and of single copies may be had on application.

For Japan: The Maruzen Company, Ltd., Tokyo.

For China: The Commercial Press, Ltd., 211 Honan Road, Shanghai. Yearly subscriptions, \$6.00; single copies, 75 cents, or their equivalents in Chinese money. Postage extra, on yearly subscriptions 80 cents, on single copies 8 cents.

Claims for missing numbers should be made within the month following the regular month of publication. The publishers expect to supply missing numbers free only when losses have been sustained in transit, and when the reserve stock will permit.

Business correspondence should be addressed to The University of Chicago Press, Chicago, Illinois.

Communications for the editors and manuscripts should be addressed to: Otto Struve, Editor of THE ASTROPHYSICAL JOURNAL, Yerkes Observatory, Williams Bay, Wisconsin.

The cable address is "Observatory, Williamsbay, Wisconsin."

The articles in this journal are indexed in the *International Index to Periodicals*, New York, N.Y.

Applications for permission to quote from this journal should be addressed to The University of Chicago Press, and will be freely granted.

Entered as second-class matter, January 17, 1895, at the Post-Office, Chicago, Ill., under the act of March 3, 1879.

Acceptance for mailing at special rate of postage provided for in Section 1103, Act of October 3, 1917, authorized on July 15, 1918.

PRINTED IN THE U.S.A.

THE ASTROPHYSICAL JOURNAL

AN INTERNATIONAL REVIEW OF SPECTROSCOPY AND
ASTRONOMICAL PHYSICS

VOLUME 82

JULY 1935

NUMBER 1

RELATIVE MULTIPLY STRENGTHS IN LS COUPLING

By LEO GOLDBERG

ABSTRACT

The relative strengths of different multiplets in LS coupling have been calculated and tabulated for sixty-five transition arrays of astrophysical interest. In arrays where the jumping electron belongs to a shell of three or more equivalent electrons, the method of Condon and Ufford was employed; all other cases were dealt with by the extension of Kronig's formulae to relative multiplet strengths, according to the methods outlined by Shortley. A description of the Condon-Ufford method is given, together with an illustration of its application to the transition array $p^3 - p^2s$. It is shown, also, that in applying this method, it is necessary to write down the zero-order states of only one configuration, that involving the smallest number of terms.

Formulae for the relative strengths of the lines within a multiplet have been known for a number of years. These have been derived independently by Kronig,¹ Russell,² and Sommerfeld and Hönl,³ from the correspondence principle, and from the sum rules of Ornstein,⁴ Burger, and Dorgelo.⁵ They have also been derived quantum mechanically by Dirac.⁶

Kronig has shown that these formulae enable us, also, to calculate the relative total strengths of the multiplets within a supermultiplet in LS coupling, by substituting L_i for S , l for L , and L for J in the formulae, where L_i refers to the orbital angular momentum of the parent term upon which are based the terms of the supermultiplet,

¹ *Zs. f. Phys.*, **33**, 261, 1925.

⁴ *Zs. f. Phys.*, **24**, 41, 1924.

² *Nature*, **115**, 735, 1925.

⁵ *Ibid.*, **23**, 258, 1925.

³ *Sitz. Preuss. Akad.*, **9**, 141, 1925.

⁶ *Proc. R. Soc., A*, **111**, 302, 1926.

l is the azimuthal quantum number of the jumping electron, and L expresses the total orbital angular momentum. The relation between the strengths of two different supermultiplets then follows from the sum rule: it can be demonstrated that the total strength of a supermultiplet is proportional to $(2L_i+1)(2S+1)$, where L_i is the L value of the parent term, and $2S+1$ is the multiplicity of the two sets of terms between which transitions occur to produce the supermultiplet. It should be remarked that all of the terms involved in the production of a supermultiplet are of identical multiplicity; i.e., inter-system combinations are forbidden.

Unfortunately, the application, in this manner, of these simple formulae to the calculation of relative multiplet strengths is definitely limited to those arrays in which the electron transition is of the sort $\gamma + a \rightarrow \gamma + \beta$, where a and β are one-electron configurations between which radiative transitions are allowed, and neither a nor β contain electrons equivalent to any in γ . An example of such a transition is: $2p^23s - 2p^23p$, where $\gamma = 2p^2$, $a = 3s$, and $\beta = 3p$. Shortley,⁷ following the theory as outlined by Johnson⁸ and others, has recently extended the application of the Kronig formulae to include arrays in which a and β contain two or more electrons, with the proviso again that radiative transitions be allowed between a and β , and that no electrons in a and β be equivalent to any in γ . An example is the electron transition $3d^24p^2 - 3d^24s4p$. Here $\gamma = 3d^2$, $a = 4p^2$, and $\beta = 4s4p$. Ufford and Miller⁹ have developed formulae for the special case in which γ is a single s-electron.

Shortley's method requires that the relative strengths of the multiplets in the transition array $a \rightarrow \beta$ be known in advance. If in either a or β the jumping electron belongs to a group of three or more equivalent electrons, the Kronig formulae will give incorrect results for the multiplet strengths in the array. Condon and Ufford¹⁰ have derived a method from quantum mechanics which is valid for all cases, including those in which the transition electron belongs to a group of three or more equivalent electrons, e.g., $3d^4 - 3d^34p$. The application of this method will be discussed in detail below.

In the present paper, the relative multiplet strengths in LS cou-

⁷ *Proc. Nat. Acad.*, **20**, 591, 1934.

⁹ *Phys. Rev.*, **46**, 283, 1934.

⁸ *Ibid.*, **19**, 916, 1933.

¹⁰ *Ibid.*, **44**, 740, 1933.

pling are tabulated for sixty-five transition arrays of astrophysical interest. In cases to which general formulae are applicable, i.e., $\gamma + \alpha \rightarrow \gamma + \beta$, the relative strengths are not explicitly listed when γ is an electron shell which is more than half-full. These may be found in the tables by replacing γ with the corresponding shell of "missing" electrons. For example, the relative strengths of the multiplets in the transition array $3d^6 4s - 3d^6 4p$ are given in the tables under $3d^4 4s - 3d^4 4p$. The configurations have been selected from those listed by Bacher and Goudsmit¹¹ and include all those involving s-, p-, and d-electrons, and in a few cases f-electrons.

All of the various methods listed above were utilized in the preparation of the tables. The Kronig formulae were applied to those transition arrays that permitted their use, and when these became inapplicable, the more involved method of Condon and Ufford was employed. The mode of attack in the former cases has been fully treated by Shortley,⁷ and further discussion in this paper would be superfluous. The complete details of the latter method are lacking, however, in the original paper,¹⁰ and a more workable description of the procedure is desirable. In the description we shall first outline the general theory and then supplement the outline with a demonstration of its application¹² to the transition array $p^3 - p^2 s$.

The intensity of a spectral line resulting from a transition between two atomic levels, γSLJ and $\gamma' SL'J'$, is given by

$$I(\gamma SLJ, \gamma' SL'J') = \frac{N(\gamma SLJ)}{2J+1} \cdot \frac{64\pi^4 \nu^4}{3C^3} \cdot S(\gamma SLJ, \gamma' SL'J'), \quad (1)$$

where $N(\gamma SLJ)$ is the number of atoms in the initial level γSLJ , C is the velocity of light in centimeters per second, and ν is the frequency in sec^{-1} . The quantity $S(\gamma SLJ, \gamma' SL'J')$, which is known as the strength of the line, is defined as the sum of the absolute squares of the matrix elements of electric moment joining the states of the level γSLJ and the states of the level $\gamma' SL'J'$:

$$S(\gamma SLJ, \gamma' SL'J') = \sum_{M, M'} |(\gamma SLJM | P | \gamma' SL'J'M')|^2. \quad (2)$$

¹¹ *Atomic Energy States* (McGraw-Hill, 1932).

¹² See note at end of paper for definitions of spectroscopic notation and terminology.

The total strength of a multiplet will be equal to the sum of the strengths of all the lines within the multiplet:

$$S(\gamma SL, \gamma' SL') = \sum_{J, J'} S(\gamma SLJ, \gamma' SL'J'). \quad (3)$$

Substituting (2) in (3), we find:

$$S(\gamma SL, \gamma' SL') = \sum_{J, J'} \sum_{M, M'} |(\gamma SLJM | P | \gamma' SL'J'M')|^2. \quad (4)$$

If we sum Kronig's formulae for the relative strengths of the lines in a multiplet, the strengths $S(\gamma SL, \gamma' SL')$ are expressed in the following form:

When $L' = L + 1$,

$$S(\gamma SL, \gamma' SL + 1) = (2S + 1)(2L + 1)(L + 1)(2L + 3) |(\gamma SL \vdots P \vdots \gamma' SL + 1)|^2.$$

When $L' = L$,

$$S(\gamma SL, \gamma' SL) = (2S + 1)(2L + 1)(L)(L + 1) |(\gamma SL \vdots P \vdots \gamma' SL)|^2. \quad (5)$$

When $L' = L - 1$,

$$S(\gamma SL, \gamma' SL - 1) = (2S + 1)(2L + 1)(L)(2L - 1) |(\gamma SL \vdots P \vdots \gamma' SL - 1)|^2.$$

Here the $(\gamma SL \vdots P \vdots \gamma' SL')$'s are the undetermined constants of proportionality occurring in Kronig's formulae. In order to determine the total strengths of different multiplets, then, we must calculate these factors $|(\gamma SL \vdots P \vdots \gamma' SL')|^2$. This may be done in the following way:

Let us first consider the line strengths in a scheme in which we characterize the states by quantum numbers L, S, M_L, M_S . The square of the matrix element between two states characterized by $\gamma L S M_L M_S$ and by $\gamma' L' S M'_L M'_S$, respectively, may be expressed in terms of the same factors that occur in (5) as follows:

$$\begin{aligned}
\begin{matrix} L' = L+1 \\ M'_L = M_L \pm 1 \end{matrix} & |(\gamma L S M_L M_S | \mathbf{P} | \gamma' L' S M'_L M_S)|^2 \\
& = \frac{1}{2}(L \pm M_L + 1)(L \pm M_L + 2) |(\gamma S L ; P ; \gamma' S L + 1)|^2. \\
\begin{matrix} L' = L+1 \\ M'_L = M_L \end{matrix} & = [(L+1)^2 - M_L^2] |(\gamma S L ; P ; \gamma' S L + 1)|^2. \\
\begin{matrix} L' = L \\ M'_L = M_L \pm 1 \end{matrix} & = \frac{1}{2}(L \mp M_L)(L \pm M_L + 1) |(\gamma S L ; P ; \gamma' S L)|^2. \\
\begin{matrix} L' = L \\ M'_L = M_L \end{matrix} & = M_L^2 |(\gamma S L ; P ; \gamma' S L)|^2. \quad (6) \\
\begin{matrix} L' = L-1 \\ M'_L = M_L \pm 1 \end{matrix} & = \frac{1}{2}(L \mp M_L)(L \mp M_L - 1) |(\gamma S L ; P ; \gamma' S L - 1)|^2. \\
\begin{matrix} L' = L-1 \\ M'_L = M_L \end{matrix} & = (L^2 - M_L^2) |(\gamma S L ; P ; \gamma' S L - 1)|^2.
\end{aligned}$$

These matrix elements vanish unless $\Delta S = 0$, $\Delta L = \pm 1, 0$, $\Delta M_L = \pm 1, 0$, and $\Delta M_S = 0$.

Let us now consider the strengths in a zero-order scheme in which each state is an antisymmetric linear combination of one-electron wave functions characterized by quantum numbers $n l m_l m_s$. In this scheme a state A of the atom is specified by giving a set $n l m_l m_s$ of quantum numbers for each electron. According to the Pauli exclusion principle, no state is allowed in which the same set of quantum numbers occurs for more than one electron, and two states are not distinct if they contain the same sets merely arrayed in a different order. In such a scheme, the M_L value of the state is just the sum of the m_l values of the electrons; $M_L = \sum m_l$; also $M_S = \sum m_s$. There is no matrix element of electric moment between two zero-order states that differ with respect to the quantum numbers of more than one electron. The square of the matrix element between two states A and A' , differing only in that one electron, the jumping electron, has quantum numbers n, l, m_l, m_s in A and quantum numbers $n', l-1, m'_l, m_s$ in A' , is given by:

$$|(A | \mathbf{P} | A')|^2 = \frac{1}{2}(l \pm m_l)(l \pm m_l - 1)\sigma^2, \quad (7)$$

when $m'_l = m_l \mp 1$, and by

$$|(A|P|A')|^2 = (l^2 - m_l^2)\sigma^2, \quad (8)$$

when $m'_l = m_l$. These matrix elements vanish unless $\Delta m_s = 0$, $\Delta m_l = \pm 1, 0$, and $\Delta l = \pm 1$. Since $\Delta m_s = 0$, and since only one electron is permitted to jump at a time, it is obvious that the matrix elements will also vanish unless $\Delta M_s = 0$. The quantity σ depends only on the configurations between which the electron jumps, and is given explicitly in terms of the radial eigenfunctions $R(n, l)$ and $R(n', l')$ of this electron by

$$\sigma = \frac{e}{(4l^2 - 1)^{1/2}} \int_0^\infty r \cdot R(n, l) R(n', l') dr. \quad (9)$$

In the $nlm_l m_s$ scheme, we have expressed the matrix elements in terms of the quantity σ^2 , which is a constant for the whole transition array. In the $LSM_L M_s$ scheme, we have expressed the matrix elements in terms of the quantities $|(\gamma SL \vdash P \vdash \gamma' SL')|^2$, which give, by (5), the multiplet strengths. Now the matrix elements in the two schemes may be related in the following way:

Consider the transition array which connects the two configurations α and α' . In α , take the set of all states characterized by one particular value M_L and one particular value M_s in the $LSM_L M_s$ scheme, and denote them by $B_1, B_2, \dots, B_i, \dots, B_n$; in the zero-order scheme take the set of all states having these same values of M_L and M_s , i.e., for which $\sum m_l = M_L$, and $\sum m_s = M_s$, and denote them by $A_1, A_2, \dots, A_i, \dots, A_n$. Similarly, in α' take the set of all states characterized by given values, M'_L and M'_s , in the $LSM_L M_s$ scheme, and denote them by $B'_1, B'_2, \dots, B'_j, \dots, B'_m$; in the zero-order scheme, consider the set of all states for which $\sum m'_l = M'_L$, and $\sum m'_s = M'_s$, and denote them by $A'_1, A'_2, \dots, A'_j, \dots, A'_m$. The principle of spectroscopic stability shows that the sum of the squares of the matrix elements joining two sets of states, $A_1 \dots A_n$ of α , and $A'_1 \dots A'_m$ of α' , remains constant when these states are subjected to a unitary transformation. Since the transformation

from zero-order states to $M_L M_S$ states is a unitary one, the principle of spectroscopic stability shows that

$$\sum_{i=1}^{i=n} \sum_{j=1}^{j=m} |(A_i | P | A'_j)|^2 = \sum_{i=1}^{i=n} \sum_{j=1}^{j=m} |(B_i | P | B'_j)|^2. \quad (10)$$

The matrix elements in (10) will vanish unless $M'_S = M_S$. Therefore, to determine the relative multiplet strengths in the transition array $a - a'$, we take each value of M_S separately, beginning with the highest, and for any pair of values M_L and M'_L , we calculate the

TABLE I
ZERO-ORDER AND $LSM_L M_S$ SCHEME FOR p^3

		M_S	
		$3/2$	$1/2$
M_L	2		$1^+ \quad 0^+ \quad 1^- \quad 2D$
	1		$1^+ \quad 1^- \quad -1^+ \quad 2D$ $1^+ \quad 0^+ \quad 0^- \quad 2P$
	0	$1^+ \quad 0^+ \quad -1^+ \quad 4S$	$1^+ \quad 0^+ \quad -1^- \quad 4S$ $1^+ \quad 0^- \quad -1^+ \quad 2D$ $1^- \quad 0^+ \quad -1^+ \quad 2P$

quantities on the left-hand side of (10) from (7) and (8), in terms of σ^2 . We then write the quantities on the right-hand side of (10) in terms of the factors $|(\gamma SL \vdash P \vdash \gamma' SL')|^2$ as given in (6). Thus, each pair of values M_L and M'_L gives us an equation of the form (10), and the set of all such equations enables us to determine, in terms of σ^2 , all the factors $|(\gamma SL \vdash P \vdash \gamma' SL')|^2$, which, by (5), yield the strengths directly.

As an illustration of the method, let us examine the transition array $p^3 - p^2s$. We are to calculate the relative strengths of the multiplets arising from transitions between $4S$, $2D$, and $2P$ of p^3 , and $4P$, $2D$, $2P$, and $2S$ of p^2s . For each configuration we make a table which classifies the zero-order states by values of M_L and M_S , and which

also classifies the states in the $LSM_L M_S$ scheme by values of M_L and M_S . Only positive values of M_L and M_S need be considered. Tables I and II make this classification for each configuration. We next calculate the squares of the matrix elements connecting the zero-order states of p^3 with those of p^2s . Since these matrix elements vanish unless $\Delta M_S = 0$, we ordinarily take each value of M_S separately, beginning with the highest, and calculate the elements for

TABLE II
ZERO-ORDER AND $LSM_L M_S$ SCHEME FOR p^2s

M_L	M_S			
	$3/2$	$1/2$		
2		1^+	1^-	0^+ 2D
1	1^+ 0^+ 0^+ 4P	1^+	0^+	0^- 4P
		1^+	0^-	0^+ 2D
		1^-	0^+	0^+ 2P
0	1^+ -1^+ 0^+ 4P	0^+	0^-	0^+ 4P
		1^+	-1^+	0^- 2D
		1^+	-1^-	0^+ 2P
		1^-	-1^+	0^+ 2S

pairs of values, M_L and M'_L . For shells of equivalent p-electrons, however, we need to consider only the states for which M_S has its lowest value, in this case $\frac{1}{2}$. These will provide a sufficient number of equations to determine all the strengths of the array. Table III gives the squares of the matrix elements for $M_S = \frac{1}{2}$, as calculated from equations (7) and (8). For example, in p^3 , for $M_L = 2$, we have the state $1_p^+ 0_p^+ 1_p^-$; in p^2s , for $M'_L = 2$, the state $1_p^+ 1_p^- 0_s^+$. Here, then, for the jumping electron, $m_s = +\frac{1}{2}$, $m_l = 0$, $m'_s = +\frac{1}{2}$, and $m'_l = 0$. Since $\Delta m_l = 0$, we substitute in (8), and find for the square of the matrix element joining the two states:

$$|(1_p^+ 0_p^+ 1_p^- | P | 1_p^+ 1_p^- 0_s^+)|^2 = 1 \cdot \sigma^2. \quad (11)$$

For the element connecting the states $M_L=2$, $1p^+o_p^+1p^-$, and $M'_L=1$, $1p^+o_p^+o_s^-$, we use the upper sign in (7), since $\Delta m_l = -1$, and find,

$$|(1p^+o_p^+1p^-|P|1p^+o_p^+o_s^-)|^2 = 1 \cdot \sigma^2. \quad (12)$$

TABLE III

p^3-p^2s , $M_S=\frac{1}{2}$

COEFFICIENTS GIVING SQUARES OF MATRIX ELEMENTS BETWEEN
ZERO-ORDER STATES WHEN MULTIPLIED BY THE CONSTANT σ^2

$M'_L=2$ $M'_L=1$ $M'_L=0$

	p^3	p^2s							
		$1p^+o_p^+1p^-$				$1p^+o_p^+o_s^-$			
		$1p^+$	o_p^+	$1p^-$	o_p^-	$1p^+$	o_p^+	$1p^-$	o_p^-
$M_L=2$	$1p^+o_p^+1p^-$	1				0	0	0	0
	$1p^+o_p^+o_s^-$					0	0	0	0
$M_L=1$	$1p^+o_p^+1p^-$	1	0*	0*	0*	0*	1	0*	1
	$1p^+o_p^+o_s^-$	0*	1	1	0*	1	0*	0*	0*
$M_L=0$	$1p^+o_p^+1p^-$	0	1	0*	0*	0*	0*	1	0*
	$1p^+o_p^+o_s^-$	0	0*	1	0*	0*	1	0*	0*
	$1p^-o_p^+1p^+$	0	0*	0*	1	0*	0*	0*	1

* Multi-electron jump.

For $M_L=2$, $1p^+o_p^+1p^-$, and $M'_L=1$, $1p^+o_p^-o_s^+$, the matrix element vanishes, since a double electron jump is involved. For the element connecting $M_L=2$, $1p^+o_p^+1p^-$, and $M'_L=1$, $1p^-o_p^+o_s^+$, we find from (7),

$$|(1p^+o_p^+1p^-|P|1p^-o_p^+o_s^+)|^2 = 1 \cdot \sigma^2. \quad (13)$$

In like manner, the matrix elements are calculated for all other pairs of states, and the coefficients of σ^2 thus determined are classified in Table III according to values of M_L and M'_L .

Now, in the $LSM_L M_S$ scheme, we calculate the squares of the matrix elements between pairs of $M_L M_S$ states in terms of the factors $|(\gamma SL \vdots P \vdots \gamma' SL')|^2$ for $M_S = \frac{1}{2}$, as given in equations (6). For example, for 2D , $M_L = 2$, and 2D , $M'_L = 2$, we have $L = 2$, $L' = 2$, $M'_L = M_L$, $L' = L$, and $M_S = \frac{1}{2}$. Hence

$$|({}^2D, 2, \tfrac{1}{2} | P | {}^2D, 2, \tfrac{1}{2})|^2 = 4 |({}^2D \vdots P \vdots {}^2D)|^2. \quad (14)$$

TABLE IV
 $p^3 - p^2s$, $M_S = \frac{1}{2}$
 COEFFICIENTS GIVING SQUARES OF MATRIX ELEMENTS BETWEEN
 $LSM_L M_S$ STATES WHEN MULTIPLIED BY FACTORS

		$ (\gamma LS \vdots P \vdots \gamma' L'S) ^2$							
		$M'_L = 2$				$M'_L = 1$		$M'_L = 0$	
		p^2s							
p^3		2D	4P	2D	2P	4P	2D	2P	2S
$M_L = 2$	2D	4	0	2	6	0	0	0	0
	2D	2	0	1	3	0	3	3	0
$M_L = 1$	2P	6	0	3	1	0	1	1	1
	4S	0	1	0	0	1	0	0	0
$M_L = 0$	2D	0	0	3	1	0	0	4	0
	2P	0	0	3	1	0	4	0	1

For 2D , $M_L = 2$, and 2D , $M'_L = 1$, we find

$$|({}^2D, 2, \tfrac{1}{2} | P | {}^2D, 1, \tfrac{1}{2})|^2 = 2 |({}^2D \vdots P \vdots {}^2D)|^2, \quad (15)$$

and similarly for other pairs of $M_L M_S$ states. The coefficients of $|(\gamma SL \vdots P \vdots \gamma' SL')|^2$ thus evaluated are given in Table IV. Each coefficient, multiplied by its corresponding factor, gives the square of the matrix element joining the particular pair of $M_L M_S$ states involved.

We have from (10) that for given values M_L , M_S in one configura-

tion, and corresponding values $M'_L M'_S$ in the other, the sum of the squares of the matrix elements joining the two sets of zero-order states characterized by $\sum m_s = M_S$, $\sum m_l = M_L$, and by $\sum m'_s = M'_S$, $\sum m'_l = M'_L$, respectively, is equal to the sum of the squares of the matrix elements joining the two sets of $M_L M_S$ states characterized by values M_L , M_S and M'_L , M'_S . Therefore, in Tables III and IV, each rectangle will yield an equation of the form of (10), and the set of all such equations determines the individual values of all the factors $|(\gamma SL \vdots P \vdots \gamma' SL')|^2$, which, by (5), give the relative strengths. Beginning with the largest value of M_L , we have for the first rectangle,

$$\begin{aligned} 4 |(^2D \vdots P \vdots ^2D)|^2 &= 1 \cdot \sigma^2, \\ |(^2D \vdots P \vdots ^2D)|^2 &= \frac{1}{4} \cdot \sigma^2. \end{aligned} \quad (16)$$

For the rectangle $M_L = 2$, $M'_L = 1$, we find

$$2 |(^2D \vdots P \vdots ^2D)|^2 + 6 |(^2D \vdots P \vdots ^2P)|^2 = 1 \cdot \sigma^2 + 1 \cdot \sigma^2.$$

Replacing $|(^2D \vdots P \vdots ^2D)|^2$ by its value in (16), we have

$$|(^2D \vdots P \vdots ^2P)|^2 = \frac{1}{4} \cdot \sigma^2. \quad (17)$$

For $M_L = 1$, $M'_L = 2$, we find

$$\begin{aligned} 2 |(^2D \vdots P \vdots ^2D)|^2 + 6 |(^2P \vdots P \vdots ^2D)|^2 &= 1 \cdot \sigma^2, \\ |(^2P \vdots P \vdots ^2D)|^2 &= \frac{1}{2} \cdot \sigma^2. \end{aligned} \quad (18)$$

For $M_L = 1$, $M'_L = 1$,

$$\begin{aligned} |(^2D \vdots P \vdots ^2D)|^2 + 3 |(^2D \vdots P \vdots ^2P)|^2 + 3 |(^2P \vdots P \vdots ^2D)|^2 \\ + |(^2P \vdots P \vdots ^2P)|^2 &= 1 \cdot \sigma^2 + 1 \cdot \sigma^2. \end{aligned}$$

Replacing the known factors by their values in (16), (17), and (18), we have

$$|(^2P \vdots P \vdots ^2P)|^2 = \frac{3}{4} \cdot \sigma^2. \quad (19)$$

Similarly, from $M_L=1$, $M'_L=0$, and from $M_L=0$, $M'_L=1$, respectively,

$$|({}^2P \vdots P \vdots {}^2S)|^2 = \frac{2}{3} \cdot \sigma^2 \quad (20)$$

and

$$|({}^4S \vdots P \vdots {}^4P)|^2 = 1 \cdot \sigma^2. \quad (21)$$

The factors thus determined are collected in Table V; and the corresponding strengths, derived by substituting these factors in equations (5), are listed in Table VI.

TABLE V
VALUES OF FACTORS $|(\gamma LS \vdots P \vdots \gamma' L'S)|^2$ FOR TRANSITION
ARRAY p^3-p^2s , IN TERMS OF σ^2

p^3	p^2s			
	4P	2D	2P	2S
4S	1	0	0	0
2D	0	1/4	1/4	0
2P	0	1/12	3/4	2/3

TABLE VI
RELATIVE MULTIPLY STRENGTHS FOR TRANSITION
ARRAY p^3-p^2s

p^3	p^2s			
	4P	2D	2P	2S
4S	12	0	0	0
2D	0	15	15	0
2P	0	5	9	4

During the process of preparation of the tables of multiplet strengths, a rather simple method of calculating the matrix elements between two sets of zero-order states was found; it requires that the zero-order scheme be set up for only the configuration in which the

jumping electron has its nl value equivalent to others. In Table I, let us consider the zero-order states characterized by $M_S = \frac{1}{2}$, and $M_L = 0$. We wish to calculate the sum of the squares of the matrix elements between these states and the states of p^2 s for which $M'_S = \frac{1}{2}$, and $M'_L = 1$. For the jumping electron, then, $m'_i = m_l + 1$. In the first of the three zero-order states under consideration, $m_{i_1} = 1$, $m_{i_2} = 0$, and $m_{i_3} = -1$. Since, for an s-electron, $m'_i = 0$, only the p-electron for which $m_l = -1$ is permitted to jump to this box of p^2 s. If any of the remaining p-electrons were to jump, we should then have m'_i s for the s-electron in p^2 s equal to 1 and 2. The square of the matrix element between two zero-order states differing only in that one electron, the jumping electron, has quantum numbers $n, l = 1$, $m_s, m_l = -1$, in one, and quantum numbers $n', l' = 0, m_s, m'_l = 0$, in the other, is by (7) equal to $1 \cdot \sigma^2$. Therefore, to calculate the sum of the squares of the matrix elements between the two sets of states in question, one simply adds the number of individual electron states for which $m_l = -1$, and multiplies the sum by $1 \cdot \sigma^2$. The result, $3 \cdot \sigma^2$, is precisely that given in Table III, evaluated from the zero-order states of both initial and final configurations. Consider now the matrix elements between the same initial states of p^3 , and the set of states for which $M'_S = \frac{1}{2}$, and $M'_L = 0$ in p^2 s. Here $\Delta m_l = 0$, and only those electron states need be considered for which $m_l = 0$. The square of the matrix element when $m_l = 0$, and $m'_l = 0$ in the array $p^3 - p^2$ s, is by (8) equal to $1 \cdot \sigma^2$. There are three electronic states for which $m_l = 0$; hence the sum of the squares of the matrix elements for $M_L = 0, M'_L = 0$, is equal to $3 \cdot \sigma^2$, the result again checking with the value given in Table III. Similarly when $\Delta M_L = -1$, we add the individual electronic states for which $m_l = 1$, and multiply by $1 \cdot \sigma^2$. The foregoing method may be applied in exactly the same way to configurations involving shells of equivalent d-electrons. Since, then, a given configuration may well involve over a thousand zero-order states, the saving effected in writing down the zero-order states of one, instead of two, configurations is alone quite considerable.

DESCRIPTION OF TABLES

The tables of strengths are numbered from I to XVI, and an index is provided on page 17 to facilitate the location of a desired transition

array. It is to be noted that in any transition array either of the two configurations may be the initial or final one. The rôles of initial and final configurations may thus be interchanged. In describing the arrangement of the tables, it will be convenient to discuss separately the three types of electron transitions with which this work has been concerned.

a) The jumping electron belongs to a group of three or more equivalent electrons. Here general intensity formulae are not applicable, and recourse must be made to the method of Condon and Ufford. In such arrays one cannot specify explicitly upon which term of the ion a given term of the "neutral" configuration is based, and thus no parent terms are listed for such transition arrays. When more than one term of a kind occurs in a given configuration, the Condon-Ufford method gives only the sum of the strengths of all the multiplets arising from transitions between these terms and a term, or set of like terms, in the final configuration. For example, in Table I (in the tables of strengths) the total strength of the transitions $d^6 2^3F \rightarrow d^5 p 7^3G$ is written as 7515. This number represents the *sum* of the strengths of all transitions between the two 3F terms of d^6 and the seven 3G terms of $d^5 p$. The strengths for the transition arrays $p^5 - p^4 d$, $p^4 - p^3 d$, $p^3 - p^2 d$, and $d^3 - d^2 p$ were first calculated by Condon and Ufford,¹⁰ and are reproduced here in the tables. Those for the arrays $d^4 - d^3 p$, $d^2 p - dp^2$, and $d^3 p - d^2 p^2$ have also been calculated by Ufford and Miller,⁹ their results agreeing with those given in the tables.

b) When the array is of the type $\gamma + a \rightarrow \gamma + \beta$ (see above, p. 2), where a and β are one-electron configurations, the relative multiplet strengths were calculated by direct substitution in the Kronig formulae, and by application of the $(2L_i + 1)(2S + 1)$ rule for supermultiplet strengths. Here transitions are permitted only between terms based on the same parent term of the ion. The parent terms are given in parentheses for the terms of the initial configuration. The parentage is generally written once for each supermultiplet or group of supermultiplets whose polyads have this common parentage. For example, in Table VI (in the tables of strengths), for the array $d^3 p - d^3 d$, the term 4F is the common parent of the set of

terms ${}^5G, {}^5F, \dots, {}^3D$, inclusive. It often happens that more than one parent term of a kind occurs in a configuration, as in Table VI, d^3p-d^3d . Here, for example, we have two 2D terms of the ion d^3 , and hence two supermultiplets

$$2({}^3F^3D^3P) \rightarrow 2({}^3G^3F^3D^3P^3S)$$

whose terms are based on $d^3({}^2D)$. These supermultiplets have the same strengths, and for economy of space, the strengths within these supermultiplets have been combined. The strength of any one multiplet may be found by dividing the value given in the table by two. Thus

$$\begin{aligned} S(d^3p \ {}^3F \rightarrow d^3d \ {}^3G) &= \frac{1}{2} S(d^3p \ {}^2F \rightarrow d^3d \ {}^2G) \\ &= 3240. \end{aligned}$$

c) We come finally to the case treated by Shortley, i.e., $\gamma + \alpha \rightarrow \gamma + \beta$, where α and β contain two or more electrons. Here transitions are permitted only between terms based on the same term of γ . The terms of γ upon which are based the terms of the various supermultiplets are given in parentheses, as in (b). When $\alpha = sp$, and $\beta = p^2$, the manner in which the terms of $\gamma + \alpha$, and of $\gamma + \beta$, have been formed is indicated in the tables. For example, in Table XIII (in the tables of strengths) the notation $d^5({}^R L) + sp({}^1 P) \rightarrow d^5({}^R L) + p^2({}^1 D)$, for a sequence of supermultiplets, implies that, for a given supermultiplet, the terms of d^5sp have been formed through the addition of $sp({}^1 P)$ to the parent term $d^5({}^R L)$, and those of d^5p^2 have been formed through the addition of $p^2({}^1 D)$ to the same parent term $d^5({}^R L)$, and similarly for $d^5({}^R L) + sp({}^3 P) \rightarrow d^5({}^R L) + p^2({}^3 P)$, and $d^5({}^R L) + sp({}^1 P) \rightarrow d^5({}^R L) + p^2({}^1 S)$. In such a transition array, transitions are permitted only between terms formed in the three ways indicated. In other words, transitions are permitted only between terms formed by adding terms of the same multiplicity in α and β to a given term of γ . In like manner, when $\alpha = s^2$, and $\beta = sp$, only the transitions $\gamma({}^R L) + s^2({}^1 S) \rightarrow \gamma({}^R L) + sp({}^1 P)$ are permitted.

These tables were prepared with the hope that they would be of use to physicists and astrophysicists. A test of their general accu-

racy is now being made by Dr. Menzel and the writer. The Rowland solar intensities are being used in the work.

In conclusion, the writer wishes to express his appreciation to Dr. George H. Shortley, of the Mendenhall Laboratory of Physics, Ohio State University, to whom he is indebted for many valuable discussions of the various methods of calculating multiplet strengths, and for advice in drawing up the tables of strengths. The work was undertaken at the suggestion and with the advice of Dr. Donald H. Menzel, of Harvard Observatory, and has been developed under his excellent counsel.

HARVARD COLLEGE OBSERVATORY

March 8, 1935

NOTE

The definitions of spectroscopic notation and terminology listed below include those given by Shortley (*Proc. Nat. Acad. Sci.*, **20**, No. 11, 591-93, November, 1934).

$\gamma SLJM$.—An atomic state, characterized by given values of the spin quantum number S , the orbital quantum number L , the inner quantum number J , and the magnetic quantum number M . The symbol γ is used to represent all quantities other than S , L , J , and M which are necessary to define the state.

γSLJ .—An atomic level, the set of $(2J+1)$ states characterized by S , L , and J . Here γ represents all quantities other than S , L , and J which are necessary to define the set of states.

γSL .—An atomic term, the set of $(2L+1)(2S+1)$ states, characterized by given values of L and S .

$(\gamma SLJM|P|\gamma' S' L' J' M')$.—The matrix element of electric moment joining the pair of states characterized by $\gamma SLJM$, and $\gamma' S' L' J' M'$, respectively.

Polyad.—A set of terms of the same multiplicity based on the same parent term in the case of the addition of one electron to a parent ion.

Line.—Radiation resulting from all transitions between two levels.

Multiplet.—Radiation resulting from all transitions between two terms.

Supermultiplet.—Radiation resulting from all transitions between two polyads.

Transition array.—Radiation resulting from all transitions between two configurations.

Strength.—Sum of the absolute squares of the matrix elements of electric moment joining the sets of states in question. The intensity of a single line is proportional to the product of the number of atoms in each state of its initial level, the fourth power of its frequency, and its strength.

INDEX TO TABLES OF RELATIVE MULTIPLY STRENGTHS

No. of Electrons	Transition Array	Table	No. of Electrons	Transition Array	Table
2	ps-p.p	XIV	5	p ^s -p ^s s	XV
	p.p-pd	X		p ^s -p ^s d	XV
	p ² -ps	XIV		d ³ s.s-d ³ sp	VII
	p ² -pd	XIV		d ³ s ² -d ³ sp	IV
	pd-pf	XIV		d ⁴ s-d ³ sp	II
	ds-dp	IV		d ⁴ s-d ⁴ p	IV
	dp-d.d	VI		d ⁴ p-d ⁴ d	VII
	d ² -dp	I		d ⁵ -d ⁴ p	I
3	p ² s-p ² p	VI	6	d ⁴ s.s-d ⁴ sp	V
	p ² .p-p ² d	X		d ⁴ s ² -d ⁴ sp	VII
	p ² d-p ² f	XII		d ⁵ s-d ⁴ sp	II
	p ³ -p ² s	XV		d ⁵ s-d ⁵ p	IV
	p ³ -p ² d	XV		d ⁵ p-d ⁵ .d	VIII
	ds.s-dsp	V		d ⁶ -d ⁵ p	I
	dsp-ds.d	X	7	d ⁵ s.s-d ⁵ sp	V
	ds ² -dsp	IV		d ⁵ sp-d ⁵ s.d	IX, X
	d ² s-dsp	II		d ⁵ s.d-d ⁵ sf	XI, XII
	dp ² -dsp	XV		d ⁵ s ² -d ⁵ sp	VI
	dp ² -d ² p	III		d ⁶ s-d ⁵ sp	II
	d ² s-d ² p	IV		d ⁶ s-d ⁵ sf	XII
	d ² p-d ² .d	VIII		d ⁵ p ² -d ⁵ sp	XIII, XIV
	d ³ -d ² p	I		d ⁵ p ² -d ⁶ p	III
				d ⁷ -d ⁶ p	I
			8	d ⁷ s-d ⁶ sp	III
				d ⁸ -d ⁷ p	I
			9	d ⁸ s-d ⁷ sp	III
				d ⁹ -d ⁸ p	I
4	s ² p ² -sp ³	XIV	10	d ⁹ s-d ⁸ sp	III
	p ³ s-p ³ .p	VI			
	p ³ .p-p ³ d	X			
	p ³ d-p ³ f	XIV			
	p ⁴ -p ³ s	XV			
	p ⁴ -p ³ d	XV			
	d ² s.s-d ² sp	V			
	d ² sp-d ² s.d	X			
	d ² s ² -d ² sp	XVI			
	d ³ s-d ² sp	II			
	d ² p ² -d ² sp	XIV			
	d ² p ² -d ³ p	III			
	d ³ s-d ³ p	IV			
	d ³ p-d ³ .d	VI			
	d ⁴ -d ³ p	I			

TABLE I

TABLE II

TABLE II

TABLE III

Diagram showing relative multiplet strengths for various atomic transitions. The diagram consists of several interconnected nodes, each representing a specific atomic state. Each node contains a set of numbers (e.g., 4500, 4900, 5300) and a set of quantum numbers (e.g., 5s, 5p, 5s). The nodes are connected by lines, indicating transitions between states. The numbers represent relative strengths or intensities of the transitions.

TABLE III

TABLE IV

Diagram showing relative multiplet strengths for various atomic transitions. The diagram consists of several interconnected nodes, each representing a specific atomic state. Each node contains a set of numbers (e.g., 21, 15, 9) and a set of quantum numbers (e.g., 4f, 4d, 4p). The nodes are connected by lines, indicating transitions between states. The numbers represent relative strengths or intensities of the transitions.

[illegible]

TABLE VII

TABLE VIII

TABLE VIII

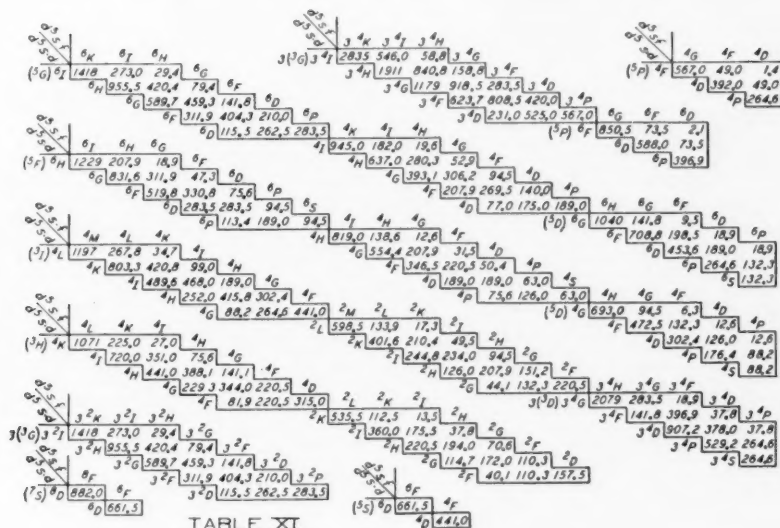


TABLE XI

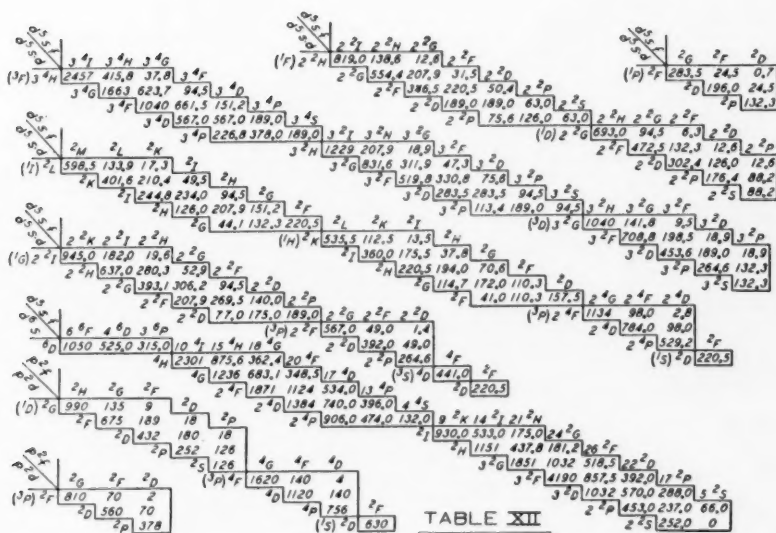


TABLE XII

Handwritten mathematical work showing a series of calculations, likely related to a cryptographic or mathematical problem. The work is organized into several columns and rows, with numbers and symbols (such as α , β , γ , δ , ϵ , ζ , η , θ , ι , κ , λ , μ , ν , ξ , \omicron , π , ρ , σ , τ , υ , ϕ , χ , ψ , ω) used to denote variables or constants. The calculations involve arithmetic operations (addition, subtraction, multiplication, division) and are often grouped by brackets or subscripts. The work is dated 1909 and includes a signature "J. P. (20)".

TABLE XIII

TABLE XIV

TABLE XV

Diagram illustrating the relative multiplet strengths for various atomic configurations, showing energy levels and transitions. The configurations include $d^2(p_L) + sp(p_L) \rightarrow d^2(p_L) + p^2(s)$, $d^2(p_L) + sp(p_L) \rightarrow d^2(p_L) + p^2(p)$, $d^2(p_L) + sp(p_L) \rightarrow d^2(p_L) + p^2(s)$, $d^2(p_L) + sp(p_L) \rightarrow d^2(p_L) + p^2(p)$, $d^2(p_L) + sp(p_L) \rightarrow d^2(p_L) + p^2(s)$, $d^2(p_L) + sp(p_L) \rightarrow d^2(p_L) + p^2(p)$, $d^2(p_L) + sp(p_L) \rightarrow d^2(p_L) + p^2(s)$, $d^2(p_L) + sp(p_L) \rightarrow d^2(p_L) + p^2(p)$, $d^2(p_L) + sp(p_L) \rightarrow d^2(p_L) + p^2(s)$, $d^2(p_L) + sp(p_L) \rightarrow d^2(p_L) + p^2(p)$.

TABLE XVI

Diagram illustrating the relative multiplet strengths for various atomic configurations, showing energy levels and transitions. The configurations include d^2s-s and d^2s^2 .

Erratum.—The configurations d^2s-s and d^2s^2 in Table XVI should be interchanged.

MEASUREMENT OF THE VELOCITY OF LIGHT IN A PARTIAL VACUUM*

By A. A. MICHELSON,¹ F. G. PEASE, AND F. PEARSON

ABSTRACT

The observations were made by the rotating-mirror method, the light passing through a steel tube 1 mile long, evacuated to pressures which ranged from 0.5 to 5.5 mm mercury. By multiple reflections the path length was increased to 8 or 10 miles.

The distance was obtained by reference to a carefully measured base line adjoining the tube.

The time was measured stroboscopically through successive steps by use of a tuning fork synchronized with the rotating mirror, a free swinging pendulum, a chronometer, and wireless signals from Arlington.

There were made 2885.5 determinations of the velocity, the simple mean value of which is 299,774 km/sec., with an average deviation of 11 km/sec. from the mean.

INTRODUCTION

The following is a report on the measurements of the velocity of light made at the Irvine Ranch near Santa Ana, California, during the period September, 1929, to March, 1933. The undertaking was proposed and planned by A. A. Michelson, professor of physics at the University of Chicago and research associate of the Carnegie Institution. Professor Michelson also obtained the funds for the project and lived to see the apparatus installed but was unable to take part in the measurements, which were carried out by F. G. Pease, of the Mount Wilson Observatory, and F. Pearson, of the University of Chicago.

It will be recalled that a series of measurements of the velocity of light had been made between Mount Wilson and Mount San Antonio in 1924-1926 which gave a value of 299,796 km/sec.² Since the internal agreement of these measures was good, some explanation is desirable as to why it was thought necessary to repeat the experiment at the Irvine Ranch. The measurements involve two distinct

* *Contributions from the Mount Wilson Observatory, Carnegie Institution of Washington*, No. 522.

¹ Dr. Michelson died on May 9, 1931, when 36 of the 54 series of 1931 observations had been completed.

² *Mt. W. Contr.*, No. 329; *Ap. J.*, 65, 1, 1927.

MEASUREMENT OF THE VELOCITY OF LIGHT IN A PARTIAL VACUUM*

By A. A. MICHELSON,¹ F. G. PEASE, AND F. PEARSON

ABSTRACT

The observations were made by the rotating-mirror method, the light passing through a steel tube 1 mile long, evacuated to pressures which ranged from 0.5 to 5.5 mm mercury. By multiple reflections the path length was increased to 8 or 10 miles.

The distance was obtained by reference to a carefully measured base line adjoining the tube.

The time was measured stroboscopically through successive steps by use of a tuning fork synchronized with the rotating mirror, a free swinging pendulum, a chronometer, and wireless signals from Arlington.

There were made 2885.5 determinations of the velocity, the simple mean value of which is 299,774 km/sec., with an average deviation of 11 km/sec. from the mean.

INTRODUCTION

The following is a report on the measurements of the velocity of light made at the Irvine Ranch near Santa Ana, California, during the period September, 1929, to March, 1933. The undertaking was proposed and planned by A. A. Michelson, professor of physics at the University of Chicago and research associate of the Carnegie Institution. Professor Michelson also obtained the funds for the project and lived to see the apparatus installed but was unable to take part in the measurements, which were carried out by F. G. Pease, of the Mount Wilson Observatory, and F. Pearson, of the University of Chicago.

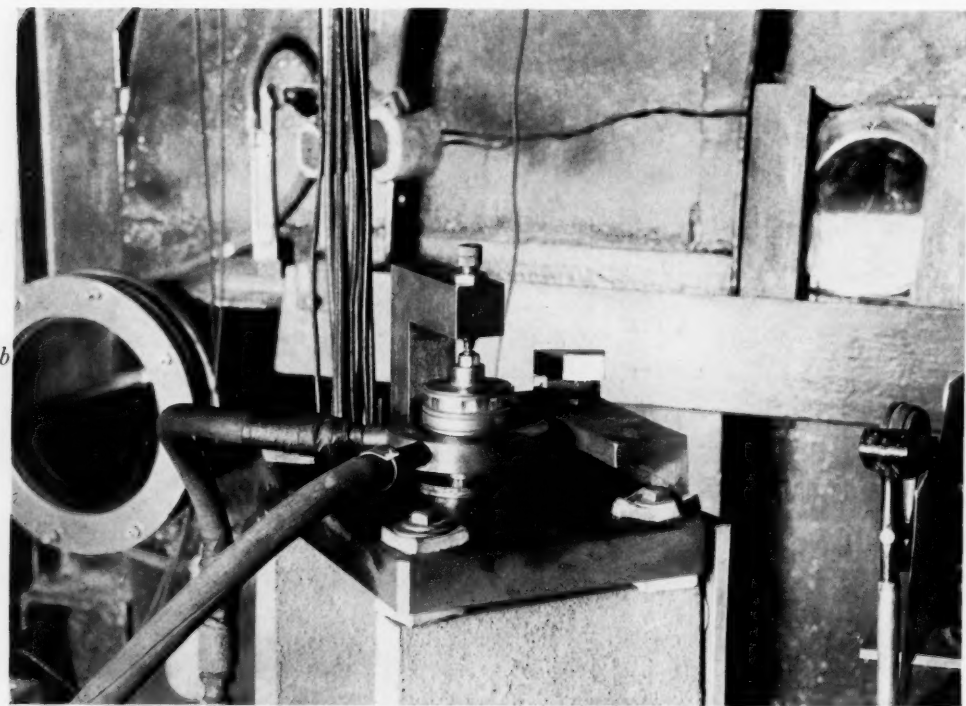
It will be recalled that a series of measurements of the velocity of light had been made between Mount Wilson and Mount San Antonio in 1924-1926 which gave a value of 299,796 km/sec.² Since the internal agreement of these measures was good, some explanation is desirable as to why it was thought necessary to repeat the experiment at the Irvine Ranch. The measurements involve two distinct

* *Contributions from the Mount Wilson Observatory, Carnegie Institution of Washington*, No. 522.

¹ Dr. Michelson died on May 9, 1931, when 36 of the 54 series of 1931 observations had been completed.

² *Mt. W. Contr.*, No. 329; *Ap. J.*, 65, 1, 1927.

PLATE I



a) VACUUM PIPE LINE AND OBSERVING ROOM
b) THE ROTATING MIRROR

elements: first, the time; and, second, the distance. It was estimated that with a rated tuning fork and stroboscopic methods the time of rotation of the mirror could be measured to one part in a million. The time element could therefore be determined with sufficient accuracy.

In the 1924-1926 experiments the determination of the distance required the measurement of a long base line and an extended triangulation from this base into the mountains. Since the Observatory was not prepared to carry out this part of the work, the United States Coast and Geodetic Survey kindly consented to undertake it. Although the splendid work of the Survey in the resulting investigation³ had never been excelled, it was felt that the direct measurement of a short base line, without subsequent triangulation, might yield an even higher order of accuracy. Moreover, there was the fact that the results for the velocity of light depend upon the refractive index of the air between the stations, about which little is known except that the total effect is small. The use of a vacuum tube a mile long would eliminate this factor and have the added advantage of giving a small, well-defined image, unaffected by atmospheric disturbances. By allowing the beam of light to traverse the tube eight or ten times, the length of path would be such that the speed of the rotating mirror need not be excessive.

Funds for repeating the investigation with these improvements were generously supplied to the University of Chicago and the Mount Wilson Observatory by the Rockefeller Foundation and the Carnegie Corporation. Through the courtesy of Mr. James Irvine, Jr., a level, unobstructed site on the Irvine Ranch near the city of Santa Ana, California, was selected for the location of the vacuum tube. Preliminary experiments late in 1929, on a tube 1100 feet long, gave results which were so promising that the construction of the mile-long tube was begun in the winter of 1929-1930 (Pl. Ia).

The United States Coast and Geodetic Survey was again called upon for three successive years to determine the length of the new base line, this time a simple distance between two points about a mile apart. The mean result obtained in these measurements by

³ A detailed account by William Bowie is given in the *U.S.C. and G.S. Report of Geodetic Observations*, 1923.

Commander Garner and Lieutenant Latham, as furnished by the Coast Survey, is 1594.2658 m.

The simple mean of all the readings for the velocity of light is 299,774 km/sec. *in vacuo*. Since the values fluctuate somewhat with the time, this mean may differ slightly from what would be obtained if observations were made continuously over an extended period. Series of measures 1-13 and 26-54, made from February 20 to July 14, 1931, gave 299,775 km/sec. Series 14-25, made from March 25 to April 3, 1931, gave 299,746 km/sec. The fact that these mean results differed from each other and from the value 299,796 km/sec. obtained on Mount Wilson necessitated additional readings.

Further readings made from March 3 to August 4, 1932, gave a mean value of 299,775 km/sec. If, however, the readings be divided into two groups with an equal number of individual determinations of the velocity, series 55-110 give a value of 299,780 km/sec., while series 111-158 give 299,771 km/sec.

Readings were resumed in December, 1932, giving a mean high value of 299,785 km/sec., which dropped to a mean of 299,765 km/sec. on January 15 and rose again to the earlier value on February 28. The mean velocity for the 75 series was 299,775 km/sec.

Attempts to explain these variations in velocity as a result of instrumental effects have not thus far been successful.

DESCRIPTION OF APPARATUS

Optical layout.—A diagram of the optical arrangement of the apparatus is shown in Figure 1. Light from an arc lamp *A* was imaged on the slit *C* by the condensing lens *B*. For the first 46 series of the 1931 observations it passed above the right-angle prism *I* to the upper half of the rotating mirror, *D*, thence through the plane-parallel glass window *L* into the tube to the diagonal flat *E* and the concave mirror *F*. It next passed above the flat mirror *H* and then, by means of repeated reflections at the flat mirrors *G* and *H* until the desired distance had been traversed, formed on the surface of *G* or *H* a magnified conjugate image of the slit *C*. The beam then retraced its path directly below the incoming path and emerged from the tube, striking the lower half of the rotating mirror *D*; it then passed through the reflecting prism *I* onto the crosswires *J* and was observed in the eyepiece *K*.

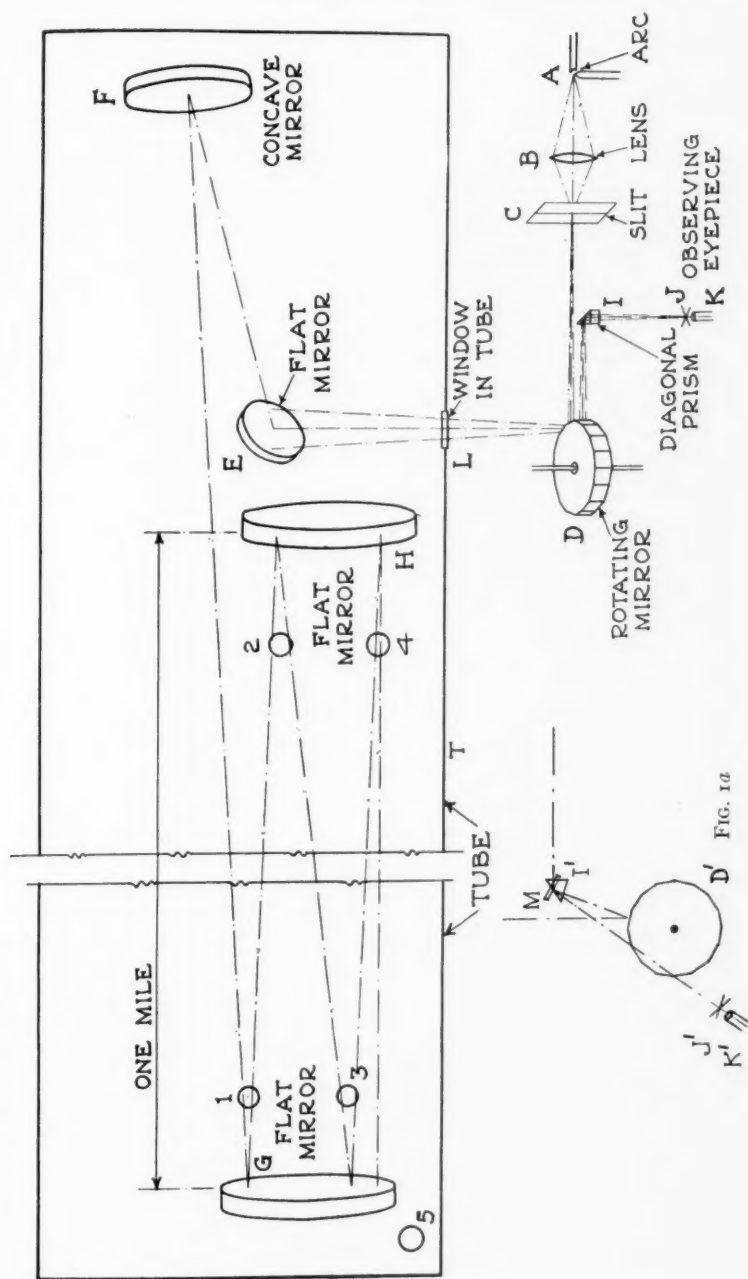


FIG. 1.—Diagram of optical system

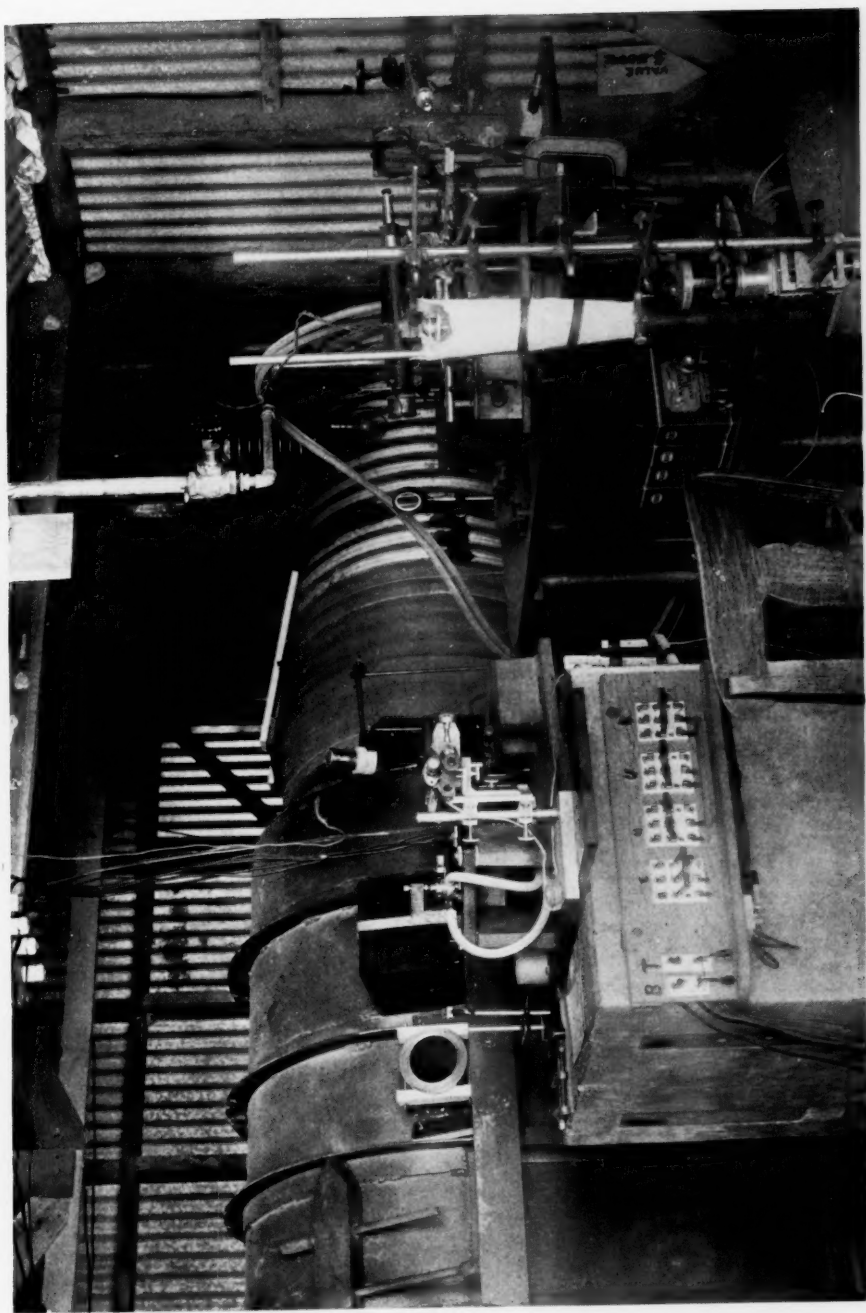
For series 47-54, to eliminate the effect of any lateral shift of the rotating mirror, the light after passing through the slit entered the 90° prism I' (Fig. 1a) and was reflected to the lower half of the rotating mirror at nearly perpendicular incidence, thence into the tube of the flat mirror at an equivalent distance of 4 or 5 miles. The returning beam struck the upper half of the rotating mirror and was then reflected by the silvered surface M , which stands directly above the 90° prism, onto the crosswires J' and into the eyepiece K' . Since the advantages of this setup were found to be negligible, the original arrangement of the prism (Fig. 1) was used in the 1932 and 1933 measures. It was originally intended to pass parallel light from F to G and H , thence under G to a concave mirror about 51 feet beyond it, which would converge the light onto a small concave mirror and thus form a system similar to that used in the Mount Wilson-San Antonio experiments. This auto-collimating system was used in the earlier work because it requires no delicate adjustment, whereas, without the auxiliary mirrors, the flat must be kept accurately aligned.

Actual observations showed, however, that the light returned from the conjugate image was brighter than that given by the auto-collimating system; the former arrangement was therefore used throughout the experiments.

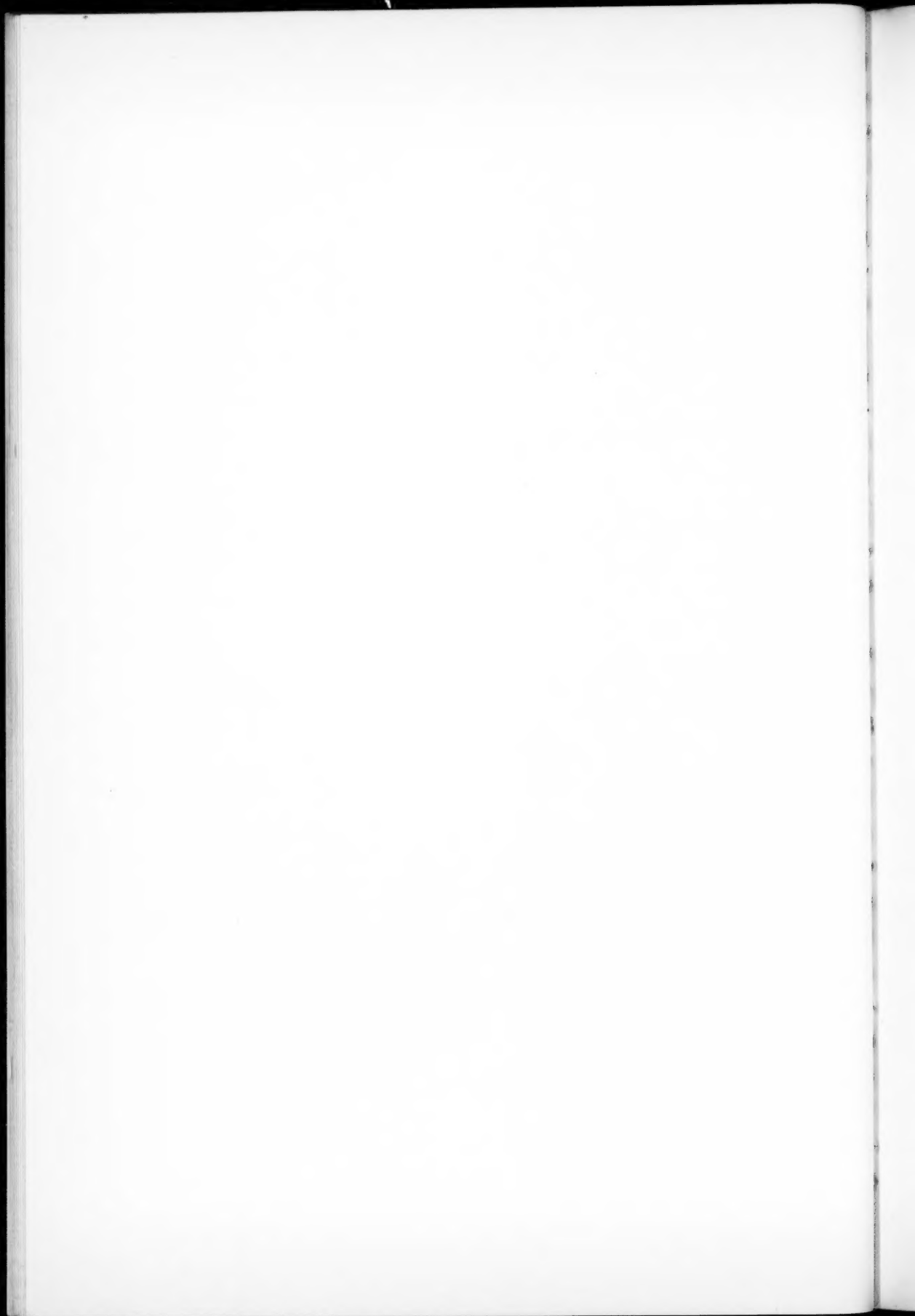
The vacuum tube T (Figs. 1 and 2) is 3 feet in diameter and approximately a mile long. The pipe is interrupted at H and G (Fig. 2) by steel tanks which house the 22-inch flats and ended at R and N by tanks containing the concave mirrors.

All operations were conducted from the observing room at H (Fig. 2 and Pl. II). Here the optical axis was located about 5 feet above the floor, and in the 1931 experiment the slit, condensing lens, rotating mirror, air controls, etc., were mounted outside the tube on a metal table bolted to the cement floor. In the 1932-1933 experiments the slit, prism, rotating mirror, and observing eyepiece were mounted on a heavy cast-iron base, fastened to a solid concrete pier. The pier, together with the metal table and the pendulum case, was fastened to a single massive concrete pier 3 feet thick, whose top lay flush with the floor. The arc lamp, which stood outside the observing room, was surrounded by a metal shield, provided with

PLATE II



INTERIOR OF OBSERVING ROOM



red-glass window for observing the arc itself. A blackened tube extended from the wall to the condensing lens, and the use of a small aperture, about 0.5 inch square, at the inner end of the tube eliminated much of the undesirable light.

To assist in lining up the mirrors, small 6-volt lamps were inserted at 1, 2, 3, 4, and 5 (Fig. 1). Lamps 1 and 3 were placed 100 feet in front of the *N* 22-inch flat and opposite the centers of the upper and

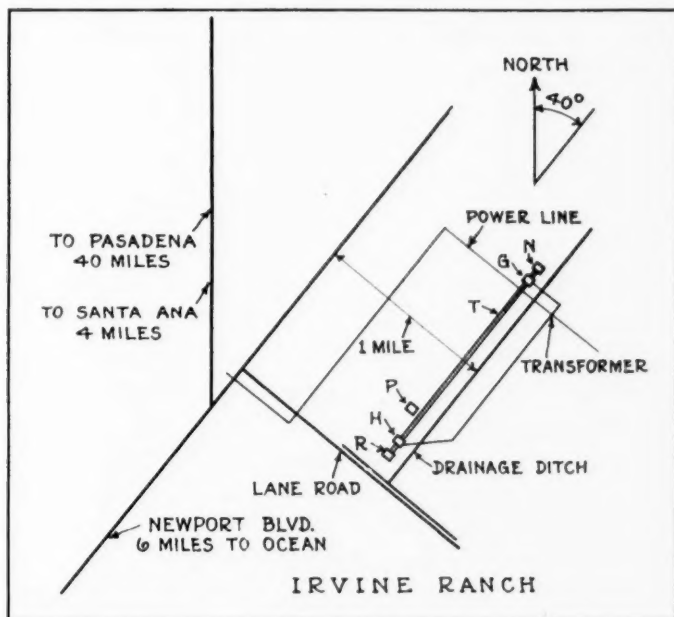


FIG. 2.—Plan of experiment

lower halves, respectively, of the mirror. Lamps 2 and 4 were similarly placed in front of the *S* 22-inch flat. Lamp 5 was opposite the center of the *N* concave. Lamps 1 and 3 and 2 and 4 were mounted on semaphore arms (electric windshield-wipers) which could be swung into position when needed for aligning. The arc lamp *A* (Fig. 1) was a Mole-Richardson semi-automatic projection lamp, using National cored carbons. It operated on 110 volts and 40 amperes. The arc ran steadily over long periods of time, needing only occasional adjustments by the attendant. The slit *C* (Fig. 1) was adjustable horizontally and vertically and racked for focus. The

slit aperture was limited vertically by occulting bars; the slit width was about 0.003 inch.

The rotating mirror *D* (Fig. 1 and Pl. Ib) used in these experiments is of well-annealed optical glass and has 32 faces. It is 0.25 inch thick and 1.5 inches across its diagonals and has a central hole to define its position on the axis. Its angles are correct to 1"0 and its surfaces flat to 0.1 wave. The operating aperture in each direction is 9/64 inch wide and 1/8 inch high. The mounting is one of those used in the Mount Wilson-San Antonio experiments having compressed-air turbine drive capable of rotation in either direction. A slight amount of oil suffices to lubricate the plain journal bearings and the single-ball step-bearing below.

The plane-parallel window *L* is of crown glass 6 inches in diameter and 0.75 inch thick. At first cemented to the tank flange, it was later held by clamps and atmospheric pressure against a rubber gasket. The diagonal flat mirror *E* is 5 inches in diameter and 0.5 inch thick. It has motor-driven slow motions about vertical and horizontal axes. The concave mirror *F* is of glass, 40 inches in diameter and 3.9 inches thick, and has a focal length of 49.28 feet. It is covered with a cardboard screen having an elliptical aperture 12×15 inches. The mirror and its mounting were built for the Mount Wilson-San Antonio experiment. The mounting is of cast-iron, in two sections. The lower ribbed base frame rests on three legs, the front one of which is adjustable by motor, which tilts the mirror about a horizontal axis at right angles to the tube axis. The base stands on three cylindrical steel plugs, set in a pier separate from that holding the tank and projecting through three holes in the bottom of the steel tank. Rubber sleeves connecting the tank and the cylinders form a flexible, air-tight joint, thus leaving the mirrors free from any motion the tank itself might have. The upper section of the mounting rests on three balls and has a slow motion in rotation about a vertical axis directly under the face of the mirror. The mirror is held in its cell by three pivoted edge-arcs, the top one having spring contact to prevent excessive loading. Three tangential grooves in the edge of the mirror fit corresponding lugs in the edge-arcs.

The flat mirrors *G* and *H* are $22\frac{3}{8}$ inches in diameter and 4 and 5

inches thick, respectively, and are adjustable about horizontal and vertical axes. The details of the mountings are similar to those of the concave mirrors already described. It was found that the silver coatings of the mirrors deteriorated rapidly; Dalton, of the Observatory optical shop, succeeded in coating them with a very thin silver lacquer in such a manner that their optical properties were not impaired. The 90° prism *I* is blackened on its top surface and silvered and blackened on its diagonal face to prevent any unnecessary illumination in the field of view. For series 1-25 it was mounted directly on the rotating-mirror support, but for the remaining work it was mounted on a shelf attached to the table, thus eliminating displacements due to any possible turbine reaction. Later experiments showed that these displacements were negligible. The micrometer is a simple slide with a single vertical crosswire, moved by a screw of 40 threads per inch, the head of which is divided into 25 parts, making each division equal to 0.001 inch. An eyepiece of 2.5-inch focus was used. A 6-volt lamp with push-button control illuminated the head.

Vacuum pump.—For exhausting the 1100-foot tube, and for preliminary work with the 1-mile tube, a small Kinney rotating-plunger vacuum pump was used. This pump performed so well that in the final work a Kinney rotating-plunger pump of 350 cubic feet of free-air capacity driven by a 15-hp motor was used. These pumps have no internal packing, are oil sealed, and on a closed system produce a vacuum of 0.05 mm. The pump was connected with the tube by a 6-inch steel pipe and was fitted with an automatically controlled check valve to prevent oil from passing into the tube when the pump accidentally stopped. A gate valve, placed at the outer end of the pipe, allowed air to enter the tube when it was necessary to let down the vacuum.

The compressed-air system.—To drive the turbines of the rotating mirror, compressed air at a pressure of 100 lb. was supplied by an ordinary motor-driven compressor. The air was piped to a tank outside the operating room, thence to the valve on the operating table.

The regulating valve *V* (Fig. 3) is an escape valve, consisting of a chamber with an open top fitted with a flat plate with ground sur-

face. A V-socket in the top of the plate holds a $\frac{1}{4}$ -inch ball, across which extends a lever held in compression by a spring. The least upward lift by the operator changes the nearly balanced pressures and allows a slight escape of air. After passage through the valve and regulator, the air stream branches, running to the *R* and *L* turbines in the rotating mirror.

Electrical system.—Power is obtained from a high-tension A.C. line which crosses the tube about 4000 feet from the *S* end, where it is stepped down to 110–220 volts and feeds a line paralleling the tube. The power plant located at *P* (Fig. 2) houses the vacuum pump, the air compressor, and the 6-kw motor-generator set supply-

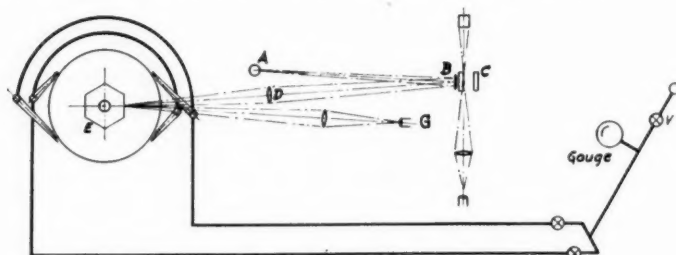


FIG. 3.—Diagram showing mirror speed control

ing current to the arc. All the mirror slow motions are operated by the observer at the micrometer. Those at the *S* end are handled by direct switches. Those at the *N* end are worked by a common push-button line, the proper contact being made through a selector operated by a Selsyn motor.

Pipe.—The pipe is of 14-gauge galvanized Armco steel sheets, 26 inches wide, rolled and corrugated and then formed into sections 60 feet long. The longitudinal seams are double riveted, the circumferential seams single riveted, and all of them soldered. The sections are mounted on wooden trestles shown in Plate Ia and make contact on shoes at the bottom, at 45° , and at the sides.

The pipe sections, *A–A* are separated about an inch, each joint being treated as shown in Figure 4. Over each junction was placed a rolled sheet of 12-gauge galvanized iron 8 inches wide, forming a sleeve *B* whose overlapping ends are bolted to the two ends of the pipes with loosely fitting stove bolts.

Two pieces of canvas *C*, 11 inches wide, were placed over the sleeve, the inner one tied with a large rope *D* to fill the groove and the outer one with string. A 32×6 -inch circular molded inner tube *G*, previously slit along its inside circumference and stretched over the end of one of the pipe sections away from the canvas, was then drawn over the canvas so that it extended about 2 inches beyond either edge. The edges of the rubber tube were rolled back a few inches and the steel pipe and the inner side of the rubber smeared with rubber cement. The rubber was then rolled flat, smeared for an inch or two with cement, and the joint then wound with several laps of friction tape *H* and coated with glyptal. In the earlier trials the rubber tube

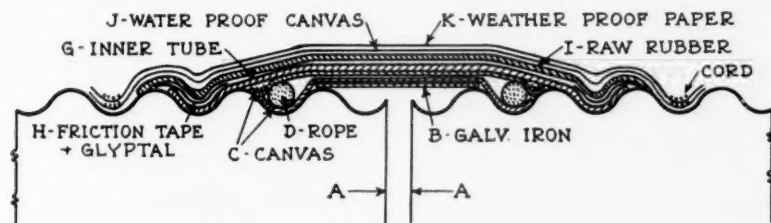


FIG. 4.—Cross-section of pipe joint

was then directly covered with canvas, but later it was smeared with cement and then covered with a sheet of raw rubber *I*, 15 inches wide, which becomes tacky with heat and closes any cracks occurring in the inner tube. Waterproof canvas *J* and a sheet of weatherproof paper *K* form the outer covering, each tied with stout cord. After completion the seams and joints were painted with glyptal to seal any leaks which might occur in them.

Four manholes give access to the tube, one at each end between the 22-inch flats and the concaves, and two others in the main section of the tube.

Tanks.—The four tanks housing the mirrors and their mountings within the vacuum tube are constructed of $\frac{3}{8}$ -inch steel plate, reinforced with appropriate steel sections welded on. The tanks consist of a flat base plate and a removable upper box section, fitting into a groove in the base, which is sealed only with a strip of solder serving as gasket and with Hydroseal. No bolts are used to tie the sections together. The base is a $\frac{5}{16}$ -inch flat steel sheet, reinforced with 8-

inch *I*-beams and stands on four small concrete piers. The upper sections are rectangular in shape up to the optical axis and semi-cylindrical above that. Openings in the ends, with flanges 3 feet in diameter and 1 foot long, make the standard flexible connection with the pipe.

The concave mirror tanks *R* and *N* (Fig. 2) are 4 feet and 4 inches long, 5 feet and $\frac{1}{2}$ inch high, and 4 feet and 6 inches wide, inside measure. The outer ends are fitted with steel drumheads, 3 feet in diameter and 9 inches long, which are joined to the tank with the standard wrapping and supported by a steel frame on two separate piers. Two $\frac{7}{8}$ -inch diameter rods about 15 feet long tie these heads to plates sunk about 4 feet underground. Turnbuckles adjust the heads when the 7-ton air pressure is removed from the tube.

The flat mirror tanks *H* (Pl. II) and *G* (Fig. 2) are 6 feet long, 3 feet and 8 inches wide, and 5 feet and 7 inches high inside. A port-hole 8 inches in diameter, at a point opposite the face of the 22-inch flat mirror, permits a transfer of measures from the mirror systems inside the tube to the measured-mile piers outside. Tank *H* has an additional port through which the light passes to and from the rotating mirror. A 4.5-inch i.d. sleeve with a turned outer flange is welded to the tank, the outer end being inclined 10° so that multiple reflections from the window do not interfere with the working beams.

The mirrors and their mountings are those used in the previous velocity experiments, altered to fit the new arrangement and equipped with motor mechanisms for adjustment, all of which are controlled by the observer at the micrometer eyepiece.

SYSTEMS OF MEASUREMENT

Measurement of time.—In velocity-of-light measures made previous to the Mount Wilson-San Antonio experiment the outgoing and return beams were reflected from the same face of the rotating mirror. The return image could always be observed by shifting the eyepiece sideways. In the null method used in the Mount Wilson-San Antonio, and in the Irvine Ranch experiments, the light emerges from one face and is received on some other face—the adjacent face in the Irvine experiment. As the mirror starts rotating, the image gradually passes from the field of view and reappears in

the other side of the field only when the rotating mirror is approaching its proper speed.

While several methods are available for measuring the velocity of light with this arrangement, the one chosen is as follows: The rotating mirror is brought into synchronism with a tuning fork whose period of vibration is determined; the position of the image is then read with a micrometer for the right- and left-hand rotations of the mirror. The distance remains fixed. The time interval to be measured is therefore that during which the rotating mirror turns $1/32$ revolution, plus or minus a small angle derived from the readings of the micrometer. The period of the fork is determined by stroboscopic methods in terms of free-pendulum beats. Since the period of the tuning fork varies with temperature, comparisons between the fork and the pendulum are made before and after each set of readings. The true time of the pendulum beats was determined before and after each annual series of experiments.

Mirror-speed control.—The light from a 6-volt lamp *A* (Fig. 3), after striking the small mirror *B* on the tuning fork *C*, was imaged by the small achromatic lens *D* on the one polished face of the nut *E*, which clamps the rotating mirror to its shaft. Since the fork stood vertically, the image vibrated up and down on the nut. The focal length of the lens *D* was such as to give sufficient amplitude to the motion of the image. Since the nut rotated in a horizontal plane, the image, as the mirror speeded up, passed through a series of vibrating and stationary states and finally reached a permanent stationary state when the beats heard between the fork and the rotating mirror ceased. At this point a second observer made a setting on the return image and a reading of the micrometer. A reversal of the direction of motion of the mirror eliminated any necessity for making a zero reading.

The observer at the eyepiece *G* (Fig. 3) controlled the air supply to the mirror turbines by means of the regulator *V* already described. The tuning-fork period was adjusted as follows: The light-path was first measured with an ordinary tape. The best available value of the velocity of light divided by thirty-two times this distance gave the whole number of vibrations of the fork per second (*N*). A fork having a slightly greater period of vibration was selected and filed off

until it was very close to the desired pitch. The fork was then mounted in its frame and, while the mirror was rotating in synchronism with it, micrometer readings were made for right and left rotations. This procedure was repeated until the pitch of the fork, as indicated by the small difference between the right and left read-

ings, was a trifle high. The final correction was made by adding a small lump of universal wax to each prong.

Fractional number of beats of the tuning fork.—Light from a filament lamp *A* (Fig. 5) was focused on a narrow slit *C* and reflected into the pendulum case, whence it was returned by the mirror *F* on the pendulum and focused by the achromatic lens *D* on an edge of tuning fork *I*. When the fork was vibrating, the flashes of light from the pendulum illuminated the fork in various positions and showed to an observer at the telescope *J* a series of sawtooth images. When the period of the fork was an exact multiple of that of the pendulum, the images as seen against a pointer in the field of view appeared stationary. When the period differed

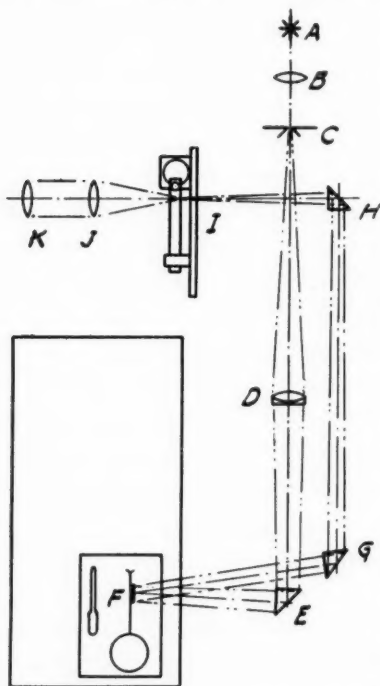


FIG. 5.—Stroboscopic timing system showing pendulum and fork.

from an exact multiple, the teeth appeared to travel across the field of view. Cognizance was taken of the flashes in one direction only; when the images traveled in the same direction as the flash, the fork was losing on the pendulum and the sign of the fractional correction was minus. If the image traveled against the flashes, the sign was plus. If n denotes the number of flashes occurring during the passage from one tooth to the next, the fraction $\pm 1/n$ added to the whole number N gave the period of the fork in terms of the free pendulum.

True period of free pendulum.—The determination of the period of the free pendulum in terms of mean solar time was made in two steps: first, a comparison of beats between the pendulum and a flash box operated each second by a contact-making chronometer; second, a comparison of the chronograph records of second marks from the chronometer with signals (1931 by hand, 1932–1933 by self-recording wireless) recording true time sent by long-wave wireless from Arlington four times each day. This determination was made several times during 1931 and before and after each experiment in 1932–1933, temperatures of the pendulum box and the time intervals being recorded. Since the period of the pendulum varies slightly with the length of swing, readings were taken for several lengths of swing and interpolations made for other swings. The pendulum is one of those formerly used by the United States Coast and Geodetic Survey in the determination of gravity. It is set in motion by an outside lever, swings in a vacuum chamber, and beats half-seconds. Its knife-edges are of agate, rocking on a flat agate plate. When not in operation it rests on auxiliary edges. On the pendulum near its point of suspension and on the shelf which carries it are mounted small speculum-metal mirrors. A dummy bob hangs inside the case carrying a thermometer. The box is of heavy bronze and is provided with adjusting screws and levels. Windows permit observation of the graduated arc and the thermometer and allow the passage of light to and from the mirrors. Consistent readings could not be obtained with the pendulum in 1931, but its inclosure in a constant-temperature case in 1932–1933 eliminated this difficulty. Throughout the experiment the pendulum case was connected with the main vacuum tube.

The flash box used for comparing beats of the pendulum with those of the chronometer consists of a rectangular box and a laboratory telescope mounted on a stand. In the forward end of the box is a 6-volt lamp, a slit, and a shutter, operated by relay with the 6-volt contact circuits of the clocks and controlled by a trigger mechanism which works with great rapidity, giving flashes of very short duration. The images of the slit reflected from the two small mirrors in the pendulum case are seen in the telescope together with a scale on glass placed at the focus. The flash box is usually placed at a

given distance from the pendulum box, and the stationary pendulum mirror is adjusted to bring the two images close to one another in the eyepiece field.

The object of the flash box is to determine the times of coincidence between the beats of the pendulum and the chronometer. When the pendulum is started, the chances are that only the fixed-mirror flash will be seen. In a few moments the second image will appear flashing, say in the bottom of the field, and gradually approach the center. When the images are in coincidence, the time indicated by the chronometer is noted. At approximately half the period the moving image appears at the top of the field, and when the down coincidence occurs, the time is noted. The comparisons are continued until coincidences have been obtained over the whole range of temperatures covered by the experiment.

Since the time of vibration depends upon the length of arc of the swing, readings are taken both for the maximum swing and for about one-half the maximum.

If n be the number of seconds between coincidences, then $n/(n \pm 1)$ is the time of one vibration of the pendulum in chronometer seconds, the plus sign being used if the flash travels in a direction opposite to that in which the pendulum swings, and minus if the two travel together. With the apparatus used the pendulum beat faster than the chronometer, and the period of coincidence was roughly 18 minutes.

Two timepieces were used, one a Bond ship's chronometer beating seconds on the relay and missing every fifty-ninth second. The rate was quite constant for a period of 24 hours following its winding. The other was a Constant Frequency Assembly of General Radio make (used late in 1931 only), controlled by an oscillating quartz crystal whose period $50,000\sim$ was reduced through two multi-vibrators to $1,000\sim$. A unipolar motor of $1,000\sim$ drives a shaft at 10 r.p.s., operating a seconds relay and a synchro-clock. (The rate of this clock was distinctly more constant than that of the chronometer.) The chronograph was a small one of Henson make, driven by a phonograph synchronous motor at a paper speed of 1 inch per second. In 1931 two ink pens were supplied, one operated by the

clock circuit beating seconds and the other by hand. In 1932-1933 the records were traced on paraffined paper by self-recording styli.

Time of light-transit.—Let a_1 and a_2 be the right and left readings of the micrometer and r the distance from the mirror to the cross-wires. Then the small angle by which the rotating mirror differs in position from $1/32$ revolution is

$$\frac{a_1 + a_2}{4r} = \frac{a}{4}.$$

If $1/n$ be the period of the optical beats between the fork and the pendulum and $1/\nu$ that of the coincidence between the pendulum and the true seconds, and if N be the nearest whole number of the fork, then the correct time elapsed during the passage of the light from the rotating mirror through the tube and back is

$$T = \frac{\frac{2\pi - a}{32} \frac{a}{4} (1 - \nu)}{2\pi(N + n)},$$

which reduces to

$$\frac{\left(1 - \frac{4a}{\pi}\right) (1 - \nu)}{32N \left(1 + \frac{n}{N}\right)}.$$

Putting

$$\frac{4a}{\pi} = a, \quad \frac{n}{N} = b, \quad \nu = c,$$

the formula becomes

$$T = \frac{(1-a)(1-c)}{32N(1+b)}.$$

Measurement of distance.—After a conference with Commander C. L. Garner, assistant chief of the Division of Geodesy of the United States Coast and Geodetic Survey, it was decided to lay out the base line about 10 feet to the west of the pipe and place six piers along the line.

Piers *E* and *B* (Fig. 6) are opposite the flats in tanks *G* and *H*, and *A* and *F* opposite the concaves in tanks *R* and *N*. Piers

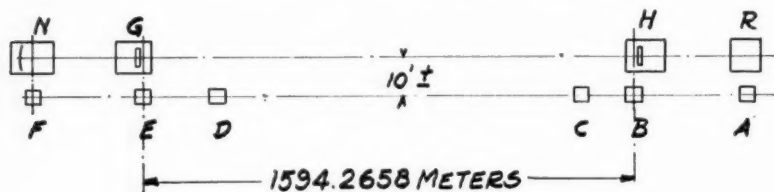


FIG. 6.—Plan of base-line piers

C and *D* were intended for use in triangulating into the tube but were not actually used. The mean length of this base line was found by the United States Coast and Geodetic Survey to be 1594.2658 m. The

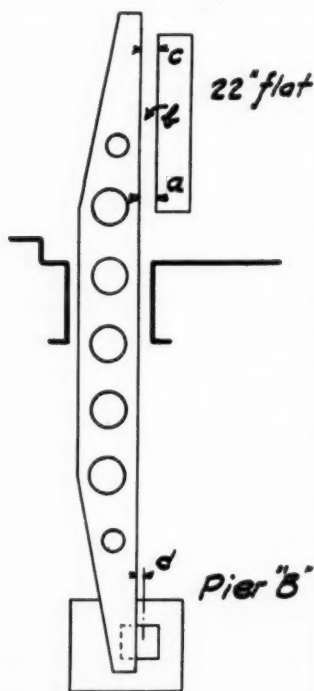


FIG. 7.—Diagram showing method of transferring mirror position to base-line pier.

transfer from the base line into the tube and the measurement of the internal distances were made by ourselves in the following manner: Before and after measuring the distance the alignment of the apparatus was carefully checked optically, with the arc on and the rotating mirror stationary, and intersecting marks were drawn on the small diagonal flat at the center of the cone of light. An excellent straight edge (Fig. 7) (used to align the tracks of the 50-ft. interferometer on Mount Wilson) 12 feet long was passed through the 8-inch diameter opening and supported on frames in a horizontal position. The straight edge was carefully adjusted parallel to the face of the flat by calipering at *a*, *b*, and *c*, and the separation *a* noted. A mercury plumb bob was then dropped from its edge and its position marked on the bronze plate in

the pier. The bob was rotated to determine its neutral position and allowance made for the thickness of the string. If *d* be the distance

of the bob from the bench mark, the simple summation $d \pm a$ gave the position of the south flat with respect to pier *B* and of the north flat with respect to pier *E*. The distance between the top of the *S* 22-inch flat and the center of the *S* concave was measured with a steel tape under 16.7-lb. tension, to which a steel scale was clamped to make contact with the concave. Temperatures were recorded and the mean of three readings taken as a correct one. This inclined distance was then corrected to give the horizontal distance between

TABLE I
LENGTH OF BASE LINE, PIERS *B-E*

Date	Observer	No. of Traverses	Distance in Millimeters
U.S. Coast and Geodetic Survey			
1931 Feb. 27—Mar. 2.....	Garner	9	1594259.2
1932 Jan. 11—Jan. 14.....	Latham	8	1594265.8
1933 Jan. 14—Feb. 17.....	Latham	31	1594272.3
Mean.....			1594265.8
Mount Wilson Observatory			
1933 July 17-20.....	Pease	8	1594263.8

the mirrors. The distance from the *S* concave to the small diagonal flat was measured with the same tape, tension, and scale. The addition of a trammel bar clamped to the tape at the end near the flat allowed its point to be adjusted to a center mark on the flat.

The distance from the small diagonal flat to the rotating mirror was taken through the window-opening by means of a trammel bar and measured on the tape. Corrections were then made for the path length through the glass 19.33 mm thick, at an inclination of 10° ($n_d = 1.52$) equivalent to a vacuum thickness of 29.39 mm. The air path outside the window was reduced to vacuum thickness by using 1.000295 as the index for air.

Table I gives the various results for the length of the base line as measured by the United States Coast and Geodetic Survey. The

data show a slight progressive increase in the means of each year's measures, which may be considered as a real change in the earth's surface. Interpolated values of the distance might have been used for the computations of the velocity of light, but, owing to large variations in the velocity results, it was thought that the simple mean value could be used without prejudice to the results. An earthquake which occurred on March 10, 1933, may explain the reduced value of the base line measured by Pease in July, 1933. Table II gives the various lengths involved in the light-path.

TABLE II
LENGTH OF LIGHT-PATH IN MILLIMETERS

Path	1931	1932	1932-1933
Rotating mirror to 5-in. diagonal corrected for air path.....	1661.3	1662.9	1661.9
5-in. diagonal to <i>S</i> concave.....	13092.7	13098.6	13102.2
<i>S</i> concave to <i>S</i> 22-in. flat.....	13714.1	13713.5	13716.8
D_1 =sum of above three.....	28468.1	28475.0	28480.9
<i>S</i> 22-in. flat to pier <i>B</i>	0.6	2.0	0.6
Pier <i>B</i> - <i>E</i> (mean).....	1594265.8	1594265.8	1594265.8
Pier <i>E</i> - <i>N</i> 22-in. flat.....	14.4	14.4	16.3
D_2 =sum of above three.....	1594280.8	1594282.2	1594282.7
$D_{10}=2D_1+10D_2$	15999744.2		
$D_8=2D_1+8D_2$	12811182.6	12811207.6	12811223.4

CALCULATION OF VELOCITY

The formula for calculating the velocity of light from the observed data is

$$V = \frac{D}{T} = \frac{32ND(1+b)}{(1-c)(1-a)},$$

or, with sufficient approximation, since b and c are small,

$$V = 32ND(1+a+b+c).$$

The presence of a slight residuum of air in the tube at temperature T necessitates a small correction e , whence the formula becomes

$$V = 32ND(1+a+b+c+e) = 32NDf.$$

The value of e is computed from the formula for the refractive index of air given in the *Smithsonian Physical Tables*:

$$n-1 = \frac{0.0002931 \times P' \times 1333.2}{1 + 0.00367t \times 1.0136 \times 10^6},$$

where P' is the pressure in millimeters of mercury and t the temperature in degrees centigrade. For the 10-mile distance a tuning fork giving 585 v.p.s. was used. For the 8-mile distance a fork was used, for which the whole number of vibrations was 365 or 366, N thus being either 2×365 or 2×366 . The various values of $32ND$ used in the experiment are shown in Table III.

TABLE III
VALUES OF $32ND$

Velocity	Vibrations per Second	1931	1932	1932-1933
V_{10}	585	299515.2
V_8	365×2	299269.2	299269.8	299270.2
V_8	366×2	300089.1	300089.7

METHOD OF OBSERVATION

With the pump running continuously, the vacuum remained approximately constant, the pressure ranging from 0.5 to 5.5 mm according to the amount of leakage. During the day the influence of the sun on the air in the tube was such as to distort and blend the several images corresponding to the various distances and thus prevent work at such times. After sundown the images improved rapidly and in a half-hour were easily separable from each other. The tuning fork was started in advance in order to give it a chance to warm up. The procedure in lining up the mirrors was as follows: With the arc lamp on, the outgoing beam from the rotating mirror was centered on the upper half of the S concave mirror by means of the 5-inch diagonal flat. The arc lamp was then cut off; lamp 1 was turned on and the concave mirror in the S end adjusted until the light appeared in the center of the field. The N 22-inch flat was then adjusted until the image of the lamp as seen in the mirror G ap-

peared superposed on the light itself. Next, lamp 2 was turned on, and a more careful adjustment of the *N* 22-inch plane was made in order to bring lamps 1 and 2 into superposition. Lamp 1 was then turned off, and the image of lamp 2 reflected from the *S* 22-inch flat was superposed on itself by adjusting the flat. Light 3 was next turned on and the *S* mirror again carefully adjusted to superpose lamps 2 and 3. When this had been done, lamps 3, 4, and 5 were all superposed. A number of images other than the one desired appeared in the field of view; but a study of their positions and foci soon showed which one was wanted.

This method of alignment was evolved when use of the *N* concave mirror was contemplated. It was found convenient to use the same method when adjusting for work without this concave, save that a small alteration in the inclination of the *S* 22-inch flat slightly raised the beam so that at the last reflection it fell with normal incidence on one or the other of the 22-inch flats. During all these operations the images were observed through the widened slit, which was then narrowed and placed in the observed focus of the light corresponding to the distance at which one wished to work. Since the field was divided, images also appeared in the eyepiece field. A slight adjustment of the 5-inch flat made the images in the eyepiece and behind the slit of equal intensity. The position of the image in the slit was carefully defined by occulting bars, and care was taken to line up the arc on the axis thus defined. When finally the arc was again turned on, the return light was visible in the eyepiece.

When the rotating mirror was set in motion, images corresponding to each of these reflections (because of diffusion and spreading of the beam) were seen in the field at distances from the crosswire proportional to the distance the light had traveled. Experience enabled one to make slight adjustments which concentrated the light in the image which was to be used. The apparatus was then ready for measurements. Observer A made a reading for the stroboscopic comparison of the fork and the pendulum (*n*), then read the temperature of the pendulum case (*t*). The mirror was then brought up to speed by manipulating the air control until the stroboscopic image was stationary. Observer B set the crosswire on the image and re-

corded the reading. In series 1-25 of 1931, 10 such readings were taken before the direction of rotation was reversed. To minimize the effect of a slight drift which had been noticed, subsequent readings (series 26-46, 1931) were made, 5 in the first direction, 10 in the opposite, and finally 5 more in the first direction. In series 47-54, 1931, 5 alternate sets of 5 readings were taken; the mean of 1 and 3 was used against 2, 2 and 4 against 3, and 3 and 5 against 4. The first readings of the successive group were alternately *L* and *R*. This method was used in all the remaining work except a few cases in which 7 sets were made. Observer A repeated the readings for *n* and *l* between each two sets, and the mean for the beginning and end of each set was used for the set.

Since the total angle measured was exceedingly small, the lever arm *r* was measured with an ordinary rule. Allowance was made for the prism thickness except for series 47-54 (1931), for which a mirror was used. Even with the vacuum as low as 0.5 mm, sufficient air remained in the tube to be affected by temperature conditions. The best images were obtained when a quiet fog settled around the tube, evidently providing a constant temperature throughout the tube. On days when the sun shone, the images drifted completely out of the field, usually returning again at night. A tube wet with dew gave comatic images when the wind blew. In 1931 it was noted that the interval during which work could be done became less and less as summer advanced, owing to the fading of the image and the necessity for constant readjustment. A satisfactory explanation for fading may be found in temperature deformations of the 22-inch flat glass mirrors which dispersed the light. In 1932 and 1933 it became the practice to work principally during the early hours of the night, since otherwise much valuable time during the interval of good observing conditions would be lost in resetting on the following night. A few observations were, however, made around midnight and 3:00 A.M.

Typical observation.—Table IV shows a typical set of observations, together with the values of the various factors calculated from the data. Columns 1, 3, and 5 give the micrometer readings made for a left-hand, columns 2 and 4 for a right-hand, rotation of the

mirror, the unit being $1/1000$ of an inch. Immediately below are their sums and mean values. The mean of the differences,

$$\frac{L_1+L_3}{2}-R_2, \quad \frac{R_2+R_4}{2}-L_3, \quad \frac{L_3+L_5}{2}-R_4,$$

shown farther below, gives the value of d in column 6 which is used to calculate $a=d/r$. Column 6 also lists the time of starting and various other data as follows: p is the pressure in the tube; n_b and n_e

TABLE IV
SAMPLE SET: OBSERVATIONS AND REDUCTIONS,
JUNE 30, 1932

(1) L	(2) R	(3) L	(4) R	(5) L	(6)
13.6	19.2	14.0	18.8	13.2	$N=365 \times 2$ $B \ 7:24 \text{ P.M.}$ $E \ 7:30$ $p \ 3.4 \text{ mm}$ $n_b \ 2/26 \ 0.07692$ $n_e \ 3/35 \ 0.08571$ 0.16263
13.8	19.6	14.2	18.9	14.2	
13.7	20.0	14.0	19.2	13.5	
13.4	19.9	13.1	19.5	13.6	
13.9	20.0	13.5	19.4	14.2	
68.4	98.7	68.8	95.8	68.7	$n + 0.08132$ $t_b \ 29^\circ.7, t_e \ 29^\circ.7, t \ 29^\circ.7 \text{ C}$ $s_b \ 4.1, s_e \ 4.1, s \ 4.1 \text{ mm}$ $r \ 11.80 \text{ in.}$ $d - 0.00571 \text{ in.}$ $a - .0006161$ $b + .0002228$ $c + .0008314$ $e + 0.0000012$ $f \ 1.0016715$ $V \ 299769.81 \text{ km/sec.}$
13.68*	19.74	13.76	19.16	13.74	
13.76	19.16	13.74			
13.72	19.45	13.75			
19.74	13.76	19.16			
- 6.02	- 5.69	- 5.41			
- 5.69					
- 5.41					
- 17.12					
- 5.71					

* Mean of five readings above.

the observed and n the mean value of the fractional number of vibrations of the fork; t_b and t_e the observed and t the mean temperature of the pendulum case; s_b and s_e the observed and s the mean swing of the pendulum; r is the measured distance from the rotating mirror to the crosswires, with corrections added for glass thickness when the prism is used. Values of $a=4a/\pi$, $b=n/N=n/365 \times 2$ are

calculated from the data. The value of $c = v$ is taken from the chart showing the true time of the pendulum beat for the mean temperature t and the swing s . The residual air correction e is taken from the chart showing the relation between n , p , and the tube temperature t ; f is the algebraic sum, $1 + a + b + c + e$, by which $32ND$ is multiplied to give the velocity V .

OBSERVATIONS

Table V shows two typical series of observations on successive nights. Column 1 indicates the number of the series, column 2 the date and hour of observation, column 3 the itemized values of the deflections found by subtracting the midvalue of the micrometer reading from the mean of those each side of it, and column 4 the mean value of the deflection. Columns 5, 6, 7, 8, and 9 give the values of a , b , c , e , and f . Column 10 gives the resulting velocity of the set of three velocity determinations, column 11 the residuals in km/sec. for the velocity relative to the mean for the group, and column 12 the number of single determinations of the velocity.

Table VI shows the results from each of the 233 series of observations. Details are as follows:

Hours of observation (col. 3).—Many of the records of the 1931 observations are incomplete as to the time of beginning and ending of the observations. Where inspection permitted or other notes supplied information, approximate times have been inserted. Hours between 12^h0^m and 4^h0^m are A.M.; all others are P.M.

Mean velocity (col. 4).—Each set of observations usually furnished three values of the velocity. Several sets were arbitrarily grouped into a series covering about an hour's time. Some special groupings will be noted, made either to cover a scattered series or to divide a night's readings into several small series. The velocity V given is the simple mean for the series.

Residuals (col. 5).—The residuals are the values which, applied to the mean velocity for a series, give the individual values for each set.

Average deviations (col. 6).—The mean without regard to sign of the residuals in column 5.

Weights (col. 7).—The weight is the number of single determina-

TABLE V
TWO TYPICAL SERIES OF OBSERVATIONS

SERIES	DATE, P.S.T.	<i>d</i>		<i>a</i>	<i>b</i>	<i>c</i>	<i>e</i>	<i>f</i>	<i>V</i>	<i>v</i>	WT.
		Individual	Mean								
(1)	(2)	(3)	(4)	(5)	(6)	(7)	(8)	(9)	(10)	(11)	(12)
98.....	1932 Apr. 28										
	8 ^h 25 ^m	421,417,392	-0.00410	+0.0003934	+0.0004475	+0.0008327	+0.0000014	1.00016750	299,771	-14	3
	8 40	340,377,391	369	3541	4852	8340	14	16747	771	-14	3
	9 5	450,445,446	447	4289	5125	8347	14	17775	802	+17	3
	9 16	357,382,400	380	3646	5518	8359	14	17528	794	+9	3
	9 24	318,313,301	-0.00311	+0.0002984	+0.0005819	+0.0008354	+0.0000014	1.00017171	299,785	0	3
	Mean	299,785	± 11	15
99.....	1932 Apr. 29										
	8 ^h 31 ^m	704,688,697	-0.00606	+0.0006103	+0.0003086	+0.0008340	+0.0000017	1.0017546	299,795	+16	3
	8 40	660,648,628	648	5682	3255	8347	17	17301	788	+9	3
	8 50	591,541,510	550	4823	3479	8354	17	16073	769	-10	3
	9 5	530,542,523	535	4584	3923	8357	17	16881	775	-4	3
	9 18	505,518	511	4378	4012	8357	17	16764	772	-7	2
	9 31	558,521,513	-0.00531	+0.0004549	+0.0004065	+0.0008303	+0.0000017	1.0016994	299,778	-1	3
	Mean	299,779	± 8	17

TABLE VI
OBSERVATIONS

(1) Series	(2) Date	(3) P.S.T.	(4) Mean Veloc- ity	(5) Residuals	(6) A.D.	(7) Wt.
	1931		km/sec.		±	
1.....	Feb. 19	9h25m - 10h 5m	299,792	+8, -7	7	2
2.....	20-21	- 2 0	774	+26, -27, -45, +4, +27, +15	24	6
3.....	23	9 0 -10 20	767	+27, +7, -34	23	3
4.....	24	9 50 -11 10	760	-1, +18, -17	12	3
5.....	26	12 30 - 2 40	773	-15, +37, -24, -8, +10	19	5
6.....	26	8 20 -10 0	768	+40, +10, -15, -17, -18	20	5
7.....	26	10 1 -11 10	758	-8, +17, +1, 0, -10	7	5
8.....	26-27	11 10 - 2 2	766	-1, -11, -30, +20, +9, +10, -6	14	7
9.....	27	8 16 - 9 26	796	+66, +33, +33, -23, -38, -12, -35, -25	33	8
10.....	27	9 27 -11 5	772	+26, -9, +2, -12, -13, +5, +9, -8	10	8
11.....	Mar. 1	9 0 -11 10	795	-2, +18, -8, -2, -6	7	5
12.....	2	8 22 - 9 4	750	-28, -29, +49, -23, +31	32	5
13.....	2	9 5 - 9 46	772	+23, +9, -22, -3, -7	13	5
14.....	25	750	+14, +19, -17, -21, -18, +22	18	6
15.....	26	750	-21, -3, +25, -4, +2	11	5
16.....	26	745	-28, -9, +20, +7, -10, +10	10	7
17.....	27	8 33 - 9 31	748	-10, +6, -16, +9, +6, +6	9	6
18.....	27	9 35 -11 0	743	+10, -3, -11, -3, -11, +18	8	6
19.....	30	9 0 - 9 50	744	-14, +18, +43, -31, -13, 0, -3	17	7
20.....	30	10 0 -11 12	745	-17, +5, -3, +13, +24, -12, -11	12	7
21.....	31	1 20 - 1 43	728	-2, +4, -24, +22	13	4
22.....	31	8 30 - 9 24	755	+10, +36, -33, +6, -24, +6	19	6
23.....	31	9 25 -10 0	757	0, +11, 0, -17, +7	7	5
24.....	Apr. 3	9 55 -10 34	741	+14, +1, -1, -11, -3	6	5
25.....	3	10 36 -11 18	741	+1, +8, -14, +16, -11	10	5
26.....	8	8 25 - 9 0	755	-52, +38, +14	35	6
27.....	15	8 0 - 9 28	754	+5, -63, +31, +11, +15	25	10
28.....	15	10 14 -10 40	770	+7, +15, -22	15	6
29.....	16	7 50 - 9 12	775	+8, -13, -27, +10, +11, +13, +1, +2	11	16
30.....	16	9 17 -10 31	776	-2, -12, -7, -4, +16, -1, -6, +16	8	16
31.....	17	8 23 - 9 18	771	+4, +12, -7, -7, -2	6	10
32.....	17	9 10 - 9 51	776	-7, -11, +18, 0	0	8
33.....	21	7 45 - 8 38	793	+37, +11, -12, -6, -13, +1, -18	14	14
34.....	21	8 39 - 9 30	779	-20, +10, -6, +8, +4, +4	0	12
35.....	21	9 41 -10 33	772	+5, -14, +1, -3, +8, +3	6	12
36.....	22	7 54 - 8 22	778	+6, +5, +1, -12	6	8
37.....	May 7	9 35 -10 24	789	-13, +14, +12, -13	13	8
38.....	14	7 40 - 8 30	774	-7, +1, +3, +2, +6, -6	4	12
39.....	14	8 31 - 9 41	770	+8, -11, -2, -7, -3, -8	6	12
40.....	14	9 42 -10 30	777	-7, -17, +6, +15, +3	10	10
41.....	14-15	11 48 -12 36	773	0, -3, -1, 0, +5, -2	2	12
42.....	15	12 37 - 1 15	775	+1, -8, -7, +3, +11	6	10
43.....	15	7 20 - 8 23	779	+15, +4, -0, +9, -19, -11, +11	11	14
44.....	15	8 52 - 9 39	767	+10, -4, -9, +9, +7, -7, -6	7	14
45.....	15	9 56 -10 38	775	-6, -4, -3, +15, +12, -16	9	12
46.....	16	12 5 -12 58	778	-1, -9, -12, +1, +6, +2, +10, +2	5	16
47.....	July 1	8 8 - 9 52	776	-10, +12, -18, -5, -9, +30	13	16
48.....	3	7 15 - 8 18	775	+6, 0, -7, +14, -13	7	13
49.....	6	7 33 - 8 22	774	+8, +1, -8	6	9
50.....	7	7 15 - 8 3	773	-23, -25, -2, +25, +25	20	15
51.....	7	8 14 - 9 18	764	-12, +26, +2, -7, -10	11	15
52.....	8	7 15 - 8 45	777	+12, +13, +6, -16, -6, -9	7	18
53.....	13	7 6 - 8 25	779	-30, +21, +5, +15, +30, -41	24	18
54.....	14	7 25 - 8 24	778	+20, -6, -10, +9, -14	12	15
55.....	1932 Mar. 3	9 20 - 9 49	299,815	-2, +1	1	6

TABLE VI—Continued

(1) Series	(2) Date	(3) P.S.T.	(4) Mean Veloc- ity	(5) Residuals	(6) A.D.	(7) Wt.
	1932		km/sec.		±	
56.....	Mar. 4	7 ^h 23 ^m —8 ^h 11 ^m	299,772	-2, -2, -1, +7	3	12
57.....	4	8 20 — 10 1	814	+16, -37, +16, +8, -15, -6	17	14.5
58.....	4	10 23 — 11 14	815	-4, +1, +12, -7	6	12
59.....	8	7 55 — 8 45	796	-3, -6, +5, +4	4	12
60.....	8	8 49 — 9 54	782	+1, +6, -18, +12	9	12
61.....	8	9 56 — 10 59	789	-5, +16, +24, -19	14	10
62.....	9	7 39 — 8 40	800	-4, +11, +11, -1, -14	8	15
63.....	9	9 6 — 9 52	821	+25, -12, -1, -10	12	12
64.....	9	10 15 — 11 11	800	-12, -1, +11, -6, +9	8	15
65.....	10	7 35 — 9 39	751	+14, +14, +7, -8, -16, +5	11	13
66.....	11	7 58 — 8 40	780	+23, -11, +4, -15	12	12
67.....	11	8 49 — 10 11	766	+1, +10, -11, -2	6	12
68.....	11	10 12 — 10 57	772	-17, +10, +5, +1	8	12
69.....	15	7 59 — 9 34	773	+11, -7, +10, -16	11	12
70.....	15	10 13 — 10 41	774	-5, -15, +20	13	9
71.....	16	7 51 — 8 27	775	-2, -7, 0, +11	5	12
72.....	16	8 30 — 9 25	779	+5, -5, -6, +6	5	12
73.....	16	9 50 — 10 42	784	+2, +10, -0, -18, +0	10	13
74.....	16	11 3 — 11 46	764	-20, +4, +15, +4	11	12
75.....	17	7 7 — 8 3	794	+58, +1, -17, -31, -11	24	15
76.....	17	8 6 — 9 37	776	+16, +23, -30, -1, -10	16	15
77.....	18	7 35 — 8 53	743	-19, -37, -7, 0, +21, +43	21	18
78.....	18	9 10 — 9 50	702	+9, -11, +3	8	9
79.....	Apr. 7	9 28 — 9 36	736	3	
80.....	8	9 50 — 10 40	787	-42, +31, +11	28	9
81.....	12	7 26 — 8 44	770	+11, +9, +12, -10, -13, -11	11	18
82.....	12	9 31 — 10 13	779	+9, 0, -12, +4	6	12
83.....	13	7 35 — 8 22	780	-18, +30, -1, -2, -9	12	15
84.....	13	8 25 — 9 02	783	-6, -2, +0	6	9
85.....	14	7 25 — 8 27	788	0, -7, +6, +20, -32	15	14
86.....	14	8 36 — 9 22	768	+4, +7, -10, -1	5	12
87.....	15	7 23 — 8 11	768	-57, -51, +17, +36, +30	38	14
88.....	15	8 27 — 9 8	807	+16, -1, +17, -16, -15	13	15
89.....	18	8 32 — 10 9	786	-22, +20, -12, +13, -1	8	25
90.....	20	8 2 — 8 30	789	0, 0	0	10
91.....	21	7 14 — 8 18	773	+7, +45, -28, -23	15	20
92.....	21	8 23 — 9 26	761	-24, +21, +1	8	15
93.....	26	7 34 — 8 15	776	-20, +19, +7, +6	15	12
94.....	26	8 43 — 9 26	783	-16, +0, +5, 0	7	12
95.....	27	7 50 — 8 55	759	-23, -27, +23, +14, +16, -2	17	18
96.....	27	8 59 — 10 16	790	-35, +5, +5, +5, +13, +5	11	18
97.....	28	7 34 — 8 23	784	+21, +6, +3, -25, -3	12	15
98.....	28	8 25 — 9 33	785	-14, -14, +17, +9, 0	11	15
99.....	29	8 31 — 9 40	779	+16, +9, -10, -4, -7, -1	8	17
100.....	May 3	7 44 — 8 25	766	+3, +7, +10, -21	10	12
101.....	3	8 41 — 9 58	776	+6, -11, +5, +16, -16	11	15
102.....	4	7 39 — 8 33	787	+1, -3, +14, -2, -10	6	15
103.....	4	8 34 — 9 40	780	+6, -12, +3, -3, +6, -2	5	18
104.....	5	7 31 — 8 03	770	+10, -5, -6	7	9
105.....	6	7 34 — 8 16	779	0, +8, -0, 0	4	12
106.....	10	7 37 — 8 57	770	+7, -10, +4	7	9
107.....	11	7 40 — 9 1	786	+1, +25, +1, -14, -8, -8	9	18
108.....	12	7 36 — 8 25	767	-6, +2, -6, +2, +8	5	15
109.....	8	8 47 — 9 34	775	-7, +1, +2, -3, +7	4	15
110.....	13	7 38 — 8 38	765	-4, -11, +19, +13, -8, +1, -13	10	21
111.....	13	9 0 — 9 18	770	-4, +4	4	6
112.....	17	7 40 — 9 9	773	+9, -10, +4, -3	6	12
113.....	18	7 36 — 9 5	775	-42, +21, +14, +7, +23, +26, +7, +11	19	20
114.....	19	7 45 — 9 7	781	+6, -9, +16, -8, 0, +2, -8	7	21
115.....	20	7 32 — 8 42	299,759	-7, +50, -12, -4, -9, +5	10	11

TABLE VI—Continued

(1) Series	(2) Date	(3) P.S.T.	(4) Mean Veloc- ity	(5) Residuals	(6) A.D.	(7) Wt.
	1932		km/sec.		±	
116.....	May 24	7 ^h 39 ^m - 8 ^h 41 ^m	299.774	+9, +4, 0, -11, -2	5	15
117.....	26	7 27 - 8 23	765	+8, -15, -11, -7, +15	11	13
118.....	27	7 34 - 7 42	760	3	3
119.....	June 1	8 5 - 9 13	778	-28, +4, +20, +13, -10	15	15
120.....	2	7 34 - 8 47	787	-11, -3, +6, +2, -1, +12, -5	6	21
121.....	3	7 24 - 8 14	780	+7, +12, +6, -6, -18	10	15
122.....	3	8 16 - 8 58	775	-2, -17, +1, +18	10	12
123.....	6	7 38 - 8 55	750	-6, +8, -8, +2	7	8
124.....	7	7 32 - 8 56	758	-11, -7, -5, +1, +10, +12	8	18
125.....	8	12 12 - 12 21	781	3	3
126.....	9	7 32 - 8 52	762	-13, -5, -2, -8, +4, +17, +6	8	21
127.....	10	7 36 - 8 45	757	-11, -11, +12, +7, -9, +8, +5	9	21
128.....	13	7 31 - 8 52	782	-13, +4, +14, +4, +3, -6, -5	7	21
129.....	14	7 24 - 8 41	781	0, -4, +10, +23, -14, -7, -18	12	21
130.....	15	7 24 - 9 11	774	-1, +15, -2, +2, -7, -3, -4	5	21
131.....	16	7 27 - 8 38	772	-23, +11, +13, +13, -17, +4, 0	12	21
132.....	17	7 46 - 8 32	763	-7, +10, +1, -3, -1	4	15
133.....	20	7 46 - 8 24	735	+4, -11, +45	12	6.5
134.....	21	7 44 - 8 43	762	-2, -6, -12, 0, +9, +11	8	18
135.....	22	7 35 - 8 54	762	-2, +12, -4, -20	7	10
136.....	23	7 23 - 8 33	772	+11, -3, +9, -21, +1, +1, +2	7	21
137.....	24	7 21 - 8 30	770	+16, -8, -4, -5, +4, +1, -5	6	21
138.....	27	7 28 - 8 35	785	+3, -25, +11, -8, -8, +18, +3	11	20
139.....	28	7 25 - 8 27	773	+7, -2, -10, +5, -15, +12, +3	8	21
140.....	29	7 45 - 8 47	770	-20, -14, +6, +2, +12, +21, -8	12	21
141.....	July 30	7 15 - 8 19	786	-4, -16, +21, +14, 0, -11, -5	10	21
142.....	1	7 50 - 8 35	776	+8, -11, +11, +1, -10	8	15
143.....	5	7 28 - 8 34	768	-11, -1, -1, +10, +3, +12, -10	9	20
144.....	6	7 22 - 8 24	757	-10, +4, -2, +8, +13, +1, -14	7	21
145.....	7	7 37 - 8 15	775	+1, +3, +1, -5	2	12
146.....	July 8	7 24 - 8 21	773	-9, +6, +11, +4, -6, -5	7	18
147.....	11	7 23 - 8 11	775	-5, +5, -7, -1, +9	5	15
148.....	12	7 56 - 8 42	768	-16, -2, +25, -2, -5	10	15
149.....	13	7 28 - 8 23	778	-8, -12, +1, +25, -4, 0	9	16
150.....	14	7 27 - 8 41	781	-23, +12, 0, +21, -10	13	15
151.....	15	7 22 - 8 37	770	-28, -57, +22, +13, +16, -3, -4	14	15.5
152.....	18	8 2 - 8 43	776	+5, -9, -16, +6	7	9
153.....	20	8 1 - 8 43	760	-5, +4, +11, -5, -6	6	15
154.....	21	7 28 - 8 13	783	+1, +1, +10, -9, -3	5	15
155.....	22	7 27 - 8 15	765	-6, -9, +12, +10, -7	8	15
156.....	25	8 7 - 8 43	777	-8, +1, +20	7	7
157.....	Aug. 3	7 38 - 8 33	752	-9, -20, +24, +21, -17	18	15
158.....	4	8 7 - 8 48	779	-4, -13, +18, -2	8	10
159.....	Dec. 3	8 5 - 9 10	805	-2, +1, +1	1	9
160.....	5	8 36 - 9 30	756	+2, -2, 0	1	9
161.....	5-6	11 55 - 12 51	776	-26, -12, +22, +12, +3	15	15
162.....	6	3 22 - 4 9	784	+8, +3, +15, -26	13	12
163.....	6	7 15 - 8 22	795	+19, +6, +2, -13, -15	11	15
164.....	7	7 19 - 8 7	792	+6, -1, +4, -10, +0	8	15
165.....	7-8	11 54 - 12 40	784	+9, +4, +1, -8, -6	6	15
166.....	8	3 6 - 3 52	772	+12, -8, -13, +6, +2	8	15
167.....	9	12 3 - 12 50	786	+11, +16, +1, -5, -23	11	15
168.....	9	3 9 - 4 5	765	-13, +6, +10, -8, -1	9	15
169.....	9	7 31 - 8 21	791	+1, +8, +8, -1, -17	7	15
170.....	10	12 25 - 1 14	797	+43, +5, -27, -25, +3	21	15
171.....	10	8 4 - 8 45	775	-17, -18, +14, +22	18	12
172.....	20	7 38 - 8 31	770	+2, +21, -2, -10, -12	9	15
173.....	20-21	11 57 - 12 44	764	-11, -3, +6, +9	7	12
174.....	22	7 14 - 8 4	779	-9, -21, -9, +16, +24	10	15
175.....	23	12 6 - 1 0	299.777	-3, +3, -9, +5, +5	5	15

TABLE VI—Continued

(1) Series	(2) Date	(3) P.S.T.	(4) Mean Veloc- ity	(5) Residuals	(6) A.D.	(7) Wt.
			km/sec.			
176.....	1932 Dec. 23	7 ^h 43 ^m - 8 ^h 34 ^m	776	+11, +14, -15, -14, +3	±	
177.....	24	12 7 -12 54	755	+29, -15, -2, -13	11	14
178.....	24	3 19 - 3 56	760	+16, -19, +21, -18	15	12
179.....	27	8 30 - 9 15	774	-7, -14, +24, -3	18	12
180.....	27-28	11 51 -12 38	777	-13, +13, +4, -3	12	12
181.....	28	2 53 - 3 42	764	+0, +2, -15, +4	8	12
182.....	28	7 36 - 8 21	776	+33, -47, +18, -4	26	12
183.....	28-29	11 46 -12 39	777	-10, -12, +5, +17	11	12
184.....	29-30	11 52 -12 26	782	+15, +9, 0, -23	12	12
185.....	30	8 29 - 9 05	774	-29, +11, 0, +17	15	11
186.....	31	12 11 -12 30	780	-35, +35	35	6
187.....	1933 Jan. 3	7 30 - 8 4	775	-5, +9, -3, -2	5	12
188.....	5	7 27 - 8 10	765	+4, -13, +13, -4	8	12
189.....	6	12 0 -12 32	796	+3, +2, -26, +21	13	12
190.....	9	8 3 - 8 28	763	+9, -9, 0	6	9
191.....	10	12 5 -12 32	770	+1, +6, -7	5	9
192.....	10	7 20 - 8 2	764	+29, -6, -15, -8	14	12
193.....	11	7 17 - 7 48	758	+39, -10, +3, -32	21	12
194.....	12	12 2 -12 48	764	+6, +9, +5, -20	11	10
195.....	12	7 6 - 7 40	753	-3, -23, +8, +18	13	12
196.....	12-13	11 54 -12 31	766	+20, -4, -21, +5	12	12
197.....	13	2 56 - 3 30	765	+21, -9, -5, -7	10	12
198.....	13	7 10 - 7 30	786	-5, +5	5	4
199.....	16	7 57 - 8 30	761	+10, +8, -5, -13	9	12
200.....	16-17	11 53 -12 24	749	+7, +8, -6, -9	8	12
201.....	17	3 3 - 3 37	767	0, -7, +2, +5	4	12
202.....	17	7 57 - 8 25	764	-10, +7, +12	13	9
203.....	18	12 0 -12 31	764	-12, -11, +23	15	9
204.....	18	7 25 - 7 56	777	-1, -18, +9, +9	9	12
205.....	19	12 13 -12 45	774	+6, +10, +5, -21	10	12
206.....	19	2 59 - 3 34	771	-2, -1, +10, -7	5	12
207.....	19	8 18 - 8 42	759	+17, -15, -2	11	9
208.....	25	7 48 - 8 28	771	-10, -4, +2, +12	7	12
209.....	26	12 16 -12 41	766	-19, +20, 0	13	9
210.....	26	3 12 - 3 42	770	+2, -22, +19	14	9
211.....	26	7 10 - 7 59	765	+4, -14, -4, +14	9	12
212.....	27	7 28 - 7 59	779	+4, -2, +4, -6	4	12
213.....	31	7 9 - 7 42	771	+3, -4, +7, -7	5	12
214.....	Feb. 1	12 4 -12 28	774	+11, -8, -3	7	9
215.....	2	7 9 - 7 48	753	+1, -3, +6, -4	4	12
216.....	2-3	11 52 -12 21	766	+3, +5, -2, -7	4	12
217.....	3	3 13 - 3 45	801	+13, -11, -1, -1	6	12
218.....	3	7 6 - 7 35	776	+16, -23, +9, -2	12	12
219.....	6	7 44 - 8 6	756	+6, -6, 0	4	9
220.....	7	7 8 - 7 40	775	-20, -20, +23, +17	20	12
221.....	8	7 10 - 7 43	785	+18, +1, -9, -11	9	12
222.....	9	7 15 - 7 44	790	+23, -8, -5, -10	12	12
223.....	10	7 15 - 7 56	763	+20, -33, -1, -4, +18	14	13
224.....	13	7 16 - 7 43	771	-11, -10, +16, +5	10	12
225.....	14	7 7 - 7 36	789	+28, -8, -16, -4	14	12
226.....	15	7 22 - 7 50	767	+8, +13, -2, -10	10	11
227.....	16	7 10 - 8 16	767	+18, +9, 0, -7, -5, -15	9	18
228.....	17	7 8 - 7 52	779	+1, +32, +5, -35, -4	6	12
229.....	20	7 11 - 7 47	782	+12, +7, -14, +5, -10	10	15
230.....	21	6 59 - 7 28	784	+14, -21, +23, -16	18	12
231.....	22	7 22 - 7 50	774	+36, -16, -14, -6	18	12
232.....	24	7 4 - 7 46	807	-18, -15, +16, +17	16	12
233.....	27	7 5 - 7 34	299,788	-4, +11, +9, -16	10	12

tions of the velocity for the series. An italicized number in the residuals column indicates that the reading has a weight less than that of the normal value for the group. For series 1-25, 1931, when 10 *R* and 10 *L* readings were made, each set of 20 readings was given a weight of 1. In series 26-46, 1931, when 5 *R* and 5 *L* and then 5 *L* and 5 *R* readings were made, each set of 20 readings was given a weight of 2. From series 47, 1931, on, practically all the readings were made 5 *R*, 5 *L*, 5 *R*, 5 *L*, 5 *R*, and each set of 25 readings was given a weight of 3. In a few cases, the set of 25 readings being incomplete, weights of $\frac{1}{2}$, 1, and 2 were allotted, and in a few others, involving seven sets of 5 each, weight 5 was given.

TABLE VII
SUMMARY OF TABLE VI

Series	Date	No. Separate Determinations	Mean Velocity	A.D.
1-54.....	1931 Feb. 19-July 14	493	299,770	± 12
55-110.....	1932 Mar. 3-May 13	753.5	299,780	11
111-158.....	1932 May 13-Aug. 4	742	299,771	9
159-233.....	1932 Dec. 3-1933 Feb. 27	897	299,775	± 11
		2885.5	299,774	± 11

The low rating given to the 1931 readings is due, first, to the way in which they were taken, which did not eliminate drift, and, second, to the fact that errors may have crept into the readings because the pendulum case was not controlled for temperature. The 1931 observations might have been considered as preliminary results and omitted altogether; but, owing to the large fluctuations in the individual values, it was decided to include every observation in the final mean velocity.

Table VII is a summary of the data given in Table VI. The average deviations in the last column are relative to the mean in the preceding column.

DISCUSSION

Distribution of velocities.—The mean velocities shown in column 4, Table VI, have been grouped into divisions covering a range of 5 km/sec. and are shown in Table VIII. A plot of these data in

Figure 8 resembles a probability-curve and indicates that the probable value of a constant velocity would be 299,774 km/sec.

TABLE VIII
FREQUENCY DISTRIBUTION OF MEASURED VELOCITIES

Velocity Range	Number	Velocity Range	Number
299000+		299000+	
726-731.....	4	776-780.....	515
731-735.....	6.5	781-785.....	270
736-740.....	3.0	786-790.....	236
741-745.....	55	791-795.....	90
746-750.....	29	796-800.....	62
751-755.....	86	801-805.....	33
756-760.....	184	806-810.....	30
761-765.....	304	811-815.....	32.5
766-770.....	353.5	816-820.....	0
771-775.....	580	821-825.....	12

Time-velocity curves.—A plot of velocity readings with respect to time is shown in Figure 9, the abscissae representing days of the year and the ordinates velocity. Four periods of the night are distinguished by the characters shown in the legend. The heavy line

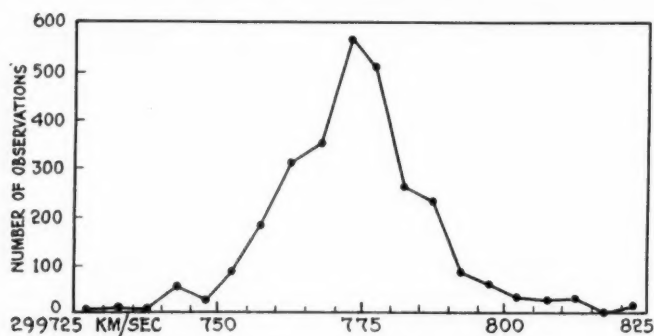


FIG. 8.—Velocity distribution-curve

joins the weighted mean values of small groups of readings covering a few days' time, while the light line shows the axis drawn at a mean value of 299,774 km/sec.

All the 1931 observations lie close to the axis with the exception of series 14-25, whose mean is 299,746 km/sec. The 1932 curve begins at 299,800 km/sec., suddenly drops to 299,776 km/sec., con-

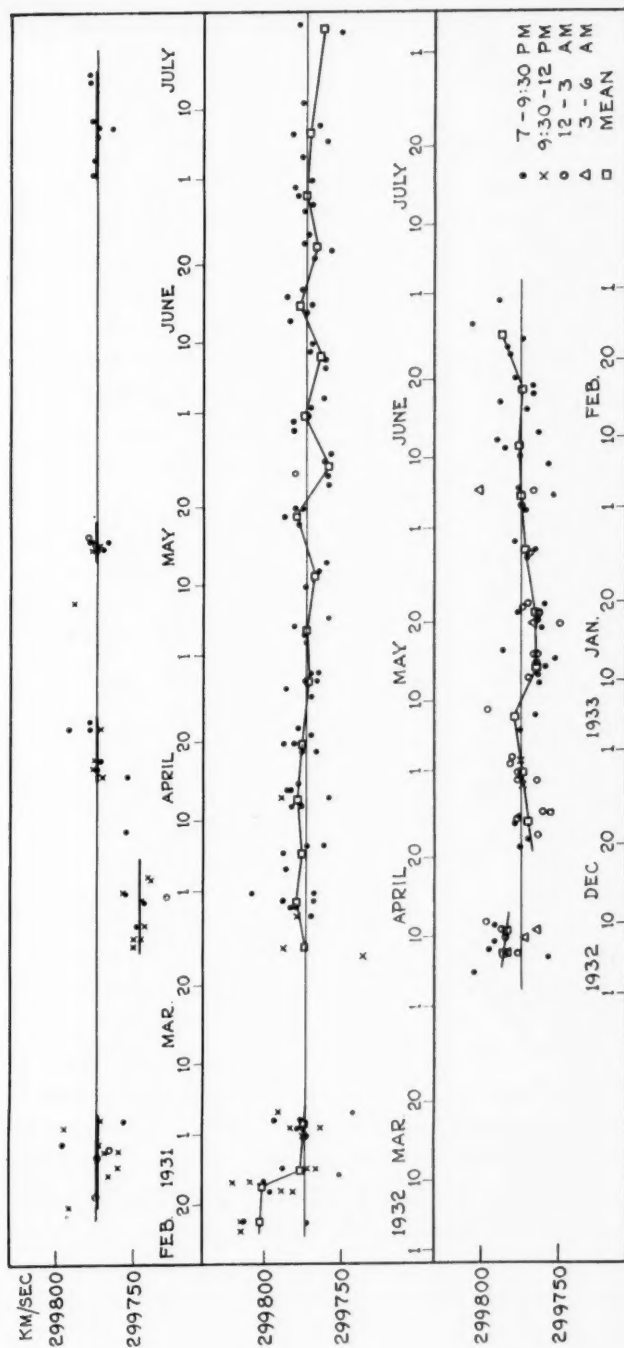


FIG. 9.—Velocity-time curve

tinues just above the axis until early in May, then drops to 299,760 km/sec. early in June. Several fluctuations occur in the curve at this time. The curve remains below the axis until the end of the observations on August 4. The 1932-1933 curve begins at about 299,785 km/sec. early in December, crosses the axis twice, and reaches a value of 299,765 km/sec. on January 15. It then gradually rises to a value of 299,787 km/sec. by the end of February.

Tidal-force-velocity curves.—When the time-velocity curves were first plotted, a curve freely drawn through the individual points appeared to resemble the tidal curve of the water depth at the nearby

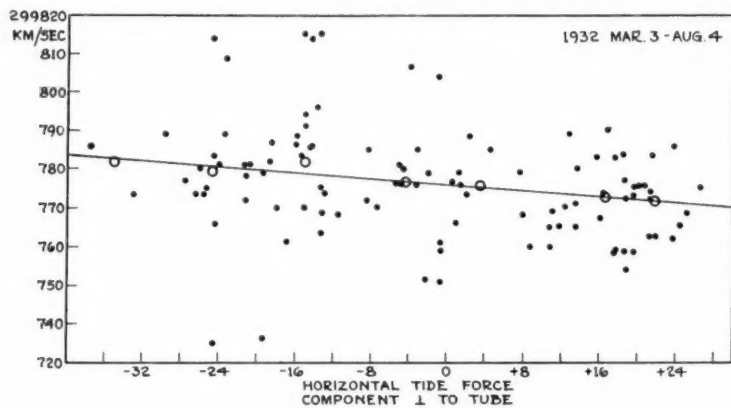


FIG. 10.—Velocity-tide-force curve

coast, if the tidal curve were displaced 10 hours forward. Since the lunital interval in this locality is 10 hours, the agreement seemed to suggest a relationship with sun-moon tidal forces acting at the time of observation and not with earth displacements due to the changing weight of water on the coast. The direct action of the tidal forces in producing earth expansion or in changing the period of the pendulum is too small to produce displacements of the order noted. Nevertheless, component curves of the sun-moon tide forces were kindly drawn by the United States Coast and Geodetic Survey on their tide-predicting machine, from which values of component tidal forces were obtained for the times of observation. A slight correlation with the velocity is suggested in the case of the horizontal component perpendicular to the tube. The plot for early 1932 readings (Fig.

10) shows large velocities for a strong tidal force pulling in a southeasterly direction, and small velocities for a force directed northwesterly. A change of 10 km/sec. corresponds to a change of 1.35×10^{-7} g. The scattering of the points is so large, however, that it is questionable whether the plot has any real significance.

Moon-diameter-velocity curves.—The diameter of the moon, which can be taken as a measure of its distance at the times of observation, was plotted against velocity for both the early 1932 and the 1932-1933 data (Fig. 11). Both curves show the same feature, namely, a curve convex downward, almost coincident in the plots, indicating high velocities for both large and small diameters of the moon and suggesting tidal effects. The scattering, however, is large and the results of low weight.

Repeated measures of the base line and checks on the clock rate revealed nothing capable of accounting for the residual differences between the mean curve and the axis. A vibration of the mirror system with a period equal to a fraction of that of the rotating mirror conceivably may have produced the rapid fluctuations observed in the individual readings. Further experiments on a more stable terrain, with improved self-recording apparatus, carried on continuously over an extended period of time will be necessary to clear up the problem.

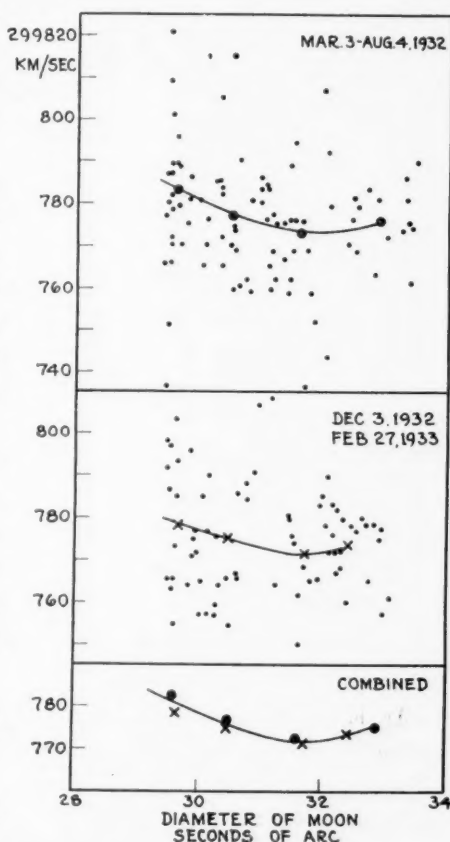


FIG. 11.—Velocity-moon-diameter curve

ACKNOWLEDGMENTS

The experiment has been carried out with the hearty co-operation of many people and institutions, and we wish to express our thanks to the following:

Dr. George E. Hale, at whose invitation the experiment was carried out in California.

Mr. Martin A. Ryerson for the initial gift of \$10,000 which started the experiments on their way. Many of the instruments built with these funds were used throughout the experiments, both on Mount Wilson and at the Irvine Ranch.

The Rockefeller Foundation for the sum of \$30,000.

The Carnegie Corporation for the sum of \$27,500.

Mr. James Irvine, Jr., for the use of land.

Dr. H. G. Gale, director of the Ryerson Laboratory of the University of Chicago.

Dr. W. S. Adams, director of the Mount Wilson Observatory of the Carnegie Institution of Washington.

The United States Coast and Geodetic Survey for its hearty co-operation in the measurement of the base line and the construction of the tidal-force curves.

The United States Naval Observatory for its co-operation in connection with the time signals.

Mr. E. C. Nichols, of the Mount Wilson Observatory, who was in charge of mechanical design; Mr. A. N. Beebe, who installed the pipe and vacuum system; and Mr. J. Kimble, who assisted throughout the experiment.

Mr. S. L. Boothroyd, of Cornell University, for the loan of a gravity pendulum.

Mr. J. W. Horton, of the General Radio Corporation, for the loan of a constant-frequency assembly.

Mr. Peter Mole, of the Mole-Richardson Company, for the loan of an arc lamp, and both Mr. Mole and the General Electric Company for the loan of a motor-generator set.

Mr. Roy Anderson, of the California Corrugated Culvert Works.

Dr. S. W. Stavely, of the Firestone Rubber Company.

Dr. Gustaf Strömberg and Dr. Seth B. Nicholson for their help in tidal-force computations and for assistance in the general discussions.

Miss Myrtle L. Richmond for assistance in the computations.

UNIVERSITY OF CHICAGO
CARNEGIE INSTITUTION OF WASHINGTON
MOUNT WILSON OBSERVATORY
September 30, 1934

STUDIES OF EXTRA-GALACTIC NEBULAE

PART I: DETERMINATION OF MAGNITUDES

By PHILIP C. KEENAN

ABSTRACT

A description is given of the method in use at the Yerkes Observatory for measuring the total magnitudes of nebulae by comparisons of extra-focal images. All comparisons are made directly with stars of the North Polar Sequence. After corrections for differential extinction and for size of image have been applied, the probable errors of the mean magnitudes are of the order of 0.06 mag. Irregularity in the shapes of the images is one of the most serious sources of error.

A catalogue of the brighter nebulae discovered on the survey plates is included.

I. INTRODUCTION

Photometry of the brighter external galaxies occupies an important place in the co-operative survey of these objects sponsored by the International Astronomical Union and organized under the leadership of Dr. Hubble of the Mount Wilson Observatory. The participating observatories have been left free to develop their own technique of observation; accordingly, we have worked out a provisional procedure for treating the zone assigned to the Yerkes Observatory, from $+50^\circ$ to the North Pole, on the basis of the equipment available. Several interesting photometric problems have arisen in the course of the work, and we feel that it may be of value to other workers in the field to discuss some of these points in advance of the publication of the survey catalogue, for which the observations will not be completed for several years. The important question of the influence of exposure time upon the measured magnitudes, and, in general, all points requiring a statistical treatment of the observed magnitudes, must be set aside until more material is available.

2. CHOICE OF METHOD

In this work we have been concerned primarily with the determination of integrated magnitudes, neglecting for the present the problem of surface brightness.

The observed magnitudes will tend to be influenced by irregularities in the shape of the galaxies and in their degree of condensation.

The effects may be expected to depend upon the type of the nebula, its size, and its brightness—the very quantities which will be required often as variables if any statistical use is to be made of the data. Thus it is clearly essential that the observations be arranged so as to make these systematic errors as small as possible. This may mean the abandonment of methods which lead to the most consistent results for individual objects or even for whole groups of homogeneous nebulae, but the most casual inspection of a few photographs is enough to show that the diversity in size and shape of the nebulae, and in the number of foreground stars, is so great as to make very low values for probable errors illusory in so far as comparisons between galaxies are concerned. It is desirable also to make supplementary investigations to detect the residual systematic errors which will necessarily be present to a greater extent than in stellar photometry.

In practice we wish to express nebular luminosities in the international system of magnitudes, so that the problem is to photograph a set of standard stars and a nebula in such a way that the images will be comparable. This can be done either by taking the images out of focus with a refractor or by trailing near-focus images with a moving-plate camera¹ so as to produce rectangular hatchings of any desired size. The latter device has the advantage of being adaptable to any type of telescope, but is a rather complicated instrument. With properly designed equipment it is possible to obtain nearly constant density across the images by either means. Since there is available at the Yerkes Observatory the Zeiss doublet of UV glass (aperture: 14.5 cm; focal length: 81 cm), giving images of excellent quality over a field of several degrees when the plate is taken inside the focus, we have decided to employ the extra-focal method for the present survey.

The size to be given the images and the method of measurement are the next points to be considered. With all minor differences of procedure disregarded, there are two possibilities:

a) Both nebula and stars are spread over an area several times wider than the maximum diameter of the nebula. Since all portions of the nebula contribute equally to each part of the image, except

¹ W. H. Christie, *Ap. J.*, **78**, 313, 1933.

near the edges, the surface brightness of the image is proportional to the total brightness of the source, and measurement is carried out with the diaphragm of the photometer smaller than the extra-focal disk.²

b) The distance from the focus for the nebular exposure is made only great enough to smooth out the irregularities in the shape of the nebula. The images will then be considerably smaller than those of method (*a*). The photometer opening is made slightly larger than the images, so that the total blackening of the plate by the nebula is measured and compared with the corresponding deflections for the comparison stars.

It appears to be generally recognized that method (*a*) is photometrically the more exact in that it more effectually smooths out the irregularities of the emulsion and the distortions of the optical image, which give rise to field corrections.

When an attempt is made to apply this method to nebulae, however, two serious difficulties are encountered. In the first place, the exposure times are considerably lengthened. Since the nature of the measurement requires a diameter at least double that of the focal image, the area will be increased by a factor of 4 as a minimum. Experience with method (*b*) suggests that its use will result in something like a twofold magnification of areas, and it may therefore be estimated conservatively that it will produce a given density with not more than half the exposure time required by method (*a*).

The second difficulty to hinder the employment of such large images is the presence of numerous foreground stars close to the nebulae. In order to see how frequently such stars intrude into the line of sight, ninety-four nebulae photographed with the 24-inch reflector were examined. The focal images of 31 per cent of these were influenced by stars, of which by far the greater part were undoubtedly foreground objects, and 16 per cent of the whole number had stars actually in front of the galaxies. In such cases, except when the stars are several magnitudes fainter than the nebula, it is practically necessary to measure stars and nebula together and then to subtract the intensity due to the stars as determined by galvanometer deflections for similar ones outside the nebula. It is clear that such correc-

² *Ibid.*

tions can only be approximated at best and will introduce considerable uncertainty into the results when the stars involved are bright. The number of wholly or partly superposed stars will increase more rapidly than the area of the images, so that the expected accuracy of measurement of large images will often be lost through the indefiniteness of the quantity measured.

For these several reasons it appears that method (a), superior though it is for compact isolated nebulae, will be applicable to a smaller range of objects, and will more frequently require the working-out of individual corrections, than will method (b), when account is taken of the great range of sizes and magnitudes to be covered by this survey. We have, therefore, chosen method (b) as our standard, but hope to employ the alternative procedure on a few selected objects as a check on the magnitude scale.

TABLE I

ΔF	Diameter
1.5 mm.....	0.31 mm
2.0.....	.40
2.5.....	.49
3.0.....	.58
3.5.....	0.69

3. OBSERVATIONS AND MEASUREMENTS

In accordance with the suggestion made by Hubble in his outline of the program for the survey, our scale of magnitudes of the nebulae is based upon exposures of uniform length. The exposure time adopted is one hour, which will give satisfactory extra-focal images with the UV camera for objects brighter than the fourteenth magnitude.

The average diameters of images of stars taken at different distances inside the focus of the UV camera are given in Table I. The data of the table apply to images dense enough to give deflections just above the toe of the calibration-curve.

In practice it is usually possible to obtain fairly uniform images of the galaxies, the values of ΔF ranging from zero, for a few diffuse nebulae, to 1.5 mm and more for nearly stellar objects. The comparison stars are then made to match the nebula by putting them out of focus by from 1.5 to 3.0 mm.

Because of the high northern declination of the zone assigned to the Yerkes Observatory, it has been found practicable to compare every nebula directly with the North Polar Sequence. The exposures are of equal length, preferably with each nebula plate taken between two calibration plates, but, since the exposures are of an hour's duration, a single calibration has to suffice in many cases. The long exposures make it necessary also to take the nebula and the pole on separate plates, not only because of the excessive density of the sky background when the exposures are superposed on a single plate, but also to avoid overlapping of the broadened images. In every case the plates to be compared are taken from the same box and are developed together in a tank, with continuous agitation of the rack in the developer, which is Eastman D-11.

In Plate III a pair of well-matched exposures are reproduced; the images shown are slightly smaller than the average.

Observers dealing with zones farther south will probably have to rely upon neighboring Selected Areas as standards, but these have the disadvantage of giving calibration-curves of unequal reliability, since some of the areas contain few stars in the magnitude range considered. At the Yerkes Observatory the zenith distance of the pole is $47^{\circ}.4$; hence the loss of light involved in taking the nebulae at approximately the same altitude as the Polar Sequence is less than 0.2 mag. Each plate is corrected for the remaining differential extinction, the amount of the correction averaging $+0.06$ mag. for the plates taken to date.

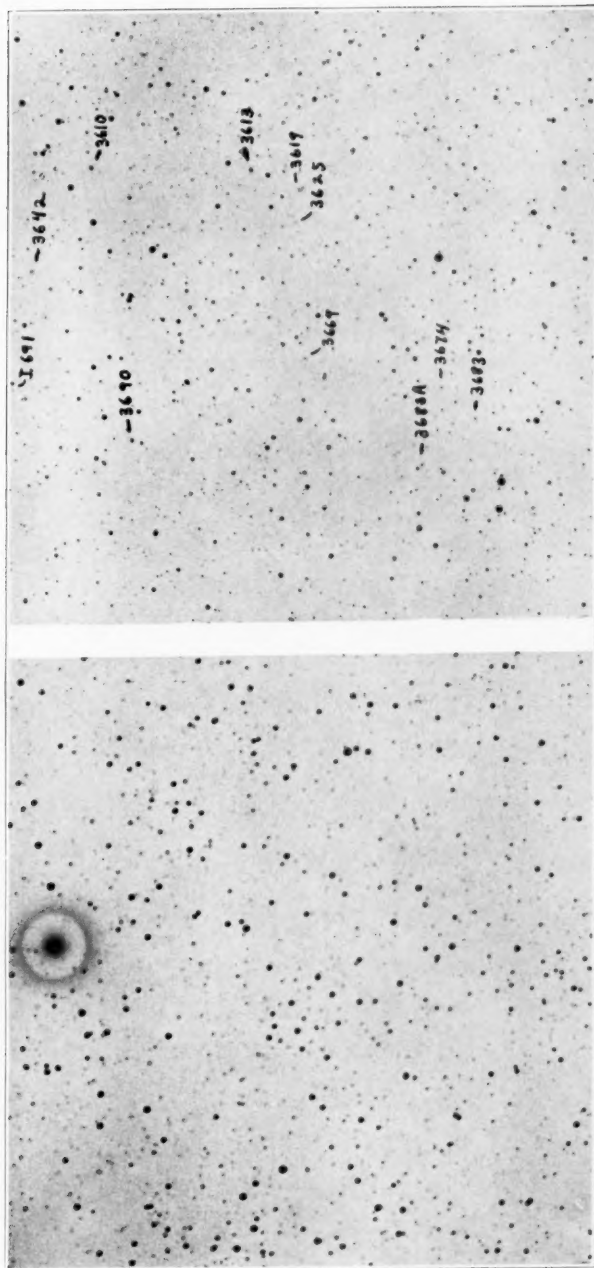
All photometric measurements on the plates have been carried out with the new thermoelectric photometer designed by Dr. F. E. Ross and constructed by Mr. Charles Ridell in the Yerkes shops. The design and operation of this instrument will be described in an article by Ross.³

In order to secure uniformly high sensitivity each series of plates is measured through a diaphragm passing a beam whose diameter, as focused on the emulsion of the plate, is just greater than the maximum diameter of the largest image to be measured. In the present arrangement all nebulae having image diameters not greater than about 1 mm ($4'$ on the UV plates) can be treated in this way.

³ To be published in the *Astrophysical Journal*.

PLATE III

A



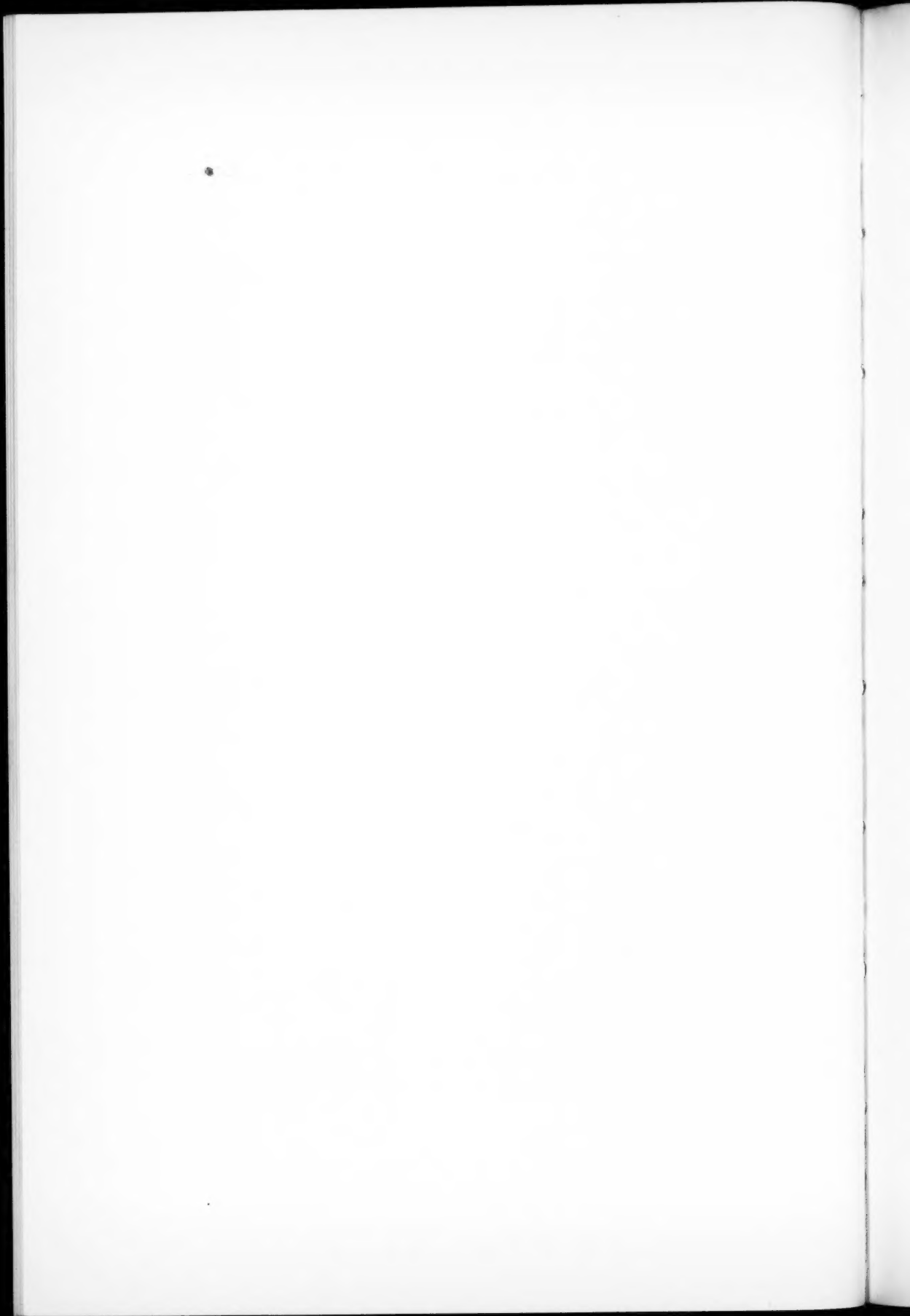
W

a

b

ENLARGEMENT 2X. SCALE: 2' = 1 MM

- a) UV 2144. North Polar Sequence. Focal distance: - 1.8 mm
- b) UV 2143. R.A. 1^h 22^m. Dec. + 58°. Focal distance: - 1.2 mm



The few larger nebulae on the program could be measured similarly by greatly reducing the magnification of the beam between the emulsion and the thermocouple, but since these objects are the ones suffering the greatest interference from foreground stars, it seemed best to deal with them on a different basis. Their total magnitudes are determined indirectly from their measured areas and from their surface brightnesses as derived from focal plates compared with large extra-focal images of the Polar Sequence. This procedure is admittedly inaccurate, but is adopted provisionally for want of a better one.

4. CONSISTENCY OF ATMOSPHERIC EXTINCTION

The direct comparison of photographs taken with the times of mid-exposure more than an hour apart requires observational justification, for these intervals are longer than those usually spanned by astronomical photometry. A critical test of the consistency of the results is made by comparing pairs of calibration plates. Such pairs allow an estimate of the maximum effect of the variation with time of the transparency of the sky, inasmuch as they are taken more than two hours apart, with a nebular exposure separating them.

In most cases the calibration plates preceding and following a photograph of a given field of nebulae are made at somewhat different focal settings in order to permit comparisons with several nebulae of varying size, particularly if the sequence of plates is continued by additional photographs on the same night. For this reason the number of plates suitable for tests of the uniformity of extinction, for which purpose the images on a pair must be as nearly identical as possible, is small. However, we have available twelve well-matched pairs taken on transparent nights, and these are sufficient to give a good idea of the reliability of the calibration-curves.

Four of these pairs of curves are plotted in Figure 1. These were selected at random and represent normal results, except that the differences between the curves for UV 2142 and UV 2144 are the greatest found on any pair yet taken on a very clear night. It is significant that the transparency on that particular night was estimated by the observer as diminishing during the exposures from 3+ to 3 on our scale. The average deviation of each curve of a pair from

the mean of the two, from all twenty-four plates used, amounted to 0.06 mag. for very dense images, 0.03 mag. at intermediate densities, and 0.02 mag. for images in the toe of the curve. The larger value found for the bright stars is due in part to slight changes in the focus, which was set separately for each plate.

The agreement is about as good as could be hoped for even if the exposures were of only a few minutes' duration. This result may seem a bit surprising at first, but is probably to be explained by the

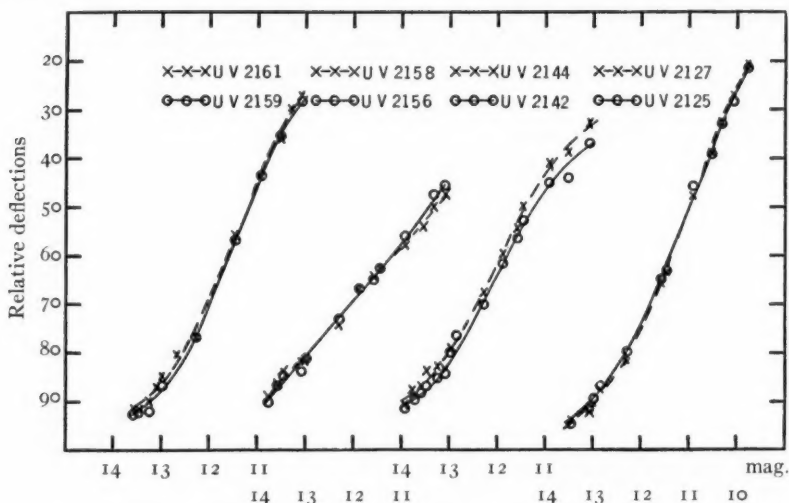


FIG. 1.—Pairs of calibration-curves. Ordinates are ratios of deflections: star to background fog.

fact that the atmosphere is frequently subject to short-period fluctuations in transparency, which are partly smoothed out by the longer exposures.⁴ In any case it may be concluded that successive one-hour exposures made on good nights can safely be compared as long as the observer does not detect changes in the transparency, as judged by the visibility of faint stars near the pole.

5. CORRECTION FOR SIZE OF IMAGE

Since the field corrections of the UV camera have been found to be caused chiefly by the change in the areas of the images in going from the center to the edge of the field, a series of plates of the Polar

⁴ I am indebted to Dr. Elvey for a discussion of this point.

Sequence at varying focal settings was taken in order to determine the relations between size of image and measured magnitude.

The resulting corrections for a diaphragm having an effective aperture of 0.9 mm are shown in Figure 2, where each curve is the

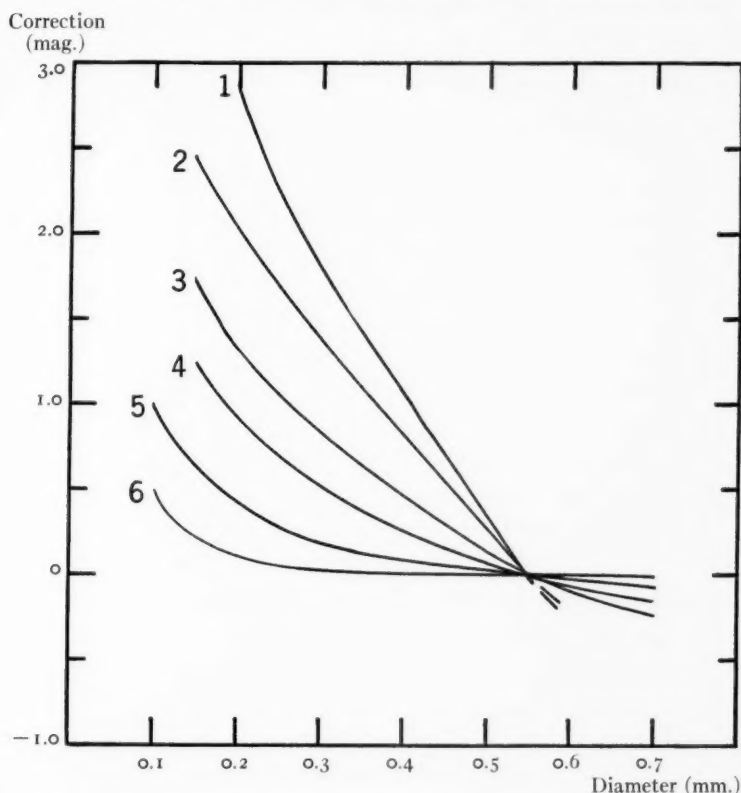


FIG. 2.—Variations in measured magnitude with diameter of image. The numbers refer to position on the calibration-curves, expressed as percentages of the total height of the curve, lower numbers corresponding to higher densities, as follows: 1, 10-20 per cent; 2, 20-40 per cent; 3, 40-55 per cent; 4, 55-70 per cent; 5, 70-85 per cent; 6, 85-100 per cent.

average for images spread over a range of about seven-tenths of a magnitude in brightness. The irregularities in the progression of the curves reflect the large scatter found in the individual points from the fourteen calibration-curves from three plates used in forming the means. The average deviation from the mean of the separate

observations going into the lower four curves is 0.09 mag. Curves 1 and 2 depend upon only a few points, but are seldom used. The diagram relates the corrections arbitrarily to a value of zero for an image diameter of 0.55 mm, which happens to occur frequently, but the curves could equally well be drawn to cross the zero line at any other diameter.

The curves behave as might be expected from a consideration of the structure of the images. For faint stars the density of images of all sizes is so low that enough light is transmitted to affect the photometer readings; consequently, the loss in density with increasing size largely compensates for the greater area of absorption, and the corrections are small. On the other hand, the images of very bright stars are effectively opaque in all sizes and should produce galvanometer deflections which are proportional to the area of clear plate around the star but are relatively insensitive to the magnitude of the star. The large and uncertain corrections for dense images are thus explained.

If Figures 1 and 2 are compared it is seen that nebulae falling just above the toe of the calibration-curve give the most satisfactory determinations of magnitude, even when they differ appreciably in dimension from the comparison stars.

For all magnitudes of nebulae measured up to this time and given a weight high enough to be regarded as satisfactory, the average correction applied due to difference in size of image is 0.05 mag., a mean of 76 values taken without regard to sign.

6. EFFECT OF SHAPE OF IMAGE

It is important and at the same time difficult to obtain direct experimental evidence of the extent to which the measures are affected by irregularities in the density distribution of the images.

Consider, first, images which are approximately circular but which differ in their radial distribution of density. The imperfections in the images formed by the 10-inch Bruce lens provide a convenient way of bringing about this condition. The lens is overcorrected for spherical aberration, so that stars taken inside the focus appear as small intense nuclei superposed upon faint disks several times as broad. On the other hand, the images formed outside the focal plane are relatively faint near their centers but are sharply bounded by

bright rings. A comparison of the same stars photographed on opposite sides of the focus will thus permit a rough estimate of the maximum differences to be expected if centrally concentrated spheroidal nebulae and open spirals were measured together on focal plates.

From a number of exposures made in this way with the Bruce telescope the systematic differences are found to be not only large but also inconsistent from plate to plate. The variations in the results are probably due in part to threshold effects connecting the fainter portions of the images with the density of the fog background. However, the general course of the measures can be seen from the typical set of calibration-curves given in Figure 3, which offers further evidence of the necessity of taking the brighter nebulae far enough out of focus to insure approximate uniformity of density.

On the two plates taken outside the focus, at -1.2 and -2.0 mm, the images have a diameter of 0.27 and 0.36 mm, respectively, throughout the greater part of the range of magnitudes covered. Only the nuclei of the images of the fainter stars appear on the exposure taken 1.4 mm inside the focus and, therefore, the toe of its curve lies a little below the corresponding portions of the other two. Passing to the bright stars, we find that the broad disk due to the axial rays has become so strong that the images have an effective diameter of about 0.65 mm, which is sufficient to raise their calibration-curve far above the others. Between the two ends there is a transition stage in which the background image is just reaching threshold density, and here the curves cross, though in this region the diameters of the images characterized by nuclei are so vague as to be practically unmeasurable.

Some information concerning the effect of comparing round and elongated images with each other has been secured from a special series of plates of the Polar Sequence, taken with the UV camera. On these the round disks had an average diameter of 0.5 mm, while the oblong images were obtained by moving the plate-holder by a hand screw back and forth over a distance of about 0.6 mm, the original diameter of the images being 0.3 mm. The trailed images produced in this way had a ratio of axes of a little less than 3 to 1 . The areas of the two types of images were almost exactly equal on the average, and corrections for the small individual differences were applied in the usual manner.

The calibration-curves for the seven sets of elongated images and six sets of round ones are practically identical in shape. The latter have a slightly greater slope; hence, the oblong images are measured as too faint by 0.20 mag. for dense images, 0.08 mag. for images of

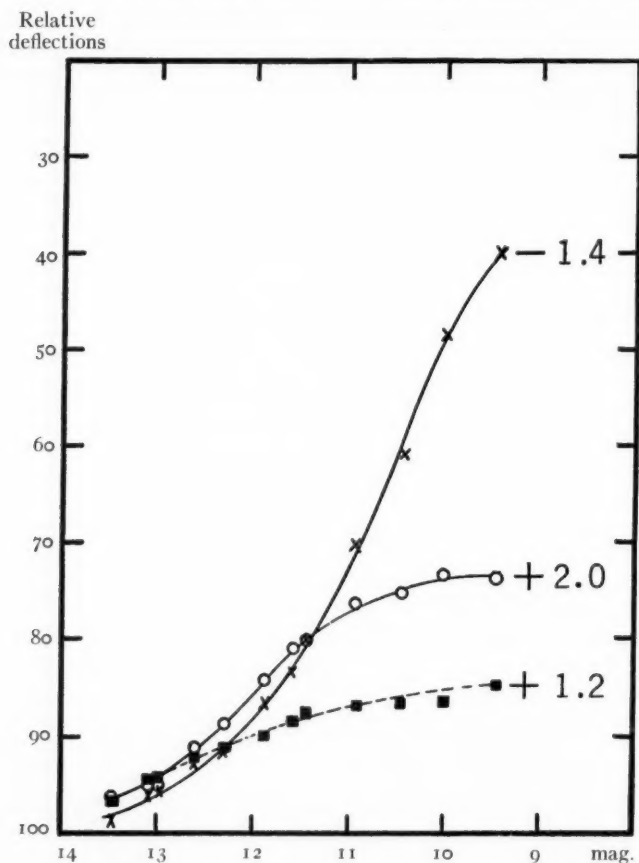


FIG. 3.—Bruce calibration-curves. Numbers at the ends of the curves refer to distances from the focus, in millimeters.

moderate strength, and 0.03 mag. for those near the toe of the curves. For densities corresponding to those obtained with most of the nebulae on our program the mean difference is about 0.06 mag., but the amount is too small to be well determined, the average deviations of individual values from the mean being of the same order.

These results indicate that as long as the densities of the images are fairly uniform their shapes are not very critical factors. There will probably be systematic differences of the indicated order between narrow spindles and nearly round spirals, but the extensive investigation necessary to determine accurate corrections for various degrees of elongation appears to be scarcely feasible at present, particularly in view of the larger errors due to other sources.

7. PRECISION OF THE MEASURED MAGNITUDES

A final evaluation of the accuracy of the integrated magnitudes must await the completion of the program, but we can estimate the errors fairly closely from the data for twelve nebulae for each of

TABLE II
ACCURACY OF NEBULAR MAGNITUDES

NGC	M_{pg}	r
2268.....	12 ^m .36	0 ^m .08
2276.....	12.08	.07
2300.....	12.25	.04
2655.....	11.00	.09
2748.....	12.44	.08
3683.....	12.90	.15
3982.....	12.26	.02
5874.....	13.33	.07
5875.....	13.27	.15
5908.....	13.02	.09
6359.....	13.59	.10
6381.....	13.38	0.05

which at least four independent measures of satisfactory weight are available. These objects are listed in order of their NGC numbers in Table II. The second column gives the weighted mean photographic magnitude, followed by the probable error of a single observation in the third. Since it is intended that the final magnitude of every nebula will be based upon at least two observations of adequate weight, the probable error of the mean magnitudes may be expected to be in the neighborhood of 0.06 mag.

Before it will be possible to tell how successfully we have reduced systematic errors, especially those discussed in the last section, a larger accumulation of material must be at hand, permitting comparisons of the results obtained with different instruments and by different methods with the same telescope.

8. NEW NEBULAE

A number of previously uncatalogued nebulae of the fourteenth magnitude or brighter appear on the plates. For the benefit of other observers Table III gives approximate positions (epoch 1950) of such

TABLE III
NEBULAE DISCOVERED ON SURVEY PLATES

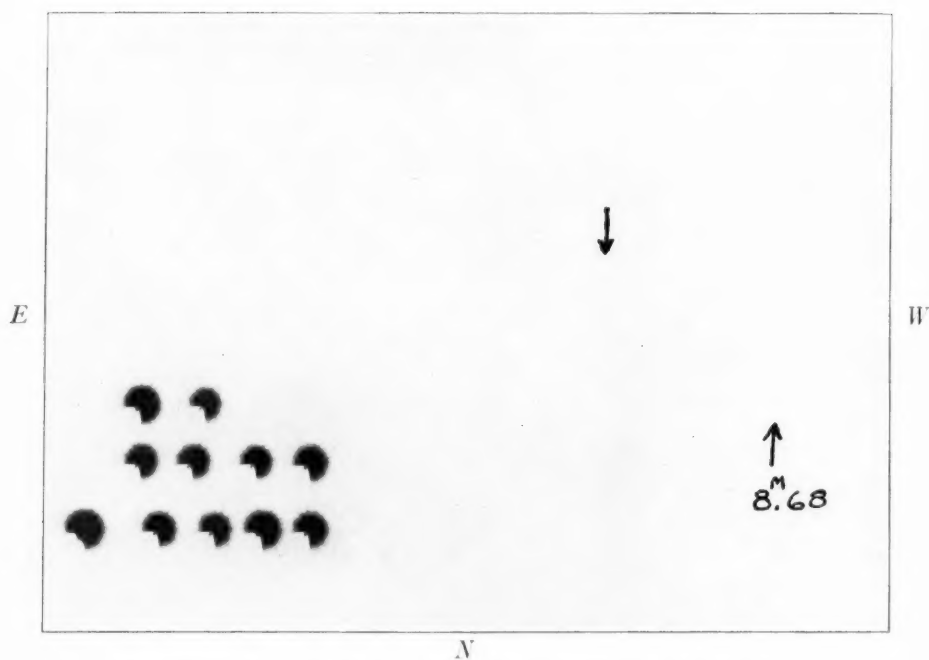
Nebula	R.A.	Decl.	Remarks
1530A.....	4 ^h 38 ^m 2	+75°37'	12 ^m 88
1573A.....	4 42.7	73 26	14 ^m 0
2146A.....	6 16.0	78 35	13 ^m 66; 3'0"×1'7" in P.A. 25°; irregular
2273A.....	6 36 :	60 07	
2273B.....	6 42.2	60 24	2'2"×1'9" in P.A. 38°; SB:
2326A.....	7 04.9	50 44	14 ^m ; 1'2"×0'9" in P.A. 14°; E ₃ :
2336A.....	7 50 :	78 19 :	
2523A.....	7 58.4	74 14	
2523B.....	8 07.1	73 44	2'3"×0'5" in P.A. 92°; Sc
2523C.....	8 12.0	73 30	0'9"×0'6" in P.A. 74°; E ₄ :
2550A.....	8 23.6	74 04	
2742A.....	9 06 :	62 22 :	13 ^m 7
2959A.....	9 41.2	68 51	0'8"×0'25" in P.A. 144°; Sb
3683A.....	11 27 :	57 23 :	13 ^m 11
3759A.....	11 34.2	55 26	13 ^m 9; 1'3"×1'2"; E ₀ :
3795B.....	11 36 :	59 03 :	13 ^m 7
3795A.....	11 37 :	58 23 :	
3846A.....	11 42 :	55 18 :	13 ^m 5
3835A.....	11 44.7	60 36 :	
3917A.....	11 48.8	52 15	13 ^m 9
4085A.....	11 58 :	51 12 :	11 ^m 6
4125A.....	12 02.2	64 42	13 ^m 8; 1'2"×0'3" in P.A. 132°; Sa:
4108A.....	12 03.3	67 32	1'2"×0'4" in P.A. 9°; Sb
4108B.....	12 04.8	67 30	0'9"×0'6" in P.A. 0°; E ₃ :
4250A.....	12 15 :	71 09 :	13 ^m 5
5216A.....	13 33.0	62 16	14 ^m
5875A.....	15 07 :	52 29 :	0'6"×0'6"; Sa:
5866B.....	15 10.9	55 58	2'2"×1'7"; Sc
5976A.....	15 35.1	59 43	
6246A.....	16 48 :	55 47 :	13 ^m 5
6493A.....	17 49.3	61 30	1'6"×0'7" in P.A. 39°; Sb
6654A.....	18 ^h 41 ^m	+73°30':	13 ^m 2. 2'6"×0'7" in P.A. 62°; Sc

objects noted to date. Temporarily each nebula is designated by the number of the nearest NGC object on the plate, followed by a capital letter. Dimensions and provisional magnitudes are included when available.

YERKES OBSERVATORY
March 1935

PLATE IV

S



ECLIPSED IMAGES OF SIRIUS A, SIRIUS B, AND COMPARISON STAR
(No reduction with rotating sector)
Enlarged about two times

HETEROCHROMATIC STUDIES OF THE COMPANIONS OF SIRIUS, OF α CETI, AND OF α_2 ERIDANI

By CHARLES HETZLER

ABSTRACT

A simple device is described whereby the components of Sirius were separated at the photographic focus of the Thaw refractor. Methods of separation in the red and ultra-violet are sketched. Magnitudes for a number of Sirius field stars are derived in terms of the B_0 field star, BD-17°1611, of magnitude 6.76. The resulting photographic and red magnitudes of Sirius B, of probable error less than 0^m.1, are 7^m.95 and 8^m.44, respectively, as compared with Wendell's visual value of 8^m.44, confirmed by Kuiper at Leiden and at the Lick Observatory, and with Vyssotsky's photo-visual value of 7^m.1. The corresponding magnitude of Sirius A is -1^m.22, without appreciable color index. Photographic positions of components A and B of Sirius relative to field stars are given at intervals since 1932; resulting values of ρ and θ are compared with calculated positions and with recent visual observations. No sign of a third component is visible.

Photographic and ultra-violet observations of α Ceti B are described. The photographic magnitude in terms of that assumed for the distant companion to α Ceti is 11.2. Several measurements of ρ and θ are tabulated.

As a comparison, the red and ultra-violet indices of α_2 Eridani B are found to agree with those of Sirius B.

SIRIUS B

Separation of the companion of Sirius at the photographic focus of the Thaw 30-inch refractor was accomplished by blocking out part of the telescope objective. The device (Fig. 1) consists essentially of a piece of blackened cardboard, cutting off that part of the aperture of the objective which corresponds to the position of the companion on the plate. The blackening surrounding the overexposed photographic image of Sirius A, owing to scattered or secondarily diffracted or aberrationally diverted light, is mostly of longer focus than the normal image. Hence the cardboard causes the photographic image of Sirius A to be partly eclipsed where the long focus light that it blocks out would fall, clearing the place for the companion (see Pl. IV). The cardboard reduces the aperture by about one-fifth. The size and shape of the eclipsing device were designed to obtain the maximum clearing effect where desired, with the least in-

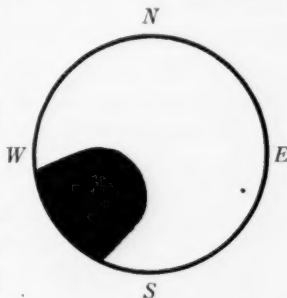


FIG. 1.—The eclipsing device

crease in exposure time and the least distortion of the fainter star images. It is, of course, impossible to cut out the center of the image of A; therefore the device does not reach to the center of the lens. Normally exposed images show no perceptible effect of the partial aperture, the extra-central light being too weak. The best results are obtained with the shortest exposures, which take advantage of moments of good seeing. For an Eastman 40 plate the exposures are as short as a second or two. Slower emulsions can be used only with exceptional seeing. With increased exposures the effect is blurred, even if Sirius is correspondingly reduced by a rotating sector. Hence there is a limit to the faintness of the comparison stars obtainable for positional work.

The red region.—Using Wratten gelatin filter No. 25A, with Panchromatic emulsions, the Thaw telescope was found to have a much sharper focus with than without the visual correcting lens. The focus is about 50 mm beyond the photographic focus in both instances. The combination of filter, emulsion, and focus gives an effective wave-length near 6400 Å. Sirius B was separated in this spectral region on several of the very best nights, when using the corrector and filter with Agfa Super-Panchromatic plates. The overexposed image of Sirius A was smaller than in the photographic region, and the eclipsing device was of no help. Since the visual corrector is of 12 inches aperture and is about one-third the way from the plate to the objective, only two comparison stars could be reached with the combined objective and correcting lens. Luckily Sirius B is of intermediate brightness. One fairly good plate, obtained with a yellow filter, seems sufficient to indicate that there is no hump in the luminosity curve of Sirius B in that region. Further, a plate of excellent focus, obtained in the region of 8600 Å, would show Sirius B were its intensity in that spectral region unexpectedly greater by several magnitudes.

The ultra-violet region.—An odd 1.5 mm “red ultra” Corning glass filter was secured. It transmits a well-defined spectral region between 3200 Å and 4000 Å, the effective wave-length being about 3600 Å. There is a fair ultra-violet focus with this filter and an Eastman 40 plate, but exposures are twenty times those in the photographic region. Blocking out part of the objective produces

almost exactly the same effect on strong images as in the photographic region without a filter. The eclipsing device was therefore used, but opportunities to observe with good seeing have been few.

Derivation of magnitudes.—With Sirius at the center of the field (Fig. 2), only the BD magnitudes of neighboring stars were known. The B₉ star, BD-17°1611, can be photographed simultaneously with Sirius when both are offset from the center of the field. The Harvard visual magnitude, 6.76, was adopted for this star, and it

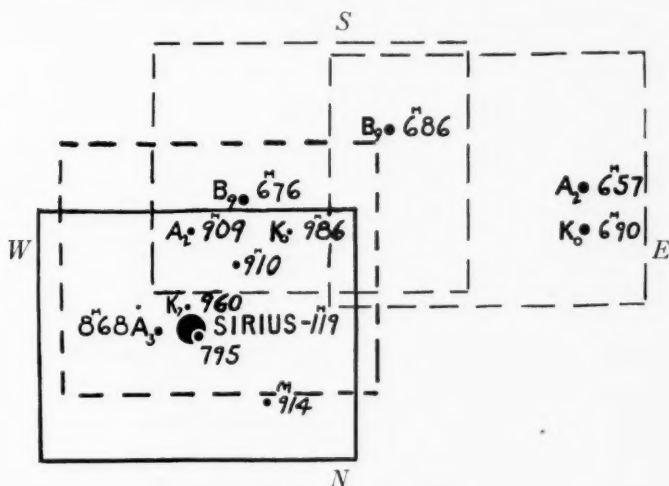


FIG. 2.—The field of Sirius

was assumed to have a color index of zero. By means of a specially constructed sector arrangement, Sirius A was reduced to approximately the same intensity as the B₉ star, and the latter in turn to the same intensity as fainter field stars, including the companion. Thus, in the photographic region, Sirius B was compared with the B₉ star both directly and indirectly: directly, by applying the sector to reduce the B₉ star to about the intensity of B; indirectly, by reducing B to the intensity of BD-16°1586, which was carefully determined from the B₉ as of photographic magnitude 8.68. A similar procedure was followed in the ultra-violet. In the red, since the visual corrector was used, no direct comparison of Sirius B with the B₉ star was made. Sirius A and the two Sirius B comparison stars, BD-16°1586

(A₃) and BD - 16°1589 (K₇), were compared with the B₉ star without the corrector but with the same filter, focus, and emulsions, employing the sector, as above, to effect approximate equality of images. Various measurements indicate agreement between photometric data obtained without and with the corrector but with the same filter, focus, and emulsions, differences probably being less than those caused by the seeing.

The star images, made approximately equal by applying the rotating sector, were further compared with a microphotometer; all additional field stars within the range of the microphotometer were also measured. The microphotometer, made by Brashear, is of the type described by Hartmann,¹ and consists essentially of a photographic wedge. Harvard standard fields near the declination of

TABLE I
CALIBRATION OF NARROW SECTOR

Region	Bright Star	Sp.	Ptg. Mag.	Comp. Stars	No. Plates	Reduction
C12.....	BD+14°4926	A	2.58	A, T, V, W, X	5	7 ^M 96
D4.....	-15°1625	B5	3.90	R, S, T, U, V, W, X, Y, Z, a, b, c	7	8.00
D9.....	-15°4467	A	2.50	U	3	7.95
Vega.....	Vega	A	0.09	BD+38°3229	4	8.06

Sirius were used to calibrate the wedge for use on the Sirius field. For magnitude ranges not exceeding 0^M.5, the accuracy, which is within a few hundredths of a magnitude, is probably greater than the agreement of plates taken on different nights. The magnitude reductions for the wider sectors presented no problem. The narrow sector employed to reduce Sirius A was constructed to transmit 0.052 per cent or to reduce the light by 8^M.2. From accurate measurements with a high-power microscope the calculated reduction was 8^M.07. The Harvard standard fields, namely regions C12, D4, and D9, which contain bright stars within the field of the plate, were used as a check on the calculated reduction (Table I). Since Vega is of nearly the same brightness and type as Sirius, the sector was also applied to it: the reduction was measured, using 6^M.87 as the photo-

¹ *Ap. J.*, 10, 321, 1899.

graphic magnitude of the A_0 star, BD 38°3229. As an additional verification, the neutral-tint gelatin filter used to reduce Sirius A for position work (see below) was calibrated, using Harvard standard region C12. The resulting magnitude of Sirius A is in satisfactory agreement with that obtained by the sector.

Any background of scattered light from Sirius A tends to make B measure brighter; the best images, in which B stands practically clear, give the least brightness for the star. By subtracting the background of the poorer images, the agreement with the better images becomes satisfactory. This probably includes the Eberhard effect, which would tend to offset the effect of scattered light and might even neutralize it. Measurements of several fields show that by allowing for differences in background, if these are not too great, accurate results are obtained. The eye tends to do this very thing: stars which appear no brighter than others against their backgrounds may be measured considerably brighter if no allowance for background is made. All plates were backed to prevent halation, and for many of the best images the background is about the same as for the comparison stars.

Photographic, red, and ultra-violet magnitudes and indices for the Sirius field appear in Table II. Sirius B is probably no brighter photographically than is here reported, but it may be slightly weaker in the red. If it is slightly weaker photographically and stronger in the red, the negative red index should be smaller; but the present value is considered fairly good. The magnitudes for B are at least as accurate as those for A, owing to uncertainty of the narrow sector reduction. Sirius is probably no brighter than is here reported, since adoption of the sector reduction from the standard fields would make it $0^m.1$ fainter. The probable error of the photographic and red magnitudes of both the A and the B components is deemed to be less than $0^m.1$. The red value of B is substantially a verification of Wendell's visual value of $8^m.44$, as against the photo-visual value of 7.1 by Vyssotsky. Kuiper² also has verified Wendell's result. The magnitude differences between A and B, namely, 9.2 mag. and 9.6 mag., are smaller than the generally accepted difference of 10 mag., but they are not nearly as small as that reported by Vyssotsky.

² *Pub. A.S.P.*, 46, 99, 1934.

The ultra-violet results, necessarily incomplete, are somewhat uncertain; Sirius B, however, is certainly not weaker in ultra-violet than in photographic light.

TABLE II
RELATIVE MAGNITUDES AND INDICES

Star	BD	Sp.	Ptg. Mag.	Red Mag.	Red Ind.	U.-V. Mag.	U.-V. Ind.
Sirius A Sirius B	Sirius Field						
	-17°1626	B9	6.85
	1645	A2	6.57
	1611	B9	6.76	6.76	0.0	6.76	0.0
	-16°1586	A3	8.68	8.57	0.11	8.73	0.05
	1587	9.98
	1589	K7	9.60	7.99	1.61
	1590	A2	9.09	8.76	0.33
	1591	A0	-1.22	-1.19	0.0	-1.1	0.1
	1591 <i>a</i>	7.95	8.44	-0.49	7.7?	0.25?
	1593	9.60	8.86	0.74
	1594	9.10	8.56	0.54
	1595	9.14
	1596	8.46
	1597	9.68
	1598	K0	9.86	8.19	1.67
	Other Fields*						
	-13°1682	B2	0.3	0.1
	1686	B2	-0.1	0.4
	-14°1605	A5	0.7
	1613	B9	0.0
	4119	G5	1.57
	4121	Ma	2.38
	+23°4317	Ma	-1.2

* NOTE: A0 field stars were used for comparison.

Measurements of photographic and red magnitudes in a number of Harvard standard fields were made, with the conclusion that the red index is greater than the color index by a factor of about 1.5. This is in agreement with recent work by Gaposchkin.³ The relation of red index to spectral classification is less constant, de-

³ *Pub. A.A.S.*, 8, 47, 1934.

pending on the individual star. This is true of the ultra-violet index as well: perusal of Miss Payne's work⁴ shows an average ultra-violet index of α^M_2 for B₅ to A₃ stars, with marked individual exceptions. At the end of Table II appear the determinations of the indices of a few stars, using the same filters, foci, and emulsions as for the Sirius field.

Photographic positions relative to fainter stars.—In the photographic region a number of pairs of plates were secured, one of Sirius A and one of B, taken successively, with the same comparison stars. For reducing A, a gelatin filter of neutral tint was placed against the plate, while B was usually reduced about α^M_6 by means of a rotating sector. The eclipsing device was used in both instances to eliminate

TABLE III

Star	Dependence	Star	Dependence
BD—16°1586.....	0.2858	BD—16°1586.....	0.5850
1589.....	.4478	1594.....	.1527
1595.....	0.2664	1595.....	0.2623

systematic effects and save time between the taking of the plates. While the comparison stars are not of equal brightness, from five to ten of the best images were measured on each plate. Measurements reduced by the method of dependences indicate that many of the plates are of excellent quality. Alternative sets of comparison stars with dependences adjusted to give the same center of gravity are listed in Table III. The resulting displacements from the center of gravity of the comparison stars, corrected for parallax (Table IV), were plotted as ordinates against the time as abscissa. The four curves, one of each component in α and δ , were drawn to give, as nearly as possible, mean values. Values of ρ and θ for several dates have been calculated from the mean positions on the graphs, and are given in Table V with the corresponding values from the ephemeris of Volet,⁵ with photo-visual values by Vyssotsky⁶ and with visual observations by Wallenquist⁷ and Aitken.⁸

⁴ *Harvard Ann.*, **89**, No. 2, 1932.

⁵ *B.A.*, **7**, 13, 1932.

⁶ *A.J.*, **53**, 997, 1933.

⁷ *Ann. Bosscha-Sterrenwacht*, **6**, 34, 1934.

⁸ *Pub. A.S.P.*, **46**, 110, 1934.

TABLE IV
POSITIONS OF SIRIUS A AND B

DATE	NO. OF IMAGES		QUALITY		PARALLAX		POSITIONS RELATIVE TO CENTER OF GRAVITY (MINUS PARALLAX)*			
	A	B	A	B	α	δ	c.g.— Ba	c.g.— B δ	c.g.— A α	c.g.— A δ
1932 Nov. 23.....		10	vg	+".23	—".20	—3".28	+5".04
Nov. 30.....		10	vg	+".20	.21	3.42	4.88
1933 Feb. 3.....		12	vg	—".21	.18	3.10	4.68
Feb. 15.....		8	g	—".27	.15	3.23	4.80
Feb. 18.....		6	f	—".28	.14	3.13	4.84
Feb. 20.....	5		g	—".29	.13	+2".77	—2".51
Mar. 24.....	2	5	f	—".37	.00	3.11	4.62	2.84	2.48
Mar. 26.....	4	5	g	—".37	.00	3.13	4.56	2.82	2.52
Oct. 31.....	5	5	vg	vg	+".32	.13	2.40	3.83	3.03	3.22
Nov. 1.....	4	6	vg	vg	+".32	.13	2.31	3.76	3.04	3.30
Dec. 24.....	4	5	p	+".05	.24	2.25	3.58	3.11
1934 Jan. 11.....	8	6	g	p	—".07	.23	2.33	3.82	3.13	3.56
Jan. 19.....	5	6	g	vg	—".12	.22	2.19	3.79	3.10	3.52
Jan. 26.....	4	6	g	vg	—".16	.20	2.28	3.83	3.07	3.49
Feb. 17.....	7	7	vg	f	—".28	.14	2.11	3.49	3.22	3.68
Mar. 20.....	7	7	vg	vg	—".36	.02	2.06	3.42	3.14	3.70
Dec. 11.....	6	8	g	+".13	.23	1.24	2.56	3.36	4.57
1935 Jan. 29.....	7	7	g	g	—".18	.20	1.25	2.37	3.33	4.81
Mar. 14.....	8	11	g	g	—".35	.04	0.99	2.24	3.42	4.94
Mar. 21.....	6	3	g	f	—".36	.02	1.09	2.19	3.47	4.94
Mar. 22.....	5	10	g	g	—".36	.02	0.95	2.13	3.48	4.85
Mar. 26.....	7	8	g	f	—".37	—".00	—0.88	+2.07	+3.55	—4.92

* A scale of 1 mm = 14".6 was used.

TABLE V
MEASURES OF SIRIUS

DATE	HETZLER		VOLET		OTHER MEASURES		
	θ	ρ	θ	ρ	θ	ρ	Observer
1932.97.....					40°.7	9".03	Vyssotsky
1933.00.....	40°.3	9".32	40°.6	9".16
1933.25.....	39.4	9.24	39.9	9.05
1933.80.....	37.4	9.02	38.2	8.77
1933.81.....					39.0	8.71	Wallenquist
1934.00.....	36.6	8.96	37.6	8.67
1934.14.....					38.7	8.52	Aitken
1934.20.....	35.9	8.89	36.9	8.56
1934.75.....	33.9	8.60	35.0	8.26
1935.25.....	31.8	8.34	33.2	7.96

In Table VI values of ρ and θ from the various pairs of plates are compared with positions calculated from Aitken's elements (1918) and from the ephemeris of Volet (1932).

Errors of observation or increased photographic effect by a visually faint third star might explain the discordances with the visual observations and with the ephemerides. It is conceivable that photographic effects might influence the apparent separation of the pair, but the photographic position angle should be quite accurate.

TABLE VI

DATE	QUALITY	HETZLER		AITKEN		VOLET	
		θ	ρ	θ	ρ	θ	ρ
1933.11.....	f	38.8	9.42				
1933.23.....	f	40.0	9.26				
1933.24.....	vg	40.0	9.25	39.7	9.14	39.9	9.05
1933.84.....	vg	37.6	8.90				
1933.84.....	vg	37.2	8.86	37.9	8.93	38.2	8.77
1933.98.....	f	37.5	8.81				
1934.03.....	p	36.5	9.18				
1934.05.....	vg	35.9	9.03				
1934.07.....	g	36.2	9.07				
1934.13.....	f	36.6	8.93				
1934.22.....	vg	36.1	8.82	36.6	8.66	36.7	8.55
1934.94.....	g	32.8	8.48			34.3	8.14
1935.08.....	g	32.5	8.51			33.8	8.06
1935.20.....	g	31.6	8.42				
1935.22.....	f	32.6	8.46				
1935.22.....	g	32.2	8.32				
1935.23.....	f	32.4	8.28			33.2	7.96

The satisfactory agreement of measurements of images of varying intensity and background argues against marked photographic effects. No visible evidence of a third star has been found on the photographic or the red plates. If it is within one magnitude of B in brightness, the separation of any such star would probably be less than a second of arc. Unfortunately, the red-sensitive plates, having only two comparison stars, cannot be measured for positions, except by trying to bisect the rather large image of Sirius A.

α CETI B

As a test of the Thaw telescope, and as worth while in itself, the separation of α Ceti B was attempted in the photographic and in the

ultra-violet spectral regions. Resolution was definitely accomplished on a number of photographic plates taken during the 1933 and 1934 minima, but not with certainty in the ultra-violet region, where the contribution of each component is puzzling. Examination of the α Ceti plates shows that photographically the total light was practically constant from mid-August until November, 1933, being about $0^M 1$ weaker than the Ma distant companion, BD-3°355, and $0^M 1$ stronger than the A₃ star, BD-3°357. The variable and the close companion were photographically about of the same brightness during this interval. In the ultra-violet the Ma star does not show even on the strongest plates, while the total light of α Ceti is still consistently $0^M 1$ stronger than that of the A₃ star. In Table II the ultra-violet index of an Ma star is seen to be large negatively. Plates of R Aquilae, χ Cygni, and R Hydrae, in both the photographic and ultra-violet regions, indicate that perhaps all the Md variables are relatively stronger in the ultra-violet than are Ma stars. While no extensive investigation was made, the photographic-ultra-violet index for the several Md variables seems to be very small, if not indeed zero. Band absorption may be greatly lessened in the ultra-violet region, as compared with the photographic. There is not much doubt that a substantial part of the ultra-violet intensity of α Ceti is due to the variable. When it had brightened on the plate of December 23, 1933, however, so that it alone contributed to normal exposures, it was at least $0^M 5$ weaker in the ultra-violet than in the photographic region, as compared with the A₃ star. But perhaps the most that can be said is that the faint companion may be strong in the ultra-violet.

During the minimum of 1933 two visual estimates were made by G. Van Biesbroeck,⁹ as follows:

September 22, 1933: "B about $2^M 5$ fainter than A, which in turn was then $0^M 2$ fainter than the distant companion."

October 1, 1933: "B about $0^M 8$ fainter than A, itself $0^M 5$ fainter than the distant companion."

A plot of the visual estimates of the American Association of Variable Star Observers indicates a visual magnitude (total light)

⁹ Private communication.

of $9^m.4$ at this time, which agrees with Van Biesbroeck's observations, since the Harvard magnitude for the distant companion is $9^m.08$. Taking the mean of Van Biesbroeck's two values, the visual magnitude of the faint component was 11.1. Based on eleven plates, my mean estimate of the photographic magnitude in terms of that of the distant companion, assumed to be 10.4, was 11.2. It might be 11.0. There is no positive evidence of any change in the magnitude of B over the period of observation.

Mira reached about the same minimum in 1934, but the seeing was generally poorer than in 1933. Three plates possibly show the

TABLE VII

Date	Emulsion	ρ	θ
Aug. 26, 1933.65....	40	$0''.80$	$122''.9$
Sept. 25, 1933.74....	40	.80	$134''.2$
		.76	$130''.1$
Oct. 31, 1933.83....	33	.75	$129''.8$
Nov. 1, 1933.83....	40	$0''.80$	$131''.3$
Mean.....	$0''.78$	$129''.8$

B component, indicating that it probably was neither brighter nor fainter than in 1933.

Several α Ceti plates were measured, under a higher power than usual, for values of ρ and θ (Table VII). A separation of $0''.8$ is really below the practical limit of the Thaw telescope, even for nearly equal pairs, to which class α Ceti belonged at these minima.

α_2 ERIDANI B

This class A3 star was compared, in the various spectral regions, with an A0 field star of nearly its own magnitude, namely BD-7779. The same filters, emulsions, foci, and methods were employed as for Sirius B and α Ceti B. The red index (photographic minus red magnitude) was found to be $-0^m.43$, and the ultra-violet index (photographic minus ultra-violet magnitude) $+0^m.24$. The measures cannot be far in error, since B is widely separated from A, and C is too faint to interfere. The agreement with the results for Sirius B,

while somewhat accidental and dependent on the particular A₀ comparison star, is nevertheless striking.

The general conclusion is that the companions of Sirius, α_2 Eridani, and possibly α Ceti seem to be, for their spectral class, unusually strong in the shorter wave-lengths. This might be correlated with other peculiarities. There is a chance that they are radiating intensely in the region absorbed by our atmosphere, like certain stars associated with nebulae. A principle for the discovery of additional stars of this type might be indicated.

Acknowledgments and thanks are due to Dr. Burns, Director Jordan, and Mr. Daniel of the Allegheny Observatory staff, for helpful interest and valuable discussion.

ALLEGHENY OBSERVATORY
UNIVERSITY OF PITTSBURGH
April 1935

ULTRA-VIOLET STELLAR SPECTRA WITH ALUMINUM-COATED REFLECTORS

III. THE SPECTRUM OF α LYRAE

By R. WILLIAM SHAW

ABSTRACT

The wave-lengths of 118 absorption lines in the spectrum of α Lyrae between λ 3000 and λ 3480 have been measured. Seventy-four of the lines have been identified with the spectra of the once ionized atoms *Al*, *Cr*, *Fe*, *Mn*, *Ti*, and *V*, and with spectra of the neutral atoms *Al*, *Fe*, and *Na*. Some of the lines appear to have variable intensities. No lines were observed between λ 3480 and the Balmer limit at λ 3646.

The lines of Ti^+ are particularly prominent. It is shown that the ultra-violet lines of this atom as observed in α Lyrae involve the same energy levels, or others of comparable excitation potential, as do known Ti^+ lines in the visible region. On this basis one might expect lines in the region $\lambda\lambda$ 3480-3646. The absence of lines in this region is discussed in terms of the hydrogen continuum and the ultra-violet energy-curve.

A close examination of the spectrum of α Lyrae from λ 3000 to the limit of the Balmer series reveals a number of extremely faint absorption lines between λ 3000 and λ 3480 but no lines between λ 3480 and the Balmer limit. For the purpose of ascertaining the identity of these weak lines a series of seven spectrograms taken¹ at intervals during the summer of 1934 have been measured. The exposures, which were never more than three minutes, were made as near the meridian as possible and were distributed throughout the summer in order to avoid any possibility of atmospheric effects. These precautions seemed desirable since the work of the previous summer indicated that the ultra-violet lines of α Lyrae were rather elusive.

The wave-lengths of the 118 lines measured, together with identifications for 74, are listed in Table I. The wave-lengths have been corrected for radial velocity.² Included in the table are eye estimates of relative intensities and the number of plates on which a given line was observed. Sixty-one of the lines were observed on two or more plates.

¹ The spectra were obtained at the Lowell Observatory with the apparatus described by S. L. Boothroyd (*Ap. J.*, **80**, 1, 1934), except that an automatic temperature control was installed in the spectrograph and the original aluminum coating of the 15-in. mirror was replaced by one of "chroluminum."

² *Pub. Yerkes Obs.*, **7**, 63, 1929.

TABLE I

λ Star	Intensity	Observations	Identification
3057.86.....	0	1	8.08 Ti^+ , 7.44 Ti^+
59.41.....	0	1	
66.34.....	0	1	6.36 Ti^+ , 6.22 Ti^+
69.33.....	0	1	
71.14.....	0	1	1.23 Ti^+
73.25.....	0	1	3.83 V , 2.97 Ti^+
74.95.....	0	1	4.67 Al^+
75.42.....	0	1	5.73 Fe , 5.22 Ti^+
78.95.....	1	2	8.64 Ti^+
88.10.....	1	2	8.03 Ti^+
90.25.....	0	1	
92.90.....	2	6	3.12 V , 2.71 Al , 2.85 Al
97.11.....	0	1	7.18 Ti^+
99.97.....	0	1	9.98 Fe , 9.89 Fe
3100.65.....	0	1	0.32 Fe , 0.68 Fe
02.62.....	1	1	2.30 V^+
05.26.....	0	1	4.80 $Mg^{+?}$
10.56.....	0	2	0.61 Ti^+ , 0.70 V^+
14.22.....	0	1	
17.23.....	1	2	
18.70.....	2	5	8.65 Cr^+ , 8.38 V^+
19.81.....	3	2	9.80 Ti^+
20.41.....	1	3	0.37 Cr^+
22.40.....	1	1	
25.03.....	3	6	4.99 Cr^+
28.63.....	0	3	8.70 Cr^+
30.63.....	1	2	0.27 V^+ , 0.81 Ti^+
31.81.....	2	3	2.05 Cr^+
35.01.....	0	1	4.93 V^+
36.96.....	2	3	6.70 Cr^+
41.12.....	0	1	
45.33.....	0	1	
47.58.....	0	1	7.23 Cr^+
51.76.....	0	1	
54.10.....	2	5	4.20 Ti^+ , 4.20 Fe
56.49.....	0	1	
58.75.....	3	4	8.88 Ca^+
59.45.....	1	4	
60.88.....	1	2	
62.52.....	1	3	2.56 Ti^+
68.54.....	1	3	8.52 Ti^+
70.39.....	0	1	
77.61.....	1	2	
79.56.....	2	4	9.34 Ca^+
80.70.....	0	1	0.71 Cr^+
81.42.....	2	3	1.42 Cr^+
82.98.....	2	4	
86.69.....	2	5	
90.60.....	1	3	0.87 Ti^+ , 0.68 V^+
91.24.....	1	3	
92.49.....	0	2	
3193.45.....	0	4	3.81 Fe^+ , 3.30 Fe

TABLE I—*Continued*

A Star	Intensity	Observations	Identification
3195.72.....	0	2	
96.74.....	2	3	6.10 Fe^+ , 7.11 Cr^+
3201.09.....	1	2	
09.12.....	1	3	9.18 Cr^+
10.54.....	1	3	0.45 Fe^+
11.27.....	1	1	
12.64.....	1	1	
13.47.....	1	3	3.31 Fe^+
17.10.....	3	5	7.04 Ti^+ , 7.10 V^+
19.48.....	2	3	
20.25.....	0	1	
22.80.....	1	1	2.82 Ti^+
24.15.....	0	1	4.23 Ti^+
25.33.....	0	1	
27.69.....	1	5	7.76 Fe^+
29.50.....	1	6	9.18 Ti^+ , 9.40 Ti^+
32.78.....	0	1	
34.39.....	2	3	4.52 Ti^+
36.33.....	2	4	6.10 Ti^+ , 6.57 Ti^+
39.07.....	2	5	9.03 Ti^+
41.73.....	1	4	1.07 Ti^+
44.84.....	0	1	
45.18.....	1	1	
46.58.....	0	1	
48.51.....	1	2	8.60 Ti^+
51.34.....	0	1	1.89 Ti^+
52.48.....	1	2	2.85 Ti^+
53.63.....	0	1	
54.18.....	0	1	4.23 Ti^+
55.95.....	2	2	5.90 Fe^+
58.79.....	0	1	
59.64.....	1	2	
61.10.....	1	3	1.59 Ti^+
63.35.....	0	1	
64.33.....	0	1	
67.55.....	0	1	7.71 V^+
71.33.....	1	2	1.63 Ti^+ , 1.14 V^+
87.43.....	0	1	7.64 Ti^+
95.34.....	0	1	5.43 Cr^+
3302.91.....	0	1	2.38 Na , 2.98 Na
04.54.....	0	1	
22.75.....	1	1	2.93 Ti^+
28.57.....	0	1	
31.05.....	0	1	
35.26.....	1	3	5.19 Ti^+
36.41.....	0	1	6.34 Cr^+
39.51.....	1	2	9.80 Cr^+
42.47.....	1	1	2.58 Cr^+
49.36.....	4	7	9.41 Ti^+ , 9.02 Ti^+
3360.61.....	2	5	0.31 Cr^+
68.06.....	2	2	8.06 Cr^+
72.50.....	0	4	2.80 Ti^+

TABLE I—*Continued*

λ Star	Intensity	Observations	Identification
3380.22.....	I	3	0.28 Ti^+
83.73.....	2	3	3.76 Ti^+
87.37.....	I	2	7.83 Ti^+
94.37.....	I	3	4.57 Ti^+ , 4.30 Cr^+
3402.98.....	I	2	2.42 Ti^+ , 3.34 Cr^+
07.79.....	I	I
20.34.....	O	I
21.91.....	O	I	1.22 Cr^+ , 2.76 Cr^+
39.22.....	O	I
41.51.....	I	2	1.98 Mn^+
43.81.....	O	2
60.28.....	I	I	0.32 Mn^+
69.25.....	I	I
73.83.....	I	I	3.97 Mn^+

The identifications were made by comparing the observed lines with the spectra³ of all the neutral or ionized atoms which have lines in the region under investigation and which might be expected in an A0 star. Special attention was given to multiplet relations. The average difference between laboratory and stellar wave-lengths is 0.14 Å. The 40 positive, 31 negative, and 3 zero residuals indicate non-systematic differences in the identifications. It happens that the average residual of those lines which were observed two or more times is also 0.14 Å. This gives some evidence for the belief that the lines observed only once are not fictitious. Moreover, α Lyrae is known to have a variable radial velocity⁴ with a period of 0.179 days and an amplitude of 4 km/sec. In the study of this variability faint lines in the visible region were used. It was found that the intensity of many lines varied through a large range. These results, together with the present observations, tend to confirm the idea that other than observational causes may be influencing the appearance or non-appearance of lines in α Lyrae.

Atoms whose spectral lines are observed in the ultra-violet spectrum of α Lyrae include Al^+ , Cr^+ , Fe^+ , Mn^+ , Na , Ti^+ , and V^+ with considerable certainty, and Al , Fe , and Mg^+ as possibilities. With

³ C. E. Moore, *Multiplet Table of Astrophysical Interest*, 1933; F. Twyman, *Wave-Length Tables*, 1931; H. Kayser, *Hauptlinien der Linienspektren*.

⁴ A. Belopolsky, *Zs. f. Ap.*, 2, 245, 1931.

less exacting requirements as to coincidence in wave-lengths more identifications, especially with *Fe* and *V*, seem reasonable. The spectrum as a whole is very similar to that observed for α Cygni, A2p, by Wright.⁵

The Ti^+ lines in particular lead to the following interesting information: The observed ultra-violet lines involve fifteen of the low-

TABLE II
MULTIPLETS OF Ti^+ IN α LYRAE

MULTIPLY	NUMBER OF LINES			
	Theory	Expected	Observed	Blended
$a^1P - a^1P^0$	7	4	2	1
$a^1F - a^1D^0$	9	8	7	3
$b^1P - a^1P^0$	7	7	2	1
$a^1F - a^2D^0$	5	3	1	1
$b^1F - a^1D^0$	7	4	2	0
$a^2D - b^2F^0$	3	2	1	1
$a^2H - b^2G^0$	3	2	1	0
$a^1F - a^1F^0$	10	10	10	3
$b^1F - b^2D^0$	5	1	1	0
$b^1P - b^1D^0$	8	6	3	1
$b^2G - a^2H^0$	3	2	2	0
$b^1F - a^1F^0$	10	4	2	0
$a^2F - a^2G^0$	3	2	1	1
$a^1F - a^1G^0$	9	7	6	2
$a^1P - b^1D^0$	3	2	1	1
Total.....		64	42	15
$b^1F - a^1G^0$	8	3		
$b^2P - b^2P^0$	4	1		
$b^2G - b^2G^0$	4	2		
$b^2P - c^2D^0$	3	1		
$a^2F - a^1D^0$	4	1		
$a^2P - a^2S^0$	2	2		

lying multiplets of the Ti^+ atom. The observations are summarized in Table II. The first column gives the abbreviated multiplet designation and the second gives the number of lines for each multiplet which are permitted by the usual ΔJ rules. Of course not all of the permitted lines are intense and not all would necessarily be observed in a stellar spectrum. The third column indicates the number of lines which might reasonably be expected and the next column gives

⁵ *L.O.B.*, 10, 100, 1921.

the number actually observed. The last column gives the number of observed lines which are blended. Of the 64 expected lines, 42 are observed, only 15 of which are blended. Not all of the blends are of the same weight, since 5 are blends of Ti^+ with itself. Examination of the individual multiplets shows that in those involving the lowest energy states practically all of the expected lines are observed. The multiplets involving higher levels show a correspondingly good agreement.

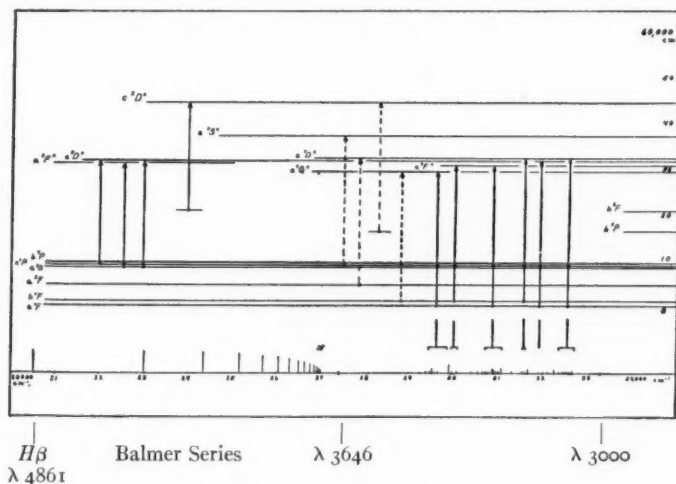


FIG. 1.—Spectrum of Ti^+ in Vega

From a study of the visible spectrum of α Lyrae⁴ and of other stars² of the same spectral class it is known that these same multiplet states, or others of comparable excitation energy, give rise to Ti^+ lines in the visible region. It follows from the known visible lines and the newly observed ultra-violet lines that, according to the known laboratory spectrum⁶ of Ti^+ , there should be a number of lines in the region from λ 3480 to the Balmer series limit—a region in which no lines were observed. At the bottom of Table II are given six multiplets of Ti^+ whose lines lie in this region. These multiplets involve the same energy levels discussed above and, on a laboratory basis, include lines just as intense as those in the observed ultra-violet multiplets. The situation is shown clearly in Figure 1 (for the

⁶ H. N. Russell, *Ap. J.*, **66**, 295, 1927.

sake of simplicity not all of the data are included in the figure). On the abscissae have been plotted in cm^{-1} the Balmer lines beginning at $H\beta$, the Balmer series limit λ 3646, the majority of the observed ultra-violet Ti^+ lines, and the atmospheric transmission limit near λ 3000. Above this spectrum the energy-level scheme for Ti^+ has been drawn. The plotted energy levels do not represent those levels which give rise to individual spectrum lines, but represent all the fine structure levels of a given multiplet. The vertical solid lines represent all the lines concerned in the electron transitions between the designated multiplet levels. The electron transition lines or arrows are placed in the energy diagram over the spectrum wave-number scale at the position in which the corresponding lines are to be observed. From the figure it seems clear that lines involving the multiplet levels indicated by the dotted arrows might be observed. These relations may also be shown, although less strikingly, by the spectra of V^+ and Cr^+ .

According to Yü,⁷ the energy-curve of α Lyrae from λ 3646 to λ 3400 is, though much lower, approximately parallel to the curve for the visible portion of the spectrum. This indicates a strong hydrogen continuous absorption which decreases only very slowly toward the ultra-violet. If this is correct, one might expect to observe no line spectra in the far ultra-violet in a case in which multiplets near the Balmer limit are missing. However, the curve of α Lyrae by Yü seems unusual in view of his curves for other stars of similar spectral type. The latter curves indicate a decreasing energy in the ultra-violet. Recent observations by Robley C. Williams,⁸ of the ultra-violet to λ 3000 in α Lyrae seem to indicate that this star, too, has increasing absorption with shorter wave-length. According to theory,⁹ the absorption coefficient for the hydrogen continuum varies as the inverse of ν^3 . It might then be necessary to suppose that the continual increase of absorption in the ultra-violet is due in part to line absorption. Undoubtedly line absorption does play a part, since a large number of the observed lines are resonance lines of ionized atoms. However, it seems difficult to explain how certain lines can

⁷ *L.O.B.*, **12**, 104, 1926.

⁸ American Astronomical Society, Philadelphia, December, 1934.

⁹ Milne, *M.N.*, **85**, 770, 1925. Quantum mechanics gives a similar result.

be so intense as to produce, with a decreasing hydrogen absorption, a continually increasing total absorption and how related lines, on the other hand, can be obscured by hydrogen absorption near the Balmer limit or appear only very weakly in the visible region.

The problem will have a solution, of course, only after this spectrum and many others of similar type have been examined in great detail. There seems hope, however, of devising means of analysis whereby the absorptions due to the hydrogen continuum and to line spectra may be separated and some knowledge gained concerning the form of the ultra-violet energy curve with these factors removed.

DEPARTMENT OF PHYSICS
CORNELL UNIVERSITY
March 1935

NOTES

VARIABLE $H\alpha$ EMISSION IN ϵ AURIGAE

ABSTRACT

Distinct $H\alpha$ absorption was present in ϵ Aurigae on October 14, 1929, during the total phase of eclipse. On January 22 and March 15, 1935, emission was evidently present, just filling up the absorption.

During the total phase of the eclipse of ϵ Aurigae a single exposure was made on a coarse-grained panchromatic plate, on October 14, 1929. This plate was greatly overexposed, but it shows distinct absorption at $H\alpha$, although it is not as strong as would be expected from the intensity of $H\beta$. Apparent narrow emission borders cannot be confidently regarded as real, as opposed to Eberhard effect.

On January 22, 1935, an exposure was made on the fine-grained Eastman III-F emulsion, for comparison with the spectrum of Nova Herculis. This plate shows the spectrum to be continuous at $H\alpha$. Evidently an emission line equal in intensity to the continuous spectrum just fills up the absorption. Another plate taken on March 15 shows no further change. All the exposures referred to were obtained with the single-prism spectrograph, having a dispersion of 175 Å/mm at $H\alpha$.

Whether the observed change is due to the eclipse of the bright-line star or is an independent phenomenon cannot be decided until more data are available.

DEAN B. McLAUGHLIN

THE OBSERVATORY
UNIVERSITY OF MICHIGAN
April 10, 1935

VARIATIONS IN THE SPECTRUM OF 29 CANIS MAJORIS

ABSTRACT

The emission lines $He\ II\ 4686$, $N\ III\ 4634$, and $N\ III\ 4640$, and the absorption line $He\ I\ 4472$, vary in intensity with the orbital period of this binary.

Recent spectrograms of this massive O7-type binary show that the emission lines $He\ II\ 4686$, $N\ III\ 4634$, and $N\ III\ 4640$, and the

absorption line *He* I 4472, vary in intensity with the orbital period of 4^d39. If the phases are counted from J.D. 2424981.613, as in Pearce's orbit,¹ maximum intensity of the emission lines occurs at 0^d5 and minimum at 2^d0. There may be a slight increase at 2^d5. The emission lines are quite narrow between 0^d and 1^d, but are broad in the neighborhood of 4^d. The maximum at 0^d5 agrees with superior conjunction of the stronger component. There is no such maximum at inferior conjunction, and the phenomenon is not caused by the overlapping of the two spectral components. Measures with the microphotometer show that the range in the intensity of *He* II 4686, expressed in units of the continuous spectrum, is from 0.5 to 1.8 A.

The absorption lines show two maxima, at 2^d5 and 0^d8, and two minima, at 3^d6 and 1^d5. Both maxima occur when the velocity of the stronger component is negative, but there is a secondary intensity minimum at the time of minimum velocity. The primary intensity minimum occurs in the neighborhood of maximum velocity. The two maxima of intensity occur when the relative velocity of the components is about 200 km/sec., so that blending cannot be responsible for the variation. In this connection it will be remembered that α Virginis, V Puppis, and μ^1 Scorpii have their maxima of intensity coincident with the minimum of velocity.

The character of the variations of the absorption lines suggests that the change is one of gradient—affecting strong lines, such as *He* I 4472, more than weak lines, such as *He* II 4542. Microphotometer measurements show that the variations affect mostly the central intensities.

O. STRUVE
C. T. ELVEY
W. W. MORGAN

YERKES OBSERVATORY
June 18, 1935

¹ *Pub. Dom. Ap. Obs. Victoria*, 6, 51, 1932. The first orbit was determined by W. E. Harper, *Pub. Dom. Obs. Ottawa*, 4, 115, 1917. A new orbit, from the Yerkes Observatory material, is being determined by Dr. Luyten and Mr. Ebbighausen.